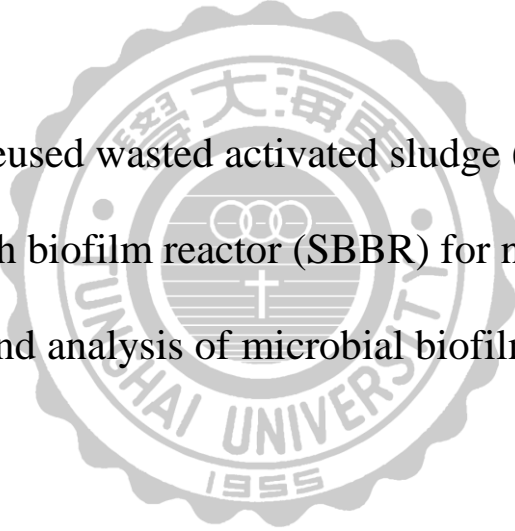


東海大學環境科學與工程研究所

碩士論文

應用重製廢棄污泥顆粒於循序批分式生物膜反應器除氮
及生物膜菌相分析

Application of recycled wasted activated sludge (WAS) pellets in
sequencing batch biofilm reactor (SBBR) for nitrogen removal
and analysis of microbial biofilm

The seal of Donghai University is a circular emblem with a scalloped outer edge. It features the university's name in Chinese characters '東海大學' at the top and 'DONGHAI UNIVERSITY' in English at the bottom. The year '1955' is inscribed at the very bottom. In the center, there is a cross-like symbol with a horizontal bar across it, and the university's name is also written in Chinese characters around the inner circle.

指導老師：張鎮南 博士

研究生：陳志哲 撰

中華民國一零四年七月

July 2015

東海大學碩士班研究生
論文指導教授推薦書

環境科學與工程學系陳志哲君所提之論文

題目：應用重製廢棄污泥顆粒於循序批分式生物膜反應器除氮及生物膜菌相分析

Application of reused wasted activated sludge (WAS) pellets in sequencing batch biofilm reactor (SBBR) for nitrogen removal and analysis of microbial biofilm

係由本人指導撰述，同意提付審查。

指導教授： (簽章)

106年 7月 6日

東海大學環境科學系碩士班

論文口試委員審定書

環境科學與工程學系碩士班陳志哲君所提之論文

題目：應用重製廢棄污泥顆粒於循序批分式生物膜反應器除氮及
生物膜菌相分析

Application of reused wasted activated sludge (WAS) pellets in
sequencing batch biofilm reactor (SBBR) for nitrogen removal
and analysis of microbial biofilm

經本委員會審議，認為符合碩士資格標準。

論文口試委員召集人 黃啟裕 (簽章)

委員 林志高

邱應志

張鎮南

中華民國 104 年 7 月 10 日

致謝

哇~研究所三年就這樣過了，實在難以想像當初我是如何有勇氣踏進這條學術路，無論如何我總算要在學校這部分先告一段了，由衷感謝我給自己一個磨練的機會，接著要感謝張老師鎮南在我求學過程中給予的指教及督促，使我在面對問題時更能獨立去完成，此外另一位要特別感謝的超級重量級人物就是黃老師啓裕，提供我一個可以做分生實驗的地方，雖然我們是在最後一年才對彼此有更深的了解，與你相識這短短的一年，我深深地覺得你是一位不簡單的人物，對我而言在學校你扮演著給予我實驗及研究上指導的老師，私下你則是扮演著我心中父親的身份與我分享你寶貴人生經驗及疼惜照顧我，我的人生旅途中能與你相識實在是我幾輩子修來的福氣，雖然我即將要畢業了，不能再常常跑去找你聊天讓你開心，但我們之間的感情會像現在一樣持續好下去，口試期間承蒙黃老師啓裕、林老師志高及邱老師應志於百忙中抽空親臨指導，提供學生許多寶貴意見及具體建議，使學生論文整體架構更加完善，也吸收到更多我還不知道的新知識。

整整三年在研究室累積的生活點滴及革命情感以及有太多說不完的事情了，慧燕學姐謝謝妳總在我失意時適時的給予我鼓勵及幫助，使我心靈上感受到溫暖，讓我渡過碩一時的黑暗期並且轉變自己的心態去迎接未來的挑戰，之後就沒辦法再幫忙訓練班監考，所以雅萍、佩萱、苓菱及于軒你們要多 carry 點學姐啊，別再出包了，理維學長謝謝你在碩一時給我的開導指教以及最後論文初稿修正上幫忙許多，佳茹謝謝你總在我傷心時聽我訴苦，使我能走到現在，祐祺、煊根學長自從你們畢業後，研究室就沒人可以陪我講一些屁話及嘴砲，文志、哲豪及好甄你們要加油唷！其實我的碩士生活過得多采多姿，因為太

常跑去其他研究室串門子，都把感情給串出來了，環管研究室的硯勳學長謝謝你在許多事情上幫助我許多，我似乎習慣你的嘴砲了，麻吉培軒說好的一起畢業呢！你卻給我先登入國軍 online，柏均謝謝你在 LOL 上的指導，事實證明我還是沒那天份 hold 住全場，最後這半年我發現環微研究室似乎才是讓我最有歸屬感的地方，想必跟那位超級重量級人物有關吧！最後一年跟能宥鈞姐一起畢業實在是太榮幸了，想到那時我們在分生實驗遇到太多瓶頸，但最後還是一一的想辦法克服及互相 cover，傻翔實在太奸詐了，拿兵單開先例後害其他人都不用玩了，所以昆翰、浩銘、皓瑋、至榮接下來就看你們的表現囉！期待你們能和我跟宥鈞姐一樣快點畢業，棟凱你的助理工作也將結束了，能在這最後這半年認識你真好，謝謝你常把身邊朋友在職場的工作經驗分享給我，讓我們朝著自己的人生目標繼續邁進，我有時間會常回來看看你們。

外環境早班的各位夥伴輪到你們囉！我很高興我能加入勞作教育這個團隊，似乎上天已經注定要讓我們互相認識，這三年的研究所生活我常向你們訴苦，還好有你們大家的鼓勵，讓我能撐到今天，如今我能過得了這一關往後的難關想必都能迎刃而解，我雖退休準備離開大家，但我的心永遠跟你在一起，同樣的我有時間會常回來找你們並且跟大家 LINE 的，最後謝謝我的家人，尤其是辛苦賺錢的老爸老媽全力支持並時常關心我在外地的狀況，讓我在求學過程中沒有任何後顧之憂，我愛你們，我終於要踏出校園準備進入人生的下個階段了。

摘要

本研究係利用台中福田水資源回收中心的廢棄活性污泥、紅土以及氧化鐵重製燒結成顆粒載體，藉由反應曲面法(RSM)找出最佳的載體配比以提升其抗壓強度、吸水率、容積密度及比外部表面積，並將重製之顆粒當作生物載體用於循序批分式生物膜反應器(SBBR)以達到同時硝化脫硝(SND)。將兩個系統分別添加40%和60%的載體比例，並且比較兩個系統在相同操作條件下去除氨氮及過程中產生中間產物羥胺(Hydroxylamine)和亞硝酸鹽的效果，利用反應器中氧化還原電位(ORP)之變化藉由能斯特方程式(Nernst Equation)導出適用線上即時監控的模式，最後針對載體上之生物膜進行菌相分析。實驗結果得知顆粒載體最佳配比污泥:紅土:氧化鐵為5:3:2，其抗壓強度為 $46.1 \pm 1.2 \text{ Kg/cm}^2$ ，吸水率為 $52.7 \pm 4.4\%$ ，容積密度為 $2.2 \pm 0.5 \text{ g/cm}^3$ ，比外部表面積為 $2.9 \pm 0.2 \text{ m}^2/\text{g}$ ，實驗發現在SBBR-60%系統中，氨氮大部分轉為亞硝酸鹽約 5.7 mg/L 且只生成微量的硝酸鹽約 1 mg/L 以下，推測反應器中進行部分硝化(nitrification)，且硝化速率(K_N)及脫硝速率(K_{DN})分別為 $9.7 \text{ mg NH}_4^+-\text{N}/\text{L-hr}$ 和 $9.5 \text{ NO}_x^--\text{N}/\text{L-hr}$ 皆比SBBR-40%系統好。由親源樹圖顯示生物膜上具有自營硝化菌和異營脫硝菌，其中好氧脫硝菌 *Dokdonella immobilis* 及 *Acinetobacter sp.* 在系統中也被發現，其間接證明溶氧在 1 至 2 mg/L 時系統也能進行脫硝反應，並且將亞硝酸鹽逐漸還原成氮氣以達到除氮效果。

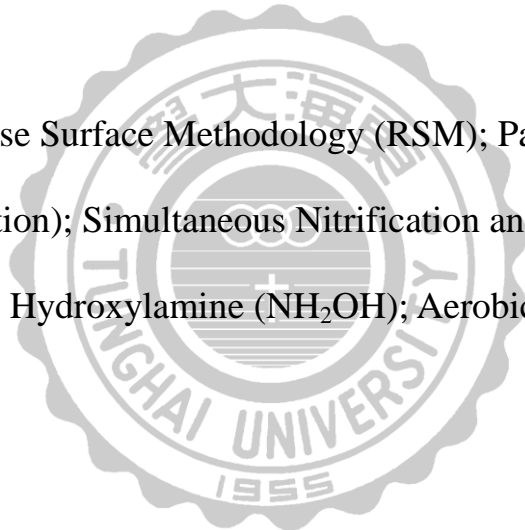
關鍵字: 反應曲面法、部分硝化、同時硝化脫硝、羥胺、好氧脫硝

Abstract

This study used recyclable materials which include wasted activated sludge, laterite and a combination of iron and sintered into pellet carrier from Futian water resource recycling center of Taichung City. The purpose was used response surface methodology (RSM) to determine the best pellet carrier ratio to rise compressive strength, water absorption, bulk density and specific external surface area, then remake of the particular materials as biological carrier molecules for sequencing batch biofilm reactor (SBBR) in order to achieve simultaneous nitrification and denitrification (SND). Two systems were added pellet carrier ratio of 40% and 60%, compared between the production amount of hydroxylamine (NH_2OH) and nitrite effect on these two systems with the same operating condition. Oxidation reduction potential (ORP) could detect the change by the Nernst Equation which was suitable for online monitoring model. Finally, biofilm of pellet carrier was used to do bacterial community analysis. The experiment resulted that the best pellet carrier ratio, sludge: laterite : iron oxide was 5:3:2, compressive strength was 46.1 ± 1.2 Kgf/cm², water absorption was $52.7 \pm 4.4\%$, bulk density was 2.2 ± 0.5 g/cm³, specific external surface area was 2.9 ± 0.2 m²/g, the experiment found in SBBR-60% system could lead most ammonium into nitrite about 5.7 mg/L, only produced few nitrate which below 1 mg/L that partial nitrification (nitritation) was speculated in the system, nitrification

rate (K_N) was 9.7 mg NH_4^+ -N/L-hr and denitrification rate (K_{DN}) was 9.5 NO_x^- -N/L-hr which were all better than SBBR-40% system. The phylogenetic tree analyzed that there were autotrophic nitrifier and heterotrophic denitrifier in the biofilm. Especially for aerobic denitrifier *Dokdonella immobilis* and *Acinetobacter sp.* were found in SBBR system. It demonstrated that denitrification reaction was activated during dissolved oxygen about 1-2 mg/L and nitrite was reduction to nitrogen gas in order to reach removal nitrogen effect in the SBBR system.

Keywords: Response Surface Methodology (RSM); Partial nitrification (nitritation); Simultaneous Nitrification and Denitrification (SND); Hydroxylamine (NH_2OH); Aerobic denitrifier



CONTENTS

Chapter 1 Introduction	1
1.1 Background information	1
1.2 Objective	3
Chapter 2 Literature Review	4
2.1 Wasted activated sludge (WAS)	4
2.1.1 Characteristic of WAS	4
2.1.2 Reuse of WAS as recycling material	5
2.2 Sintering theory	7
2.2.1 Foaming mechanism	10
2.3 Basics of immobilized-cell processes	11
2.3.1 Biofilm formation	11
2.3.2 Biofilm system	14
2.4 Biological nutrient removal (BNR)	15
2.4.1 Nitrification	15
2.4.2 Denitrification	16
2.4.3 Nitritation/denitritation	17
2.4.4 Simultaneous nitrification and denitrification (SND)	18
2.4.5 Nitrifier denitrification	19
2.4.6 Anaerobic ammonium oxidizing (Anammox)	20
2.5 Sequencing batch biofilm reactor (SBBR)	20
2.6 Nernst equation	23
2.7 Response surface methodology (RSM)	24
Chapter 3 Material and Methods	26
3.1 Experimental design and flow chart	26
3.2 Biofilm carrier produced from WAS	28
3.2.1 Source and characteristic of WAS	28
3.2.2 Toxicity characteristics leaching procedure (TCLP)	29
3.2.3 The procedure of manufacture the WAS pellets	30
3.3 The basic characteristics analysis of pellet	32
3.3.1 Water absorption	32
3.3.2 The particle size analysis	32
3.3.3 Compressive strength	33
3.3.4 Bulk density	33
3.3.5 Scanning Electron Microscope (SEM)	34
3.3.6 B.E.T analysis	34
3.3.7 Specific external surface area	34
3.4 The sequencing batch biofilm reactor (SBBR) system	36

3.4.1	Experiment set-up	36
3.4.2	Operation of SBBR	38
3.4.3	Composition of the synthetic wastewater	39
3.5	Analytical methods.....	41
3.5.1	Water quality analysis	41
3.6	Molecular community analysis of biofilm.....	43
3.6.1	Chromosomal deoxyribonucleic acid (DNA) extraction ..	43
3.6.2	DNA concentration and purity analysis	45
3.6.3	Agarose Gel Electrophoresis.....	45
3.6.4	Polymerase Chain Reactor (PCR).....	46
3.6.5	Denaturing Gradient Gel Electrophoresis (DGGE)	50
3.6.7	Sequencing analysis	54
3.6.7.1	Basic Local Alignment Search Tool (Blast).....	54
3.6.7.2	Phylogenetic Analysis	54
Chapter 4	Results and Discussion.....	55
4.1	The raw materials analysis.....	55
4.1.1	The basic characteristics of the raw materials	55
4.1.2	The TCLP of raw materials.....	57
4.2	The carrier pellet analysis.....	58
4.2.1	The characteristics of carrier pellet.....	58
4.2.2	The TCLP of carrier pellets.....	60
4.2.3	The composition and surface of the carrier pellets	61
4.3	The carrier pellets were applied for SBBR systems	63
4.3.1	The daily monitor profiles in SBBRs.....	63
4.3.2	Comparative profiles of two SBBRs	66
4.3.2.1	SBBR I (40% ratio).....	66
4.3.2.2	SBBR II (60% ratio)	67
4.3.3	Hydroxylamine produced in two SBBR systems	73
4.3.4	Biomass growth of two SBBR systems	74
4.4	Comparison of the K_N , K_{DN} and SND efficiency of two SBBR systems	77
4.5	Molecular biotechnology analysis	79
4.5.1	Bacterial community analysis at different SBBR systems by PCR-DGGE and cloning	79
4.5.2	Phylogenetic analysis.....	81
4.6	Nernst Equation Model Development in SND process	84
4.6.1	Nernst equation in the overall SND process.....	84
4.6.2	Nernst equation established in the SND process	

(ammonium and nitrite removal)	85
4.6.3 Nernst equation established in the SND process (ammonium removal).....	87
Chapter 5 Conclusions and Suggestions.....	89
5.1 Conclusions.....	89
5.2 Suggestion.....	90
Reference.....	91
Appendix	105
Appendix 1	105
Appendix 2.....	108



List of Figure

Figure 2-1 The granule agglutination response schematic drawing (a) Initial point contact; (b) Early stage neck growth; (c) Last stage neck growth; (d) Terminal condition fully coalesced spheres.	9
Figure 2-2 Schematic presentation of the formation of a biofilm.	13
Figure 2-3 Substances transportation in the biofilm for SND in SBBR.	14
Figure 2-4 Pathways of conventional nitrification/ denitrification and nitrifier denitrification via nitrite.	19
Figure 2-5 Typical sequencing batch reactor operation.	21
Figure 3-1 Flow chart of this study.	27
Figure 3-2 Flowchart preparation of pellet and analyze basic characteristic items.	31
Figure 3-3 Schematic diagram of the SBBR system with 40% (A) and 60% (B) ratios of pellets in the reactor. Both reactors were connected with on-line DO, pH and ORP sensor to a Lab VIEW® system in a personal computer to maintain the operational parameters.	37
Figure 3-5 Flow chart of the NH ₂ OH analysis (Peng, 2002).	42
Figure 4-1 Particle size distribution analysis of (a) WAS powder and (b) laterite powder.	56
Figure 4-2 Surface plot of compressive strength (CS), dry sludge and temperature from RSM analysis.	59
Figure 4-3 Surface plot of surface area, dry sludge and temperature from RSM analysis.	60
Figure 4-4 Surface of carrier pellet with the formula ratios of WAS: laterite: chemical additive are (a) 5: 3: 2 and (b) 5: 4: 1.	61
Figure 4-5 The SEM images of carrier pellets in this study and previous studies.	62
Figure 4-7 Concentration profiles of ammonium in the influent and effluent of SBBRs in this study. The daily profiles of ammonium in two types of system (SBBR with 40% and 60% filling ratio). The period of phase I (loading: 0.033 kg NH ₄ ⁺ -N/ m ³ -day) under 70 days, phase II (loading: 0.046 kg NH ₄ ⁺ -N/ m ³ -day) under 47 days and highest concentration was phase III (loading: 0.062 kg NH ₄ ⁺ -N/ m ³ -day) under 39 days, respectively.	65

Figure 4-8 Batch profiles of on-line measured parameters under three loadings with filling ratio of 40% in the SBBR system (a) DO, (b) pH and (c) ORP.....	69
Figure 4-9 Batch profiles of continuous monitoring under three loadings with filling ratio of 40% in the SBBR system (a) COD, (b) Ammonium, (c) Nitrite, (d) Nitrate, (e) Phosphate.....	70
Figure 4-10 Batch profiles of on-line measured parameters under three loadings with filling ratio of 60% in the SBBR system (a) DO, (b) pH and (c) ORP.....	71
Figure 4-11 Batch profiles of continuous monitoring under three loadings with filling ratio of 60% in the SBBR system (a) COD, (b) Ammonium, (c) Nitrite, (d) Nitrate, (e) Phosphate.....	72
Figure 4-13 Growth profiles of biomass in two SBBR systems in each pellet.	75
Figure 4-14 Total growth profiles of biomass in this study and previous study.....	75
Figure 4-15 DGGE profile of bacterial communities under different SBBR systems. 6% (w/v) polyacrylamide (acrylamide-bisacrylamide (37.5:1)) gel with a denaturing gradient of 30% to 50% and carried out in 1X TAE buffer at 250V for 8h at 60°C.	80
Figure 4-16 Phylogenetic tree of cloning from band of DGGE in two different SBBR systems. The phylogenetic tree of the interrelationship was constructed by using neighbor-joining method. Bootstrap replication values calculated from 500 times.	83
Figure 4-17 Comparison of simulation and experimental ORP profiles (ammonium and nitrite removal) for “only mix” and “mix and aeration” stages of SBBR system with filling ratio 60% carrier pellets.	86
Figure 4-18 Comparison of simulation and experimental ORP profiles (only ammonium removal) for “mix and aeration” stage of SBBR system with filling ratio 60% carrier pellets.....	88

List of Table

Table 2-1 Application of WAS in other literatures.	6
Table 2-2 Various types and temperatures of additives on overflowing gases.	10
Table 2-3 Comparison the treatment performance by using SBR and SBBR systems from other literatures.....	22
Table 3-1 The Regulation of heavy metal concentration of leaching.....	29
Table 3-3 Composition of stock synthetic wastewater in this study ¹	40
Table 3-4 Concentrations of three phase influent synthetic wastewater...	40
Table 3-5 Analytical methods and instruments used in this study.....	42
Table 3-6 Agarose gel percentage and efficient range of DNA separation.	46
Table 3-7 PCR primer used for amplification of bacterial 16S rDNA.	48
Table 3-8 Reagent and volume for PCR reaction.	49
Table 3-9 Heating program of PCR in this study.....	49
Table 3-10 Relationship between gel percentage and base pair separation.	51
Table 3-11 Reagent of 6% polyacrylamide gel of DGGE in this study....	51
Table 3-12 Reagent and volume of protocol for ligation using T&A TM cloning vector.	53
Table 3-13 LB medium for host cell growth and solution in cloning procedures.	53
Table 4-2 The TCLP tests for heavy metal concentration of Futian WAS and laterite.	57
Table 4-3 Comparison of the basic characteristics of the porous WAS pellets in this study and previous study.....	59
Table 4-4 The TCLP test for heavy metal concentration of the porous WAS pallets.....	60
Table 4-5 Comparison of removal concentration of different filling ratios in this study and other references.....	76
Table 4-6 Nitrification rate (K_N), denitrification rate (K_{DN}) and SND efficiency under different systems and comparison with other reported values.	78
Table 4-7 Results of regressive analysis on the Nernst equation for “only mix” and “mix and aeration” stages in two SBBR systems (ammonium and nitrite removal).	86
Table 4-8 Results of regressive analysis on the Nernst equation for “mix	

and aeration” stages in two SBBR systems (only ammonium removal).88



Chapter 1 Introduction

1.1 Background information

Wasted activated sludge (WAS) is generated from wastewater treatment plants (WWTPs) during the activated sludge process. There are more WAS produced in Taiwan in 2010, and the amount is increasing by an average rate of 5% every year (Huang and Wang, 2013). Sludge management is one of the main problems in WWTPs due to the large amount of sludge generated during the treatment process and the costs associated with its disposal. WAS has mainly been disposed of using two methods: landfilling and soil application (Sanchez-Monedero *et al.*, 2004; Kim *et al.*, 2005). Currently, the cost of disposing the WAS in Taiwan is reaching \$4,500 – 6,000/ton. Therefore, the present conception is to develop an effective process to minimize and reuse WAS in order to resource recovery. This way will save treatment cost and decrease the secondary pollution.

For a large number of WAS, some studies have been confirmed the reuse of processed WAS for lightweight aggregates, bricks, ceramics and carrier (Kim *et al.*, 2003; Cusido and Soriano, 2011; Tuan *et al.*, 2013). Sintering is the bonding of particles in a mass of powders by molecular or atomic attraction in the solid state, by application of heat, causing strengthening of the powder mass and possibly resulting in densification and recrystallization by transport of materials (Upadhyaya, 2001). In order to obtain the desired microstructure and final properties of solids, since improving their mechanical properties of hardness, strength, wear resistance and toughness (Chinelatto *et al.*, 2014). The main factors affect the sintering processes include: particle size distribution, chemical composition, temperature, forming pressure and react time (Tay and Yip,

1989; Volland *et al.*, 2014).

The response surface methodology (RSM) is a method to conduct minimal tests to find out the critical elements that affect the results and can reduce the time of trial and cost (da Silva *et al.*, 2001; Shahabadi and Reyhani, 2014). Besides, it can not only test the differences between various levels of each factor, but also test the interaction between the factors (Yi *et al.*, 2011). Hence, this approach had been used to gain an optimal formula to assemble the porous WAS pellets with the requirement characteristics of enough porosity and compressive strength to reuse as immobilized material.

Many types of high-performance biological treatment reactors have been developed which are characterized by a when compared to conventional wastewater treatment plants, as well as compact construction and an operation favorable to the environment have been developed. The sequencing batch biofilm reactor (SBBR) system has attracted a great deal of attention due to its ability to take advantages of both a biofilm reactor and a sequencing batch reactor (SBR) (Ding *et al.*, 2011). Besides, it has many advantages over traditional activated sludge system. SBBR not only retain the biomass in reactor but also reduce the waste sludge discharge. Simultaneous nitrification and denitrification (SND) is simultaneous heterotrophic nitrification and aerobic denitrification where both nitrification and denitrification are achieved simultaneously under reduced aeration and hence the controlling of aerobic and anaerobic consortia is not required (Kulkarni, 2013). SND process has some advantages such as decreases cost and reduces waste sludge discharge. This study will apply the rebuilt WAS pellets to set up SBBR system. Due to WAS contains the trace inorganic substance which provides additional nutrient for the biofilm attached to the surface of the

immobilized cells.

1.2 Objective

This study employs the rebuilt pellets to attach biofilm on pellets and places in the SBBR system to remove ammonium with synthetic wastewater, and then has tried to compare the performance of different pellets ratio and analysis of microbial biofilm to investigate the pathway of SBBR system. Finally, this study establishes a Nernst equation of model to simulate the entire reaction for expectation to control the status of reaction in the future.



Chapter 2 Literature Review

2.1 Wasted activated sludge (WAS)

After treating industrial or municipal wastewater, large quantities of waste activated sludge (WAS) were produced, and the WAS treatment and disposal (i.e., sanitary landfill, incineration, composting) was expensive (Weemaes *et al.*, 2000) and took up to approximately 60% of the overall wastewater treatment plants (WWTPs) cost (Saby *et al.*, 2002). In Taiwan, the annual sludge (dewatered) production from 34 industrial wastewater treatment plants was approximately 0.67 million tons. In general, the dried sludge had higher heavy metal content than that of the dewatered sludge (Weng *et al.*, 2003). Sanitary landfill and incineration were major disposed of excessive WAS. Sanitary landfills required wide land to dispose WAS in Taiwan, quick urbanization had made it increasingly difficult to discover suitable landfill site (Lin and Weng, 2001). The incineration could significantly decrease the quantity of WAS, however this treatment method required supplementary fuel to make sure the WAS burn completely (Dewil *et al.*, 2005). Therefore, WAS management would be moving towards reutilization and minimization of sludge as useful resources.

2.1.1 Characteristic of WAS

Many literatures have reported more than 50% of fly ash existed in WAS. Due to the ash consisted trace of heavy metal, hence one of the earliest used investigated was as raw material for the manufacture of bricks and tiles (Donatello and Cheeseman, 2013). The characteristic of WAS were not the same from different WWTP, and therefore this study selected the wasted sewage sludge to reuse. The WAS was often dewatered by the sludge dewatering machine to reduce moisture content

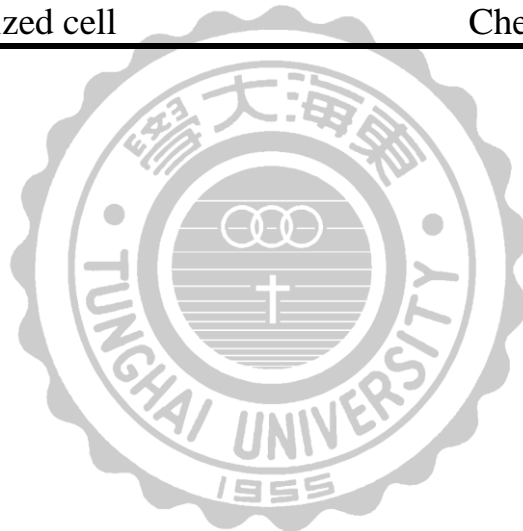
of WAS. But some factor like particle surface charge and hydration, particle size, compressibility and sludge pH etc. which would affect the dewatering efficiency (Chen, 2008). The WAS contained over moisture would increase the cost and energy consumption of WWTPs. Besides, WAS main components included suspended solids, organic matter, Fe-Al hydroxide, water and coagulant. The main chemical compounds of sludge and its ashes were Al_2O_3 , SiO_2 , Fe_2O_3 , and CaO (Fang *et al.*, 2015). Due to sludge consisted of major element Si, Al, Ca and Fe and so these qualities agreed with resource recovery that developed to manufacture the useful material (Hamer and Karius, 2002; Lafhaj *et al.*, 2008).

2.1.2 Reuse of WAS as recycling material

The WAS had to be pre-treated to stabilize, disinfect and reduce volume before it was reused. In recent years, a number of studies have been carried out to investigate the reuse of WAS as some useful material such as the lightweight aggregate, clay ceramics or biological treatment process carrier (Kim *et al.*, 2003; Weng *et al.*, 2003; Cusido and Soriano, 2011; Volland *et al.*, 2014; Volland and Brötz, 2015). Some literatures have been reused the WAS minimization and reutilization were shown in Table 2-1. This study would attempt to reuse the WAS as biological treatment process carrier that possessed high porosity and compressive strength for reusing. Among cell immobilization methods, passive immobilization (bio-film on surfaces) and entrapment (cell trapping in porous space of carrier) have been used in the bioreactor (Rafiei *et al.*, 2014). Besides, the reused porous carrier in bioreactor could enhance the wastewater removal efficiency by increasing the biomass in a sequencing biofilm batch reactor (SBBR).

Table 2-1 Application of WAS in other literatures.

The purpose of reutilization	References
Biofilm carrier	This study
Immobilized pellets and air diffuser	Su (2008)
Lightweight aggregate	Volland and Brötz (2015)
Lightweight aggregate	Volland <i>et al.</i> (2014)
Micro-media	Kim <i>et al.</i> (2003)
Brick	Lin and Weng (2001)
Cement	Xu <i>et al.</i> (2014)
Ceramic	Wolff <i>et al.</i> (2015)
Immobilized cell	Chen (2005)



2.2 Sintering theory

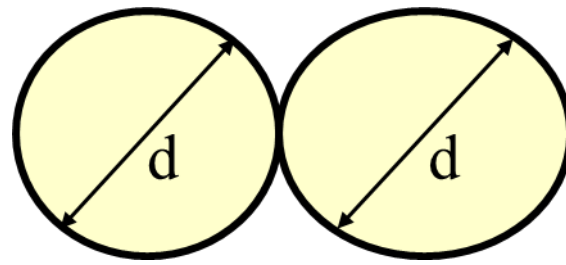
Sintering was a thermal treatment for bonding particles into a coherent, predominantly solid structure via mass transport events that often occur on the atomic scale in the physical phenomenon. The bonding leads to improved strength and lower system energy. The sintering reaction was heated under the melting point of raw materials and rearranged the internal structure of materials up to high-strength, high-density of sintered body (Li *et al.*, 2009).

1. Solid-state sintering: applied surface diffusion, lattice diffusion, boundary diffusion or solid material with the surrounding atmosphere was reaction of the mass transfer.
2. Sintering by viscous flow: Sintering was caused by the flow of non-crystalline material, viscous flow sintering mechanism of sintering as the main environment in silicate (Skrifvars *et al.*, 1994). Viscous flow sintering would form the airtight pore, the reason for the liquid surface into the boundary of lattice was diffusion and then contraction (Nowok *et al.*, 1990).
3. Liquid phase sintering: applied the fusion and solid precipitation to increase particle size and density. The process of liquid phase sintering had three stages: rearrangement, solution-precipitation and final densification.

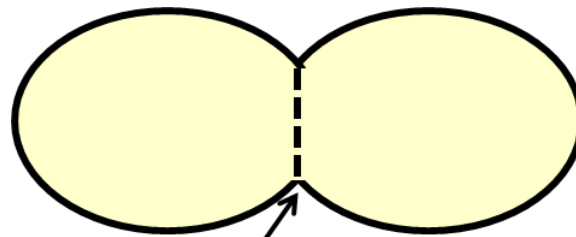
The factors of affecting sintering were sintering temperature, the time of heating, chemical composition, forming pressure and size distribution.

German (1996) built the mechanism of sintering model which was divided into four steps sintering in Figure 2-1. The four steps included initial point contact, early stage neck growth, last stage neck growth and terminal condition full coalesced spheres. German thought the mechanism of sintering that started at the point between particles to contact and then the neck growth. The new grain boundary was formed between the particles under the sufficient reaction time and then two particles were integrated into a single particle.



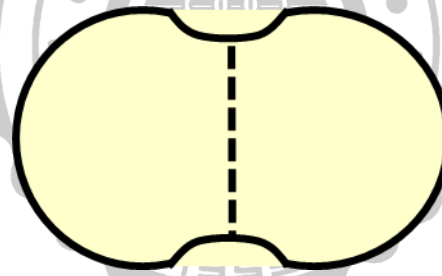


(a) Initial point contact

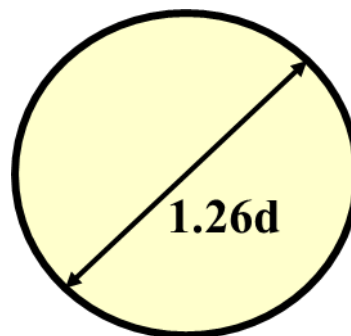


neck

(b) Early stage neck growth



(c) Last stage neck growth



(d) Terminal condition fully coalesced spheres

Figure 2-1 The granule agglutination response schematic drawing (a) Initial point contact; (b) Early stage neck growth; (c) Last stage neck growth; (d) Terminal condition fully coalesced spheres.

2.2.1 Foaming mechanism

Foaming phenomenon was between the softening point and maximum heating temperature to heat the raw material. Foaming needed some special composition, such as amphetamine sulfate, carbonate, oxide and organic wastes so as to release gases to form a cell nest structure (Kose and Bayer, 1982; Bhattu and Redit, 1989). The viscosity and gas production were two important conditions on expansion or foaming phenomenon in raw materials. If raw material without the above-mentioned conditions, it had to add additives to make the above two points occurred. Although the expansion was a factor of affection for foaming mechanism, but after heating might not be production the enough gases to cause swelling effect. Table 2-2 listed the various types of chemical composition and temperature of overflowing gases.

Table 2-2 Various types and temperatures of additives on overflowing gases.

Chemical equation	Reaction temperature (°C)
$\text{FeS}_2 + \text{O}_2 \rightarrow \text{FeS} + \text{SO}_2 \uparrow$	350 - 450
$4\text{FeS} + 7\text{O}_2 \rightarrow 2\text{Fe}_2\text{O}_3 + 4\text{SO}_2 \uparrow$	500 - 800
$\text{Fe}_2(\text{SO}_4)_3 \rightarrow \text{Fe}_2\text{O}_3 + 3\text{SO}_3 \uparrow$	560 - 775
$\text{MgCO}_3 \rightarrow \text{MgO} + \text{CO}_2 \uparrow$	400 - 900
$\text{Na}_2\text{CO}_3 \rightarrow \text{Na}_2\text{O} + \text{CO}_2 \uparrow$	>400
$\text{CaCO}_3 \rightarrow \text{CaO} + \text{CO}_2 \uparrow$	600 - 1,050
$\text{CaSO}_4 \rightarrow \text{CaO} + \text{SO}_3 \uparrow$	1,250 - 1,300
$6\text{Fe}_2\text{O}_3 \rightarrow 4\text{Fe}_3\text{O}_4 + \text{O}_2 \uparrow$	1,000 - 1,550

2.3 Basics of immobilized-cell processes

2.3.1 Biofilm formation

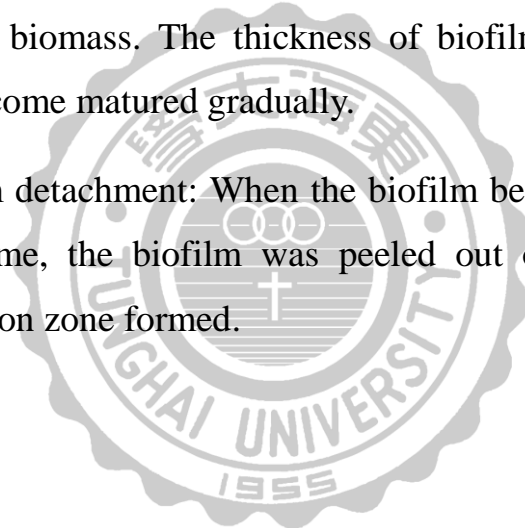
Nowadays, there are many systems for selecting to treat different characteristic of wastewater. However, immobilized bioreactor systems were confirming to be better alternatives to the conventional suspended growth bioreactor systems. The advantages are easy operation in continuous flow, lower cell losses, improved physical and chemical stability of the biocatalyst, lower power requirements and the ease with which the cells can be reused (Mudliar *et al.*, 2008). Various immobilized bioreactor configurations such as horizontal and vertical packed beds, fluidized beds and rotating biological contactor (RBC) have been reported (Das *et al.*, 2002).

The formation of biofilm could be divided into suspended-growth and attached-growth systems. The former was the microbial remained suspended such as activated sludge and the latter was microbial attached to the inert medium to form the local high-density of biofilm. Microorganisms universally attached to surfaces and produce extracellular polysaccharides, resulting in the formation of a biofilm. Organisms within biofilms can withstand nutrient deprivation, pH changes, oxygen radicals, disinfectants, and antibiotics better than planktonic organisms (Jefferson, 2004). In this study, the rebuilt pellets were utilized as bio-carriers to form the biofilm in the bioreactor system. The bioreactor was made up of support material and attached growth biomass. Figure 2-2 showed the biofilm systems were complicated as a result of a combination of factors, such as bacterial growth, substrate consumption, attachment, external-internal mass transfer of substrate and products, cell death, shear loss (biofilm loss because of erosion),

sloughing (fragments disrupting from the film), structure of the support material, competition between bacterial species, and effects of predators (Wijffels and Tramper, 1995).

The biofilm formation processes included as follows:

- (1) Microbial attachment: Microorganisms in the bulk liquid were attached onto the surface of support material (bio-carriers).
- (2) Substrate adsorption: Substrate adsorbed into the support material.
- (3) Attached growth biomass: Substrate utilized with the attached growth biomass. The thickness of biofilm can be increased and become matured gradually.
- (4) Biofilm detachment: When the biofilm become matured for a long time, the biofilm was peeled out owing to the inner starvation zone formed.



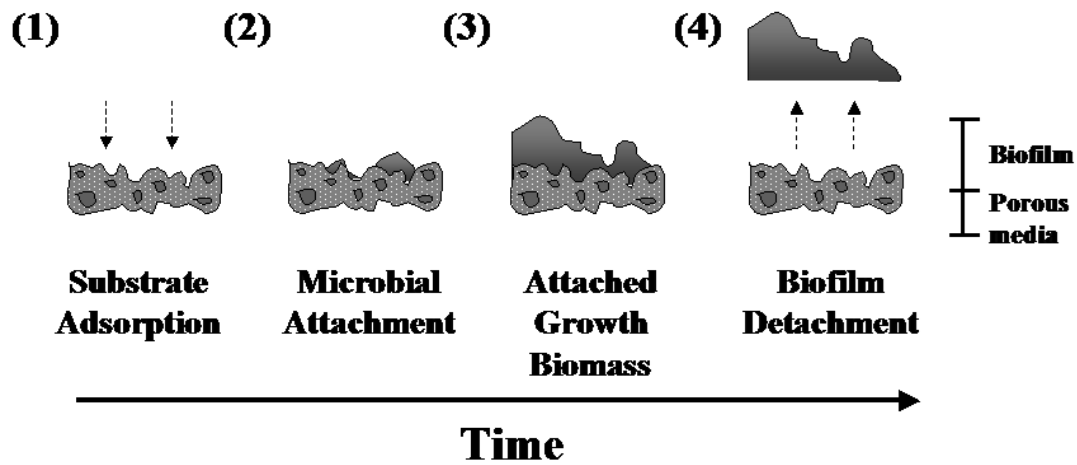


Figure 2-2 Schematic presentation of the formation of a biofilm (Wijffels and Tramper, 1995).

The immobilized system compared with traditional activated sludge system had main advantages as follows (Chiu *et al.*, 2007; Daniel *et al.*, 2009):

1. Without the need for external carbon source dosage.
2. Has a higher load capacity.
3. Lower sensitivity to toxicity effects, as well as to other adverse environmental conditions.
4. Reduce operating costs and expenses.
5. Elimination of long sludge-settling periods.

2.3.2 Biofilm system

Biofilm system was the common biological process for the polluted water treatment. Conventional biofilm treatment always used plastic carriers, which were only for biofilm support (Feng *et al.*, 2015). But in this study that used rebuilt WAS pellet for providing biofilm support and inorganic matters. The biofilm could bear a great potential for the simultaneous removal of organic matters and nutrients, such as nitrogen and phosphate in the biofilm system (Duan *et al.*, 2013). Figure 2-3 showed the biofilm was aerobic on the surface, anoxic zone was in the middle and anaerobic zone was at the point of attachment to the pellet. The concentration gradients of dissolved oxygen (DO) and organic matters were similar, being highest at the external surface of the biofilm and lowest at the surface of pellet (Semmens *et al.*, 2003). The diffusion reaction theory indicated that the growth rate of biofilm was dependent on substrate loading rate applied to the biofilm system. Hence, the substrate loading rate might represent the capability of biofilm growth, and could be regarded as the growth force of biofilm culture (Liu *et al.*, 2003).

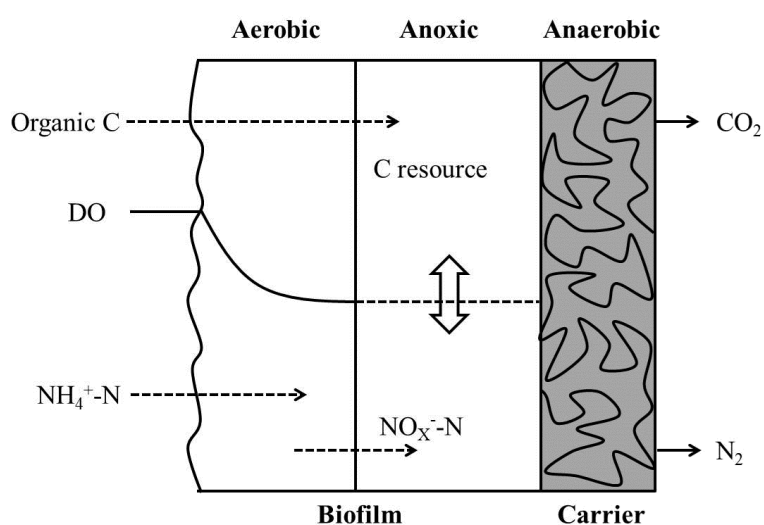


Figure 2-3 Substances transportation in the biofilm for SND in SBBR

(Zhu *et al.*, 2007).

2.4 Biological nutrient removal (BNR)

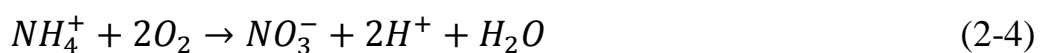
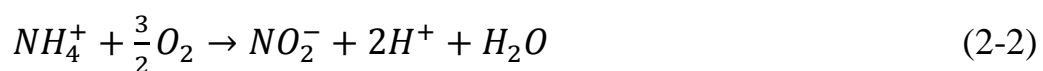
Biological nutrient removal (BNR) involved transformations and removal of inorganic nitrogen (ammonium and nitrogen oxide) by biomass synthesis and sludge wasting, and nitrification (ammonium oxidation to nitrite and nitrate) and denitrification of nitrate and/or nitrite to nitrogen gas (Czerwionka *et al.*, 2012). In a traditional BNR activated sludge system, mixed fill was comparable to the anoxic zone that was used for denitrification. Anaerobic conditions could also be achieved during the mixed fill phase. After the micro-organisms used the nitrate nitrogen, sulfate became the electron acceptor. Anaerobic conditions were characterized by the lack of oxygen and sulfate as the electron acceptor.

2.4.1 Nitrification

Nitrification is a two-step sequencing biological oxidation process (2-1). The nitrification that ammonium (NH_4^+) oxidation to nitrite (NO_2^-) (2-2) is the limiting step carried out by ammonium oxidizing bacteria (AOB), while the nitrification that nitrite is oxidized to nitrate (NO_3^-) (2-3) rapidly by nitrite oxidizing bacteria (NOB), in the presence of molecular oxygen (Henze *et al.*, 2008).



The complete nitrification reaction showed as (2-2), (2-3) and (2-4).



Oxygen was required as electron acceptor and under aerobic condition with the autotrophic bacteria, such as *Nitrosomonas* and *Nitrobacter* in the nitrification reaction (Siripong and Rittmann, 2007). Some factors affected the nitrification reaction, i.e., pH, DO and temperature. When nitrification proceeded, the alkalinity was consumed by hydrogen ion released and caused the pH to reduce. The optimal pH values were between 7 and 8.5 (Guo *et al.*, 2009). Another important issue was aeration, which must be adjusted to provide enough DO for nitrification ($3.16 \text{ g O}_2/ \text{ g NH}_4^+$) but avoiding unnecessary energy consumption. Besides, the sludge retention time (SRT) was one of the key parameters for nitrification because autotrophic nitrifying bacteria grow slowly compared with heterotrophic microorganisms and must be maintained in the system to obtain high nitrification efficiencies (Ruscalleda Beylier *et al.*, 2011).

2.4.2 Denitrification

Denitrification converted nitrate (NO_3^-) and nitrite (NO_2^-) to nitrogen gas. However, nitrate existed in drinking water or groundwater would cause public health problems, such as the Blue Baby Syndrome in infants, where nitrate bound with hemoglobin, was one of the best-known and most serious threats (Fan and Steinberg, 1996).

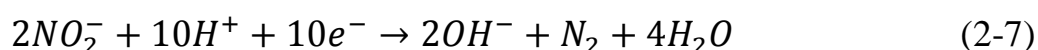
The denitrifiers bacteria needed organic matters and carry out denitrification process under anoxic environment in the traditional denitrification. Denitrifier bacteria would utilize nitrite and nitrate instead of oxygen as terminal electron acceptors. Besides, the organic carbon played the role of electron donors in the meantime. Therefore, the availability of organic carbon was one of the most important factors influencing denitrification. If organic carbon did not be enough for

electron donors, the denitrification would be inhibited. The denitrification reaction was following (2-5):



2.4.3 Nitritation/denitritation

In recent years, novel biological systems have been developed which were different from convention biological nitrification/ denitrification. These systems performed partial nitrification (nitritation) which converted ammonium to nitrite and stopped at this stage, followed directly by reduction to nitrogen gas (denitritation) in anoxic condition (Queiroz *et al.*, 2011). Nitritation/ denitritation were an economy of total energy consumption which saved 25% of oxygen demand, in comparison with the complete nitrification (2-2) and (2-4). Besides, the denitritation reduced the 40% reduction of organic matters demand, in comparison with denitrification (Jenicek *et al.*, 2004; Queiroz *et al.*, 2011). The denitritation and denitrification reaction were following (2-6) and (2-7), respectively:



The key to achieve nitritation/ denitritation that ammonium oxidation bacteria (AOB) must to become the dominant nitrifying bacteria while nitrite oxidation bacteria (NOB) need to be inhibited (Regmi *et al.*, 2014). Furthermore, the other factors affecting nitritation which included temperature (above 25 - 35°C), concentration of free ammonia (FA) and free nitrous acid (FNA), low dissolved oxygen (DO) concentration and pH (Zeng *et al.*, 2010).

2.4.4 Simultaneous nitrification and denitrification (SND)

As mentioned previously, the nitrification and the denitrification processes were usually carried out separately in aerobic and anoxic compartments, respectively. In the last decade, the nitrogen loss and simultaneous nitrification and denitrification (SND) in step feeding process were reported by Zhu *et al.* (2005). Many studies have revealed that nitrification and denitrification can also occur concurrently in the same reactor. This phenomenon is called SND.

SND eliminated the need for a separate denitrification tank and mixed liquor recycle (Zhu *et al.*, 2007). The SND process divided into two categories; pure-culture and mixed-culture systems. Pure-culture system implied the SND reactor had only one bacterium which could achieve nitrification and denitrification consecutively. Some bacteria could accomplish this process such as *Nitrosomonas europaea* and *Paracoccus denitrificans* (Stuven and Bock, 2001). However, the pure-culture had a good performance of the nitrogen removal, but pure-culture was strictly limited to apply to the small-scale and was difficult to apply in the field. Hence, the mixed-culture system was concentrated on improving the field SND treatment process.

The biodegradable organic matter availability in the deep biofilm regions and the DO concentration gradients were the two main parameters affecting SND performance. The DO limitation was 0.5 to 1.5 mg/L for SND (Chiu *et al.*, 2007). Due to the rate of nitrification was much faster than that of denitrification, so a balance controlled reaction system will insure the consecutively processes work smoothly. If DO concentration was too low that could decrease nitrification reaction rate and furthermore inhibit the denitrification process. SND was more cost

effective with respect to the conventional process in separate aerobic and anoxic tanks because the C-source consumption was 22–40% lower and the sludge yield was reduced by 30% (Sun *et al.*, 2010). The optimal C/N ratio for SND was calculated at 11.1, where the nitrification and denitrification reactions were in balance (Chiu *et al.*, 2007). Nitrification in SND could consume 8.64 g CaCO₃/ g NH₄⁺-N alkalinity in the reactor; while the denitrification reaction would produce 3.6 g CaCO₃/ g NO₃⁻-N alkalinity and maintain pH in the solution. Due to the alkalinity demand for nitrification was partially compensated for by the inorganic carbon released during denitrification, and the dependence on a pH control was reduced (Ruscalleda Beylier *et al.*, 2011).

2.4.5 Nitrifier denitrification

In nitrifier denitrification, the oxidation ammonium to nitrite was directly followed by the reduction of nitrite to nitrous oxide and nitrogen gas. The pathway of conventional nitrification/ denitrification and nitrifier denitrification reaction was followed Figure 2-4. Nitrifier denitrification contrasted with nitrification-denitrification, where different groups of coexisting microorganisms could together transform ammonium to finally nitrogen gas (Wrage *et al.*, 2001).

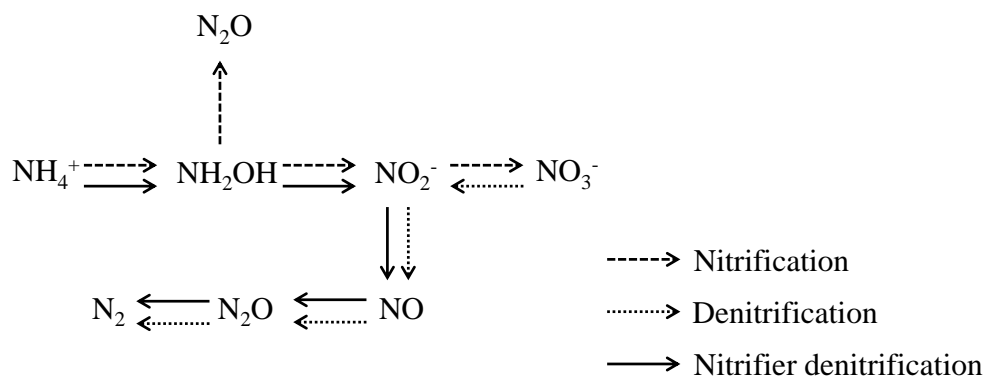


Figure 2-4 Pathways of conventional nitrification/ denitrification and nitrifier denitrification via nitrite (Wrage *et al.*, 2001).

2.4.6 Anaerobic ammonium oxidizing (Anammox)

The anaerobic ammonium oxidizing (Anammox) bacteria was a chemical autotrophic utilized inorganic carbon as carbon source which reduce operating costs compared with traditional nitrification and denitrification. Anammox was capable of ammonium oxidation with nitrite as terminal electron acceptor (Ma *et al.*, 2015). In the anammox process, about half of the ammonium oxidized to nitrite (nitrification) with nitrogen removal rates in the range 0.50-7.1 kg N/m³/d (Joss *et al.*, 2009; Kampschreur *et al.*, 2009) that had noticeable reductions in oxygen consumption and to an increase in biogas production (Siegrist *et al.*, 2008). However, Anammox bacteria had a slow growth rate was approximately 10-14 d and a high sensitivity to changing environmental conditions, which made them extremely difficult to cultivate (Ni and Meng, 2011). That caused application of the Anammox process had been restricted by the growth characteristics of the Anammox bacteria (Jin *et al.*, 2012a).

2.5 Sequencing batch biofilm reactor (SBBR)

The sequencing batch reactor (SBR) was a fill-and-draw activated sludge system for wastewater treatment. In an SBR system, wastewater was added to a single batch reactor, treated to remove undesirable components, and then discharged. SBR systems have been successfully used to treat both municipal and industrial wastewater. The sequencing series for treatment consists of the following process stages: fill, react, settle, decant and idle (Figure 2-5).

The sequencing batch biofilm reactor (SBBR) was packed with carriers covered with biofilm and operated based on a SBR. Few reports have been found on the SND when real wastewater used in the SBBR (Jun *et al.*, 2007). Besides, the SBBR system had attracted a great deal of attention due to its ability to take advantages of both a biofilm reactor and a SBR.

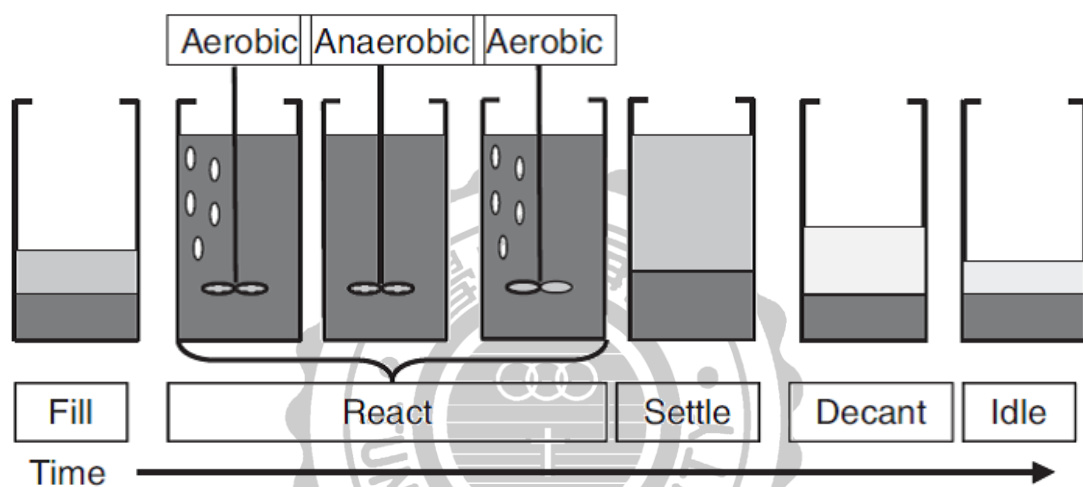


Figure 2-5 Typical sequencing batch reactor operation (Boopathy *et al.*, 2007).

The SBBR systems showed improved biomass concentration in reactors with corresponding higher specific removal efficiencies, greater volumetric loads, increased process stability toward shock loadings and are capable of covering small areas (Ding *et al.*, 2011).

Table 2-3 showed the comparison treatment performance by using the SBR and the SBBR systems from other literatures. There were different kinds of wastewater treated by using SBR and SBBR systems to provide a satisfactory effluent water quality.

Table 2-3 Comparison the treatment performance by using SBR and SBBR systems from other literatures.

Reactor	Wastewater source	Removal efficiency (%)			Reference
		COD	NH ₄ ⁺ -N	TP	
SBBR	Municipal	97.6	94.4	97.2	Jin <i>et al.</i> (2012b)
	Swine	98.2	95.7	96.2	Hai <i>et al.</i> (2015)
	Domestic	96.0	99.0	100	Ding <i>et al.</i> (2011)
	Domestic	95.0	94.0	97.0	Yin <i>et al.</i> (2015)
SBR	Synthetic	86.0	83.0	92.0	Tsuneda <i>et al.</i> (2006)
	Swine	82.0	100	20.1	Won and Ra (2011)
	Municipal	93.5	88.3	97.5	Ghehi <i>et al.</i> (2014)
	Municipal	94.0	93.0	79.0	Bagheri <i>et al.</i> (2015)

2.6 Nernst equation

Nitrification and denitrification in the biological nitrogen removal process which was an oxidation-reduction reactions during which electron were transferred from the reducing agent to oxidizing agent until the reaction reaches equilibrium. The electrochemical potential between the reducing and the oxidizing agents was known as the oxidation-reduction potential (ORP), which measured the net potential of the system (Weissenbacher *et al.*, 2007). Recently, many wastewater treatments used real-time control to monitor the water quality that not only improved effluent quality but also decreased excessive energy consumption. Therefore, many literatures pointed out that used the measured on-line ORP could provide better control of the reaction in the bioreactor (Ga and Ra, 2009; Won and Ra, 2011). The measured ORP value in biological system was correlated to the concentration changing of the reductive and the oxidative species represented in a Nernst equation (Chiang *et al.*, 2006). The general Nernst equation was shown in (2-8):

$$E = E^0 + \left(\frac{RT}{nF}\right) \ln\left(\frac{[Oxi]}{[Red]}\right) \quad (2-8)$$

where:

E = ORP (mV)

E^0 = standard ORP for the given oxidation-reduction process (mV)

R = gas constant (8.314 J mol⁻¹K⁻¹)

T = absolute temperature (K)

N = number of electrons transferred in the reaction

F = Faraday constant (96,500 C mol⁻¹)

[Oxi] = Concentration of oxidizing agent

[Red] = Concentration of reducing agent

Chang *et al.* (2004) used on-line measured data (e.g. ORP) and nitrogen compounds (e.g. ammonium, nitrite and nitrate) in the reactor to substitute terms in Nernst Equation. Deduced Nernst equation could be used to comprehend the nitrification and denitrification conditions in reactor. ORP value of any degree conversion of reactants to products in reactor can be precisely calculated (appendix 1). Therefore, on-line control strategy could effectively utilize in the bioreactor system.

2.7 Response surface methodology (RSM)

In statistics, response surface methodology (RSM) explored the relationships between several explanatory variables and one or more response variables. The main idea of RSM was to use a sequence of designed experiments to obtain an optimal response. This model was only an approximation, but used it because such a model was simple to calculate and apply, even when little was known about the process.

MINITAB[®] 14 was statistical software used to analysis the optimal analysis of operation factors (Gunawan *et al.*, 2005). Chose the major factors and after the test, a response surface and contour plot was obtained which would display the optimal operation zone for the following study.

In order to correlate the dependent variables and independent variables with the minimum possible number of experiments, a central composite design for two factors has been used. The total number of experiments (N) required for two independent variables was determined by (2-9).

$$N = 2^K + 2K + n_c \quad (2-9)$$

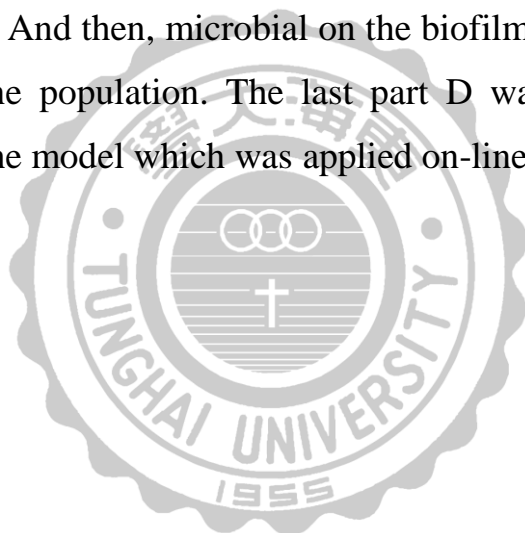
Where K represents the number of independent variables, in the present study, K=2 and n_c was the center point. The data were analyzed using MINITAB® 14 statistical software. Three replications of center point were selected for center composition design and totally, 11 experiments were predicted by the software.



Chapter 3 Material and Methods

3.1 Experimental design and flow chart

In this study, frameworks had been built for 4 parts (Figure 3-1). First part A, after materials collection had been carried out which carrier was made for applicable SBBR systems and test the basic characteristic. Second part B, the carriers in different ratio of volume for each system was attached by biofilm in process of culturing sludge. Influent loading had three phases from low level to high level. Third part C, influent and effluent of water qualities were analyzed every day and assessed the efficiency of SND. And then, microbial on the biofilm would be analyzed so as to realize the population. The last part D was to utilize Nernst equation to build the model which was applied on-line monitored.



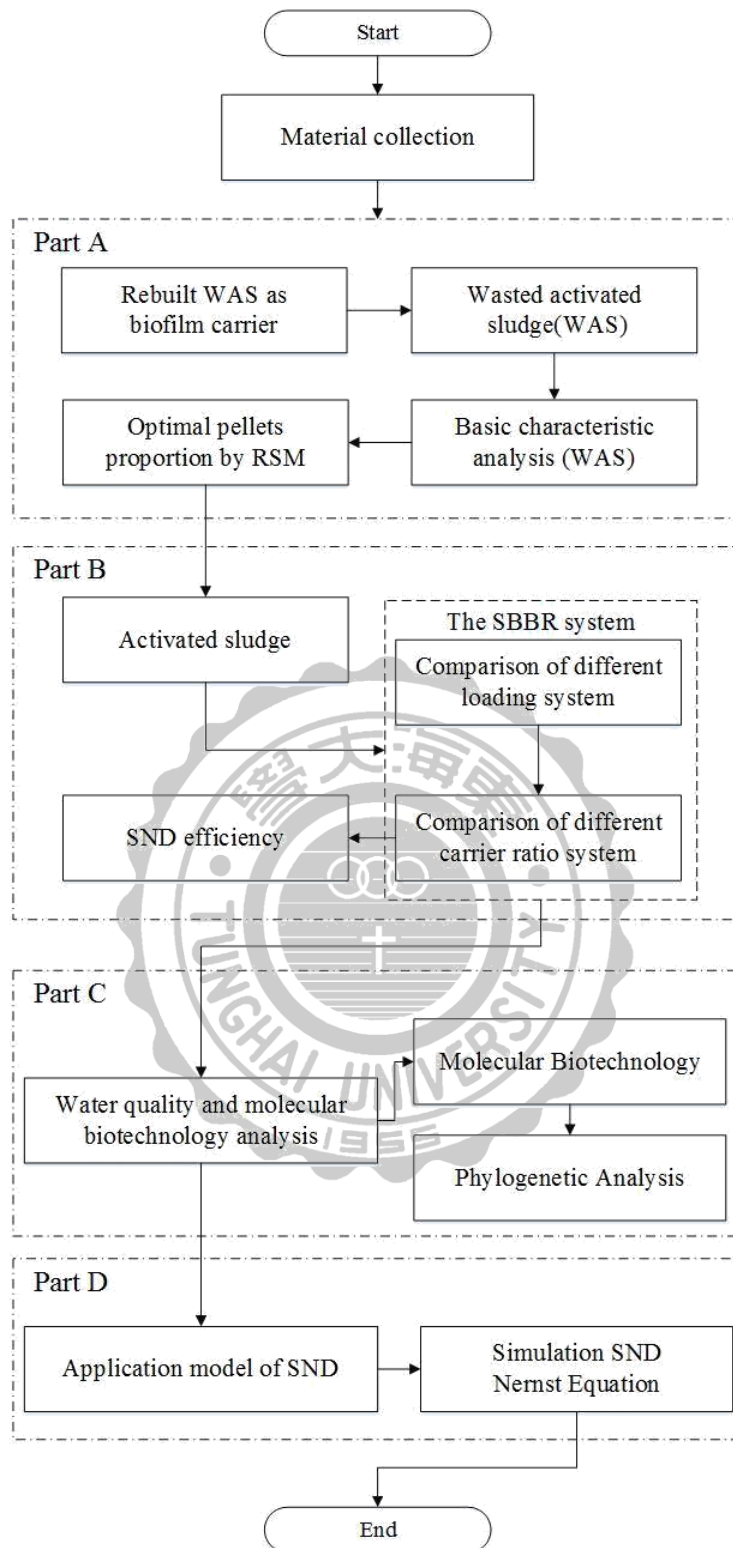


Figure 3-1 Flow chart of this study.

3.2 Biofilm carrier produced from WAS

3.2.1 Source and characteristic of WAS

The WAS was collected from Futian water resource recycling center of Taichung City which treated 55,000 CMD domestic wastewater from downtown Taichung City and produced 327 tons sludge cake daily. The wasted sludge was collected from digester, which contained 80% of moisture. The WAS was dried at 105°C for two days before sintering. The ash content of WAS was measured after baking sludge under 800°C for three hours (NIEA R205.01C). The formula of the moisture, ash and flammable contents in WAS were shown in (3-1), (3-2) and (3-3).

$$M (\%) = (W_1 - W_2) / W_1 \times 100\% \quad (3-1)$$

$$A (\%) = W_3 / W_1 \times 100\% \quad (3-2)$$

$$F (\%) = 100\% - M - A \quad (3-3)$$

where:

M : Moisture content

A : Ash content

F : Flammable content

W₁ : weight of sample before dried in the oven (25°C)

W₂ : weight of sample dried at 105°C

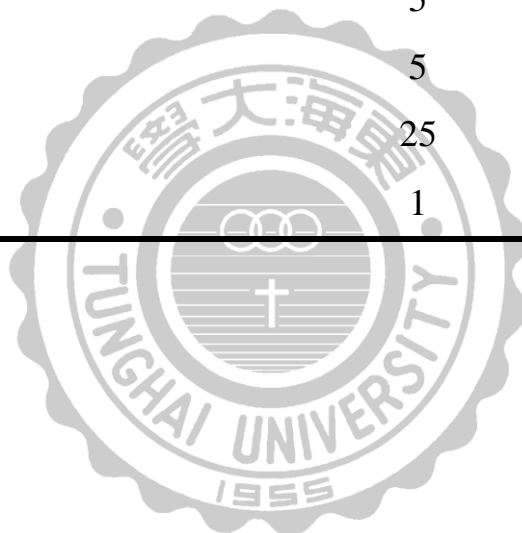
W₃ : weight of sample burned at 800°C

3.2.2 Toxicity characteristics leaching procedure (TCLP)

The WAS from the domestic wastewater plant may contain trace heavy metals. Therefore, WAS would be free from toxicity as determined by using the leaching test before rebuilt pellets. Five toxic heavy metals (Cu, Pb, Cr, Zn and Cd) were analyzed and all were found below the restriction (NIEA R201.14C).

Table 3-1 The Regulation of heavy metal concentration of leaching.

Element	Regulation of TCLP from heavy metal (mg/L)
Cu	15
Pb	5
Cr	5
Zn	25
Cd	1



3.2.3 The procedure of manufacture the WAS pellets

The process of rebuilding the WAS to the biofilm carrier which mixed the WAS, laterite and chemical additive (iron (III) oxide). The three raw materials were mixed after drying at 105°C in oven for three days. The laterite helped the WAS to shape into pellet and the chemical additive generated foam agent to increase the hardness. The tiny powder could enhance the structure strength of pellet after sintering.

The mix formula of WAS and laterite were designed by MINITAB[®]. Application RSM tested every design proportion then tried error found out the optimal formula. First, the pellets had to air-dry and then to bake after air-drying. Finally, the pellets were baked in a programmable furnace under the temperature raised from 200°C to the final temperature of 1000°C thereafter. The total time of sintering was 6.6 hours (400 min). After sintering, those pellets cooled down to the room temperature (25°C). The method of manufacture of the pellet was shown in Figure 3-2.

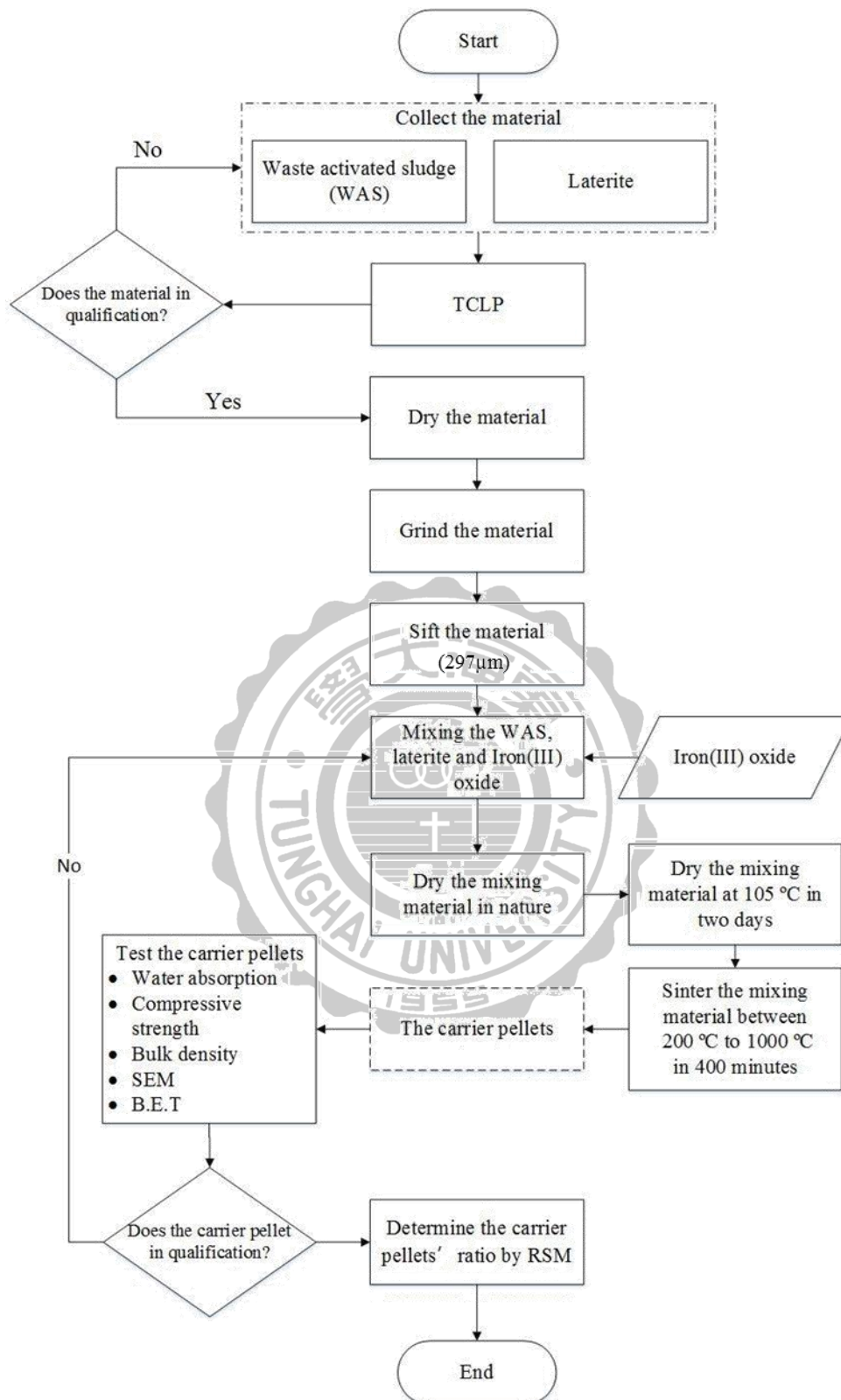


Figure 3-2 Flowchart preparation of pellet and analyze basic characteristic items.

3.3 The basic characteristics analysis of pellet

3.3.1 Water absorption

In physical characteristics of the porous pellet, the water absorption was measured by the reference density measurement (Cheeseman *et al.*, 2003). The water absorption testing was following the Chinese National Standard (CNS-487). The sample was immersed in 23°C water for 24 hours, and then removed out the water. The surface water of sample was wiped and measured the sample weight that was the weight of water saturation sample. The equation of water absorption was shown in (3-4).

$$\text{Water absorption (\%)} = (W_s - W_d) / W_d \times 100 \% \quad (3-4)$$

where:

W_s : the weight of saturation water sample (g)

W_d : the weight of dry sample (g)

3.3.2 The particle size analysis

The laser particle size analyzer (LS), BECKMAN COULTER LS230 (USA) in Cheng Kung University, according to ISO 13320 provided guidance on instrument qualification and size distribution measurement of particles in many two-phase systems e.g. powders, sprays, aerosols, suspensions, through the analysis of their light-scattering properties.

It did not address the specific requirements of particle size measurement of specific materials. The laser particle size analyzer was applicable to range of particle sizes from approximately 0.04 μm to 2 mm (appendix 2).

3.3.3 Compressive strength

Strength of various materials was measured by the compressive strength, which tested method was adopted by Chinese National Standard (CNS1010 R3032). The sample was prepared to make into a 3cm x 3cm cube and tested the value of uniaxial compressive stress in Chinese Inspection Technology Co., Ltd.

3.3.4 Bulk density

Archimedes principle indicated that the upward buoyant force that was exerted on a body immersed in a fluid, whether fully or partially submerged, was equal to the weight of the fluid that the body displaces. According to the Archimedes principle, obtained the sample volume, and the weight of sample divided by volume of sample equaled bulk density. The equation of bulk density was shown in (3-5) and (3-6).

$$\text{Volume: } V_s (\text{cm}^3) = V_w - (W_b - W_a) / \rho_w \quad (3-5)$$

$$\text{Bulk density: } \rho_s (\text{g} \cdot \text{cm}^{-3}) = W_s / V_s \quad (3-6)$$

Where:

W_s : Weight of dry sample, (g)

W_a : Weight of graduated cylinder + W_s , (g)

W_b : Weight of quantitatively to the 100 ml water + W_a , (g)

V_w : Volume of quantitatively water, (cm^3)

V_s : Volume of quantitatively sample (cm^3)

ρ_w : Density of water ($\text{g} \cdot \text{cm}^{-3}$)

ρ_s : Density of sample ($\text{g} \cdot \text{cm}^{-3}$)

3.3.5 Scanning Electron Microscope (SEM)

Scanning Electron Microscope (SEM) analysis which was a type of electron microscope, it imaged the sample surface by scanning it with a high-energy beam of electrons in a raster scan pattern. The electrons interacted with the atoms that made up the sample produced signals that contained information about the surface topography of sample. SEM and Energy Dispersive Spectrometer (EDS), JEOL JSM-7000F (Japan) in Tunghai University, was used to observe the micro morphologies and structure of original sample.

3.3.6 B.E.T analysis

Brunauer–Emmett–Teller (BET) theory explained the physical adsorption of gas molecules on a solid surface and serves as the basis for an important analysis technique for the measurement of the specific surface area of a material. The BET analysis used BECKMAN COULTER SA3100 (USA) in National Cheng Kung University. According to ISO 9277 specifies the determination of the overall specific external and internal surface area of disperse (e.g. nano-powders) or porous solids by measuring the amount of physically adsorbed gas according to the Brunauer, Emmett and Teller (BET) method.

3.3.7 Specific external surface area

It was a derived scientific value that can be used to determine the type and properties of a material. a_s was the counting-weighing method. Hence, the representative sample of dry particles was counted after the weighing. Using the particle density, the volume of the average spheres had the same volume, d_v , was calculated. Specific external surface area of the pellets was measured by the Sustainable Environment Research

Center of National Cheng Kung University. The specific external surface area was related to d_v by this expression (3-7):

$$a_s = \frac{\delta}{\rho_p d_v} \quad (3-7)$$

where:

a_s : specific external surface area, (m^2/g)

ρ_p : particle density, (g/cm^3)

δ : particle area (m^2)

d_v : equivalent diameter from the same volume, (cm^3).



3.4 The sequencing batch biofilm reactor (SBBR) system

3.4.1 Experiment set-up

This study used the type specification of experiment setup shown in Table 3-2, which includes the basic setup of bioreactor, real-time monitor probes and computerized monitoring system. Figure 3-3 showed two pilot-scale SBBRs with 40% and 60% filling ratios (v/v) of pellets in the reactor to conduct SND reaction.

The rectangular biological reactor with effective volume of 25 L was made by acrylic sheets with the height of 45.0 cm, the internal width and length of 25.0 cm and 25.0 cm, respectively. The working volume was 20L.

Table 3-2 Specification of experiment setups.

Item	Working range	Manufacture
Biological reactor	45×25×25 cm The working volume was 20 L	Made by acrylic fiber glass
Mixer	Operated at 150 rpm	Oriental Motor, Japan
Aeration pump	Maximum air flow rate is 12 L/min	Serial No. 1030114, Medo Co., Japan
pH	0 - 14	SUNTEX PC-310, Taiwan, R.O.C
ORP	-1999 - 1999 mV	SUNTEX PC-310, Taiwan, R.O.C.
DO	0.00 - 60.00 mg/L	SUNTEX DC-5100
LabVIEW	-	LabVIEW 5.1

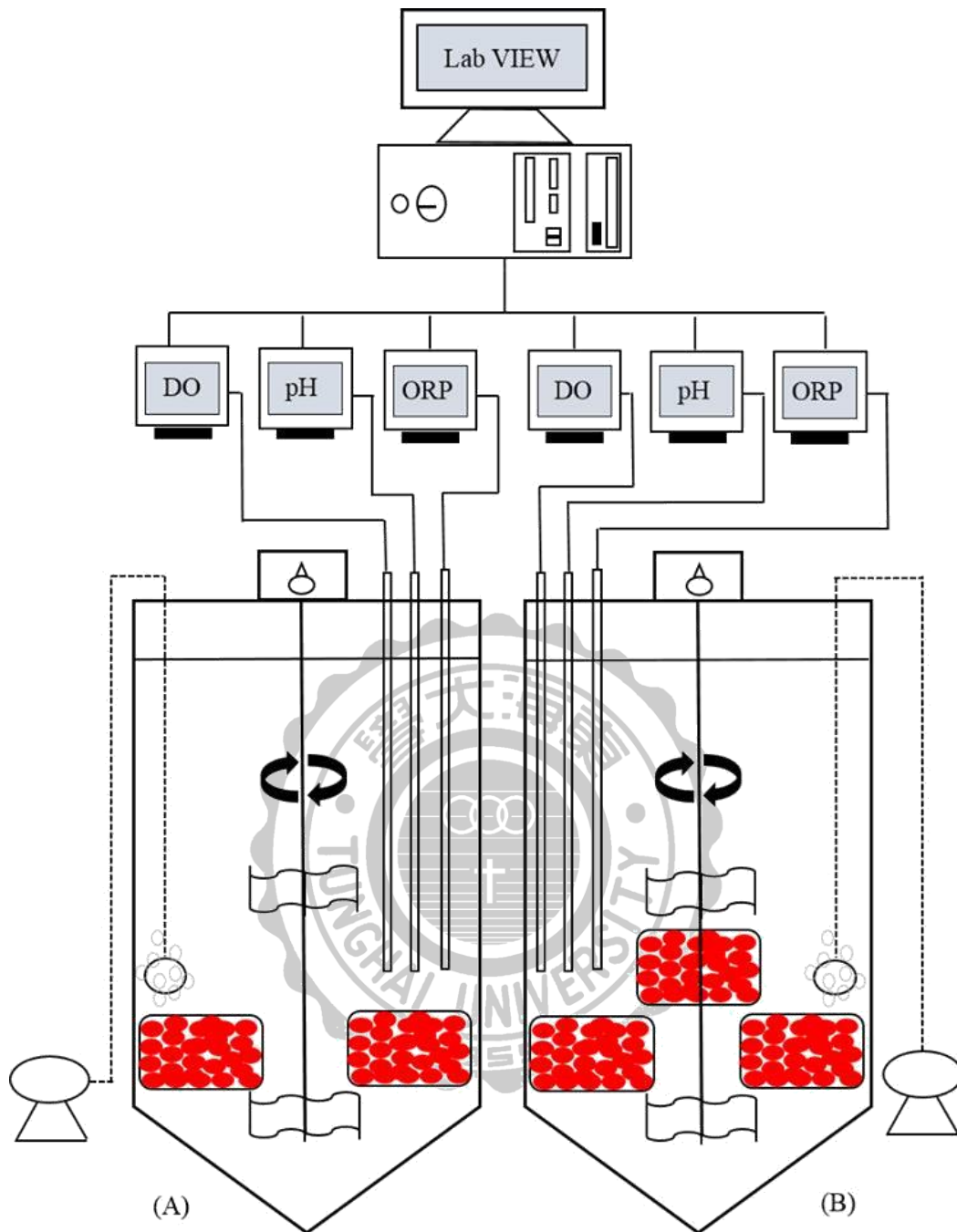


Figure 3-3 Schematic diagram of the SBBR system with 40% (A) and 60% (B) ratios of pellets in the reactor. Both reactors were connected with on-line DO, pH and ORP sensor to a Lab VIEW[®] system in a personal computer to maintain the operational parameters.

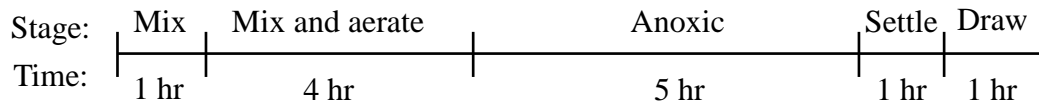
The real-time monitor of pH meter (SUNTEX PC-310, Taiwan, R.O.C.) was adjusted by using the pH 4.0 and pH 7.0 standard solutions, ORP meter (SUNTEX PC-310, Taiwan, R.O.C.) was adjusted by using the 220 mV standard solutions, DO meter (SUNTEX DC-5100, Taiwan, R.O.C.) was adjusted by using internal aero-correction process. The Lab VIEW[®] software was used for computerized real-time monitoring of the process, which included monitor software and AD/DA card. The whole system was set up in a temperature controlled room ($25\pm 2^{\circ}\text{C}$).

3.4.2 Operation of SBBR

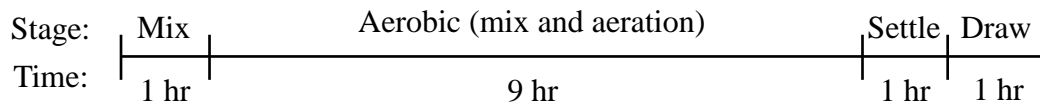
This study conducted the nitrification and denitrification reactions by adjusting different levels of airflow in the systems. Nitrogen removal could be observed, however, where DO concentrations were relatively low (i.e. 1.5 mg/L) (de Silva *et al.*, 1998; Nagaoka, 1999; Holakoo *et al.*, 2007). In order to achieve the SND reaction, the airflow was controlled under low level of DO, i.e., aerated case with 1.0L/min air flow with DO ranging from 0.8-1.5 mg/L (Phase I) and the mixed liquor in the reactor was stirred at 150 rpm. But air flow was changed with 0.5L/min at phase II and III. The SBBR systems were operated with a 12 hours cycle in a temperature controlled room. The operation periods of each cycle in SBBR systems were shown in Figure 3-4. The hydraulic retention times (HRT) of two SBBRs were 12 hours.

In the cyclical operation stages of cultured the sludge was showed in Figure 3-4 (a). In the first stage, the biomass was incubated in the system that the reactors only mixed without aerated (1 hour). In the second stage, the reactors mixed and aerated (4 hours), and then in the third stage, the reactors only mixed (5 hours). Finally, in the fourth stage, the reactors were settling (1 hour) then the supernatant was drawn (1 hour). After cultured the sludge, the cyclical operation stages was switching to only

mixed and aeration without the anoxic stage showed in Figure 3-4 (b).



(a) The cyclical operations stage of cultured the sludge in the system.



(b) The cyclical operation stage of SND process in the system.

Figure 3-4 Operation cycle in (a) the operation stage of cultured sludge (b) the operation stage of SND process.

3.4.3 Composition of the synthetic wastewater

The synthetic wastewater contained carbon source (glucose), nitrogen source (urea), phosphate buffer (KH_2PO_4) and trace nutrients. The general nutrients included acetic acid, glucose, urea, ammonium chloride and phosphate. The organic and inorganic nitrogen in the synthetic wastewater were urea and ammonium chloride. The milk powder in the formula contained protein, lactose, mineral and fat. The formula of the stock synthetic wastewater was shown in Table 3-3. The stock synthetic wastewater was stored at 4°C which avoided degradation. The concentrations of three phase influent synthetic wastewater were shown in Table 3-4. The high nutrient contented synthetic wastewater with the average COD: $\text{NH}_4^+\text{-N}$: $\text{PO}_4^{3-}\text{-P}$ ratio (100: 12.7: 2.2) was used in this study.

Table 3-3 Composition of stock synthetic wastewater in this study¹.

Content	Doses (in 3 L distilled water)
KH ₂ PO ₄	20 g
Glucose	18 g
Urea	60 g
NH ₄ Cl	125 g
FeCl ₃ (10%)	2 mL
CH ₃ COOH (99.8%)	58 mL
NaHCO ₃	256 g
Peptone	9 g
Milk powder	272 g

¹: (Su, 2008; Huang, 2010; Wu, 2012)

Table 3-4 Concentrations of three phase influent synthetic wastewater.

Components	Concentration (mg/L)		
	Phase I	Phase II	Phase III
COD	455±17.1	653±15.7	852±12.4
NH ₄ ⁺ -N	55±7.4	76±3.4	103±3.7
NO _x -N	N. D	N. D	N. D
PO ₄ ³⁻ -P	10±0.7	13±1.7	19±1.7
COD: NH ₄ ⁺ -N: PO ₄ ³⁻ -P	100: 13.6: 2.1	100: 12.1: 2.2	100: 12.4: 2.2

N. D: Not detected

3.5 Analytical methods

3.5.1 Water quality analysis

The analysis of method in this study was listed in Table 3-5. The concentration of COD, $\text{NH}_4^+\text{-N}$, and MLSS in the mixed liquor was analyzed according to the Standard Methods for the Examination of Water and Wastewater 21st Edition. NO_2^- , $\text{PO}_4^{3-}\text{-P}$ and NO_3^- concentrations were analysed by using ion chromatography (IC) (883 Basic IC plus, Metrohm, Switzerland). All samples were pre- filtered with $0.45\mu\text{m}$ glass fiber membrane before analyzing. Hydroxylamine (NH_2OH) was determined by calorimetric method (Peng, 2002), which was shown in Figure 3-5. 2 mL sample was filtered with $0.45\ \mu\text{m}$ membrane, and then 1 ml of 1% alcoholic 8-hydroxyquinolin (Alfa Aesar, USA) and 1 ml of 2N Na_2CO_3 (Merk, Germany) were added. After mixing, sample reaction was placed in room temperature for 2 hrs. The resulting indoxine of indigo was measured with a spectrophotometer (U-2000, HITACHI, Japan) at wavelength of 705 nm. The hydroxylamine standard solution was prepared by dissolving hydroxylamine powder (Alfa Aesar, USA) in deionized water, ranging from 0.0 to 1.0 mg/L of hydroxylamine and a standard curve was obtained by using the above method with a linear regression $R^2 > 0.995$.

Table 3-5 Analytical methods and instruments used in this study.

Item	The Analysis Method and Instrument
COD	Methods 5220B ¹
NH ₄ ⁺ -N	Methods 4500F ¹
NO ₂ ⁻ -N	Ion Chromatography, IC
NO ₃ ⁻ -N	Ion Chromatography, IC
PO ₄ ³⁻ -P	Ion Chromatography, IC
NH ₂ OH	Peng, 2002
pH	pH meter, Method 4500-H-B ¹ (SUNTEX PC-310)
ORP	ORP meter, Method 2580 B ¹ (SUNTEX PC-310)
DO	DO meter, Method 4500-O-G ¹ (SUNTEX DC-5100)
Temp	Temperature meter, NIEA W217.50A
MLSS	Methods 2540D ¹

¹: Standard Methods for the Examination of Water and Wastewater 21st Edition (APHA, 2005)

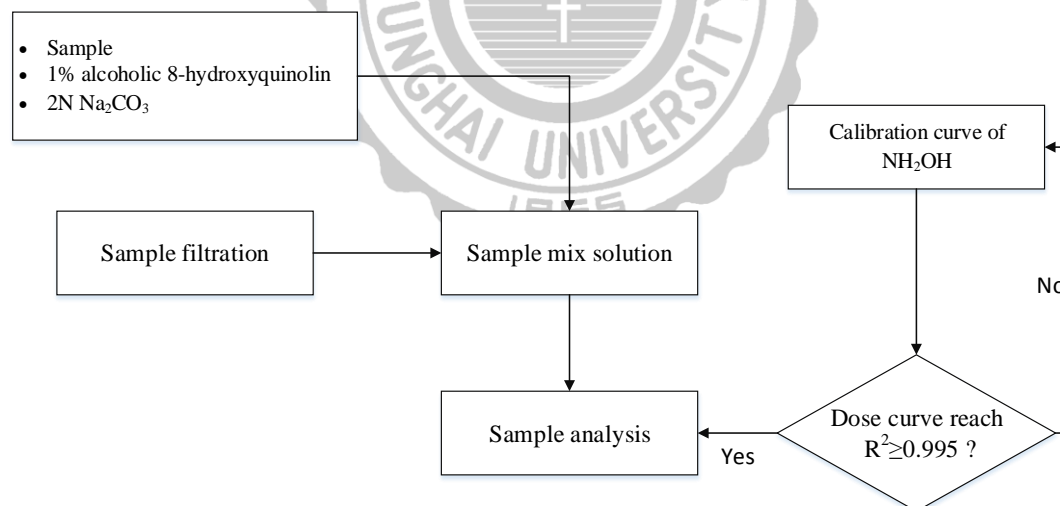


Figure 3-5 Flow chart of the NH₂OH analysis (Peng, 2002).

3.6 Molecular community analysis of biofilm

3.6.1 Chromosomal deoxyribonucleic acid (DNA) extraction

Samples were collected from different reactor (40% and 60% carriers) in phase III during aerobic stage. The soil DNA isolation kit (Mo Bio method) was used to performed DNA extraction. The steps express as follow:

1. Provide the 2 ml Bead Solution tubes, add 0.25 – 1 gm of soil sample.
2. Gently vortex to mix.
3. Check Solution S1. If Solution is precipitated, heat solution to 60°C until dissolved before use.
4. Add 60 μ l of Solution S1 and invert several times or vortex briefly.
5. Add 200 μ l of Solution IRS (Inhibitor Removal Solution).
6. Secure bead tubes horizontally using the Mo Bio Vortex Adapter tube holder for the vortex. Vortex at maximum speed for 10 minutes.
7. Make sure the 2 ml tubes rotate freely in your centrifuge without rubbing. Centrifuge tubes at 10,000 \times g for 30 seconds.
8. Transfer the supernatant to a clean microcentrifuge tube (provided).
9. Add 250 μ l of Solution S2 and vortex for 5 sec. Incubate 4°C for 5 min.
10. Centrifuge the tubes for 1 minute at 10,000 \times g.

11. Avoiding the pellet, transfer entire volume of supernatant to a clean microcentrifuge tube (provided).
12. Add 1.3 ml of Solution S3 to the supernatant (careful, volume touches rim of tube) and vortex for 5 seconds.
13. Load approximately 700 μ l onto a spin filter and centrifuge at $10,000 \times g$ for 1 minute. Discard the flow through, add the remaining supernatant to the spin filter, and centrifuge at $10,000 \times g$ for 1 minute. Repeat until all supernatant has passed through the spin filter.
14. Add 300 μ l of Solution S4 and centrifuge for 30 seconds at $10,000 \times g$.
15. Discard the flow through.
16. Centrifuge again for 1 minute.
17. Carefully place spin filter in a new clean tube (provided). Avoid splashing any Solution S4 onto the spin filter.
18. Add 50 μ l of Solution S5 the center of the white filter membrane.
19. Centrifuge for 30 seconds.
20. Discard the spin filter. DNA in the tube is now application ready. No further steps are required. We recommend storing DNA frozen (-20°C). Solution S5 contains no EDTA.

3.6.2 DNA concentration and purity analysis

After DNA extraction, using a DNA calculator (GeneQuant II, USA) set to scan at 260, and 280 nm, was used to quantify DNA based on absorbance at these wavelengths (Warburg and Christian, 1942). Absorption at UV260 nm measured the concentration of double stranded DNA, while absorption at 280 nm measured concentration of protein. DNA concentration was 50 $\mu\text{g}/\text{mL}$ when absorbance was 1 at wavelength of 260nm. The ratio of A_{260}/A_{280} could be used to illustrate the DNA purity in the solution. In general, the better purity ratio ranged from 1.8 to 2.0. When ratio of A_{260}/A_{280} was too small that represented ethanol or organic solvents might not be completely removed, on the contrary represented the proteins were not completely removed. Therefore the sample should be extraction and purification again.

3.6.3 Agarose Gel Electrophoresis

Agarose gel electrophoresis was a method of gel electrophoresis used in biochemistry, molecular biology, and clinical chemistry to separate a mixed population of DNA or proteins in a matrix of agarose. According to different length of DNA used different concentration of agarose gel (Table 3-6) had a best separation for DNA (Chong, 2001). Used 1% Tris-Acetate-EDTA (TAE) buffer to prepare 1.5% agarose gel (w/v) and heated in the microwave oven until agarose completely dissolved. After agarose dissolved, poured the agarose in the horizontal gel electrophoresis system. When agarose cooling to room temperature, DNA samples and DNA marker mixed ratio with 6x loading dye were 5:1 (v/v). Followed the previous step, slowly loaded the samples mixture and standard molecular weight marker into well of agarose gel. Closed the lid of gel electrophoresis tank and attached the electrical led so that the DNA

would migrate toward the positive anode. Apply a voltage of 100V for 20 minutes. After gel electrical that put the gel in the 0.5 µg/mL of ethidium bromide (EtBr) solution to stain for 10 minutes. The stained gel was finally visualized under UV light (Vilber Lourmat) to take photograph of gel.

Table 3-6 Agarose gel percentage and efficient range of DNA separation.

Gel concentration (%)	DNA size (kbps)
0.5	0.8 - 25
0.8	0.5 – 15
1.0	0.3 – 12
1.5	0.2 – 10
2.0	0.1 - 2

3.6.4 Polymerase Chain Reactor (PCR)

Polymerase Chain Reactor (PCR) was used for amplified the identical of genomic DNA. The whole process was divided into three parts with denaturing, annealing and extension. In denaturing period, the double stranded DNA was separated into two single stranded and the heating temperature generally used at 94°C. Then primer were bound with the two short stretches of sequence, the region which utilized the characteristics of primers in annealing period with temperature ranged from 52°C - 56°C. Expected to the higher species-specific, the selection of primers or genetic fingerprinting was shown significance (Fasoli *et al.*, 2003). Utilized the characteristics of primers, polymerase, deoxy-ribonucleoside triphosphate (dNTP) (components with dATP, dTTP, dGTP, and dCTP) and temperatures control could amplify the fragment in which we wanted to observe. Final part of PCR was extension usually heating at 72°C, where template was used to the bound

sequence (Pritchard *et al.*, 2005). The PCR had advantages on maintain the completeness of microbial communities and without cloning previous separation, because of the PCR could also amplified the dead cells which could visually as species bands on the denaturing gradient gel electrophoresis (DGGE) gels (Cocolin *et al.*, 2002). The nested-PCR technique was necessary to use for amplify the most variable regions of 16S rDNA gene targeting V3-V5 region, because of the size limited of DNA fragments for DGGE (200 - 800 bp).

The two primers used for nested PCR in this study were 27f/1522r (long fragment) and 341f/926r (short fragment). The sequence and target of two primers in this study were shown in Table 3-7. The chemical reagents and volumes for PCR reaction were shown in Table 3-8 and the heating programs of PCR were shown in Table 3-9.

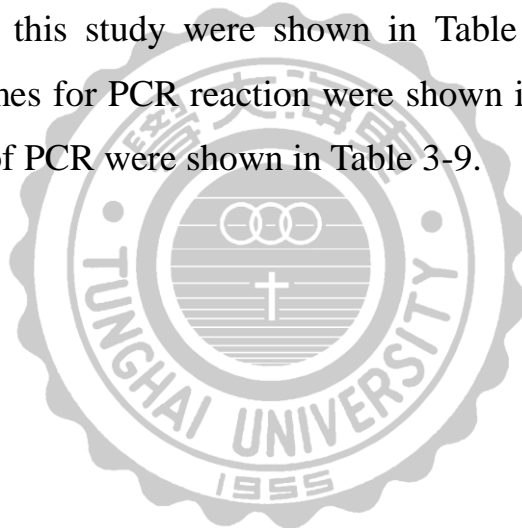


Table 3-7 PCR primer used for amplification of bacterial 16S rDNA.

Primer	Target	Sequence (5'-3')	Reference
27f	Universal	AGAGTTTGATCCTGGCTCAG	Edwards <i>et al.</i> (1989)
1522r	Universal	AAGGAGGTGATCCAGCCGCA	Edwards <i>et al.</i> (1989)
341f	Bacteria	CCTACGGGAGGCAGCAG	Hesham <i>et al.</i> (2011)
341f-GC	Bacteria	GC clamp connected to the 5' end of 341f	Hesham <i>et al.</i> (2011)
926r	Universal	CCGTCAATTCTTTGAGTTT	Hesham <i>et al.</i> (2011)

*GC clamp = 5'- CGC CCG CCG CGC GCG GCC GGG GCG GGG
GCA CGG GGG G - 3'.

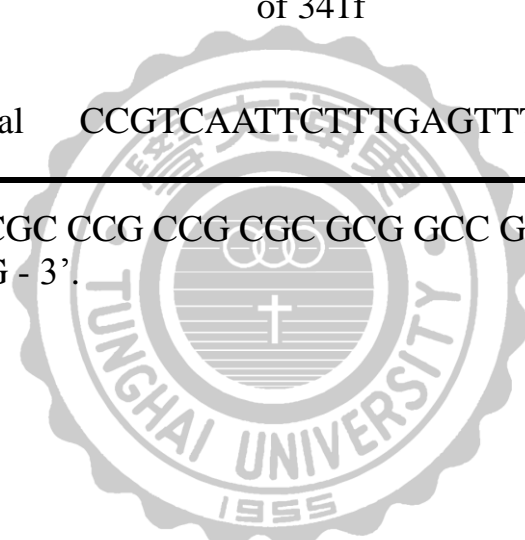


Table 3-8 Reagent and volume for PCR reaction.

Reagent	Volume (μ l)	Concentration
Master Mix	7.5	2X
Forward	2	10 μ M
Reverse	2	10 μ M
ddH ₂ O	2	-
Template	1.5	-

Table 3-9 Heating program of PCR in this study.

Primer	Temperature	Time	Cycle numbers	Reactions
27F/1522R	94°C	4 min	1	Activation
	94°C	1 min	30	Denaturation
	56°C	1 min	30	Annealing
	72°C	1 min	30	Extension
	72°C	7 min	1	Final extension
341F GC/926R	94°C	4 min	1	Activation
	94°C	1 min	30	Denaturation
	52°C	1 min	30	Annealing
	72°C	1 min	30	Extension
	72°C	7 min	1	Final extension

3.6.5 Denaturing Gradient Gel Electrophoresis (DGGE)

One culture-independent method for studying the diversity of microbial communities is analysis of PCR products, generated with primers homologous to relatively conserved regions in the genome, by using denaturing gradient gel electrophoresis (DGGE) (Muyzer *et al.*, 1993; Muyzer and Smalla, 1998). Each kind of microbial community had difference base composition, especially the content of G and C. DGGE could separate similar fragment of DNA with difference GC content from lower to higher in proper order. Different fragment of base pair had the optimal performance with different gel percentage that the relationship was shown in Table 3-10.

The matters needed attention and the method of casting parallel gradient gel with DGGE implements (DCode Universal Mutation Detection System, Bio-Rad, USA) were depicted in the next following. Before cast parallel gradient gel the glass should wash with 70% ethanol and air-dried to avoid the inaccurate analysis. The implement of cast gel was constructed with two glasses and clips then put the spacer between the glass and the bottom should be sealed by tape to avoid gel leaked. According to previous experiment, the gradient range of denaturant was decided from 30% to 60%. The reagent and concentration of DGGE gel in this study was shown in Table 3.11. A gradient delivery system (Bio-Rad Model 475 Gradient Delivery System) was used to deliver gel mixture into the mold. After pouring the gel, put the comb in the mold carefully to avoid the bubble produced and sit for at least 60 minutes for gel coagulated. 1X TAE buffer was added to each well after withdrawing the comb. Due to the gel placed in the pre-heated electrophoresis tank that the temperature would make the urea released to obstruct DNA loading. Flushing each well with 1X TAE buffer again and loaded

approximately 25 μ l of samples then ran the electrophoresis at 250V for 8 hours at 60°C. After the electrophoresis, the gel was placed to stain in the 0.5 μ g/ml of EtBr solution for 15minutes and cleansed in the ultrapure water for 10minutes. The stained gel was finally visualized under UV light (Vilber Lourmat) to take photograph of gel. Due to the results of DGGE separation was not good so used the sterile scalpel to slice target bands and then employed QIAEX II Gel extraction kit (Qiagen, USA) to re-suspend the DNA and consequently were analyzed by molecular cloning.

Table 3-10 Relationship between gel percentage and base pair separation.

Gel percentage	Base pair separation
6%	300 - 1000 bp
8%	200 - 400 bp
10%	100 - 300 bp

Table 3-11 Reagent of 6% polyacrylamide gel of DGGE in this study.

Reagent	30%	50%	Brand
40% Acrylamide/Bis	15 ml	15 ml	Bio-Rad
50X TAE buffer	2 ml	2 ml	Biokit
Formamide (deionized)	2.4 ml	4 ml	Showa Chemicals
Urea	2.52 g	4.2 g	Bio-Rad
ddH ₂ O	To 20 ml	To 20 ml	-
Ammonium persulfate (APS)	0.1%	0.1%	Bio-Rad
Tetramethylethylenediamine (TEMED)	8 μ l	8 μ l	Bio-Rad

3.6.6 Molecular cloning

First of all used the primer (341F/926R) proceeded PCR reaction to amplify the samples of re-suspending DNA to increase amount of DNA. This study adopted the T&A™ cloning kit to conduct next experiment. The plasmid DNA was T&A™ (2728 bp) and competent cell was E. Coli DH5α in this study. Inserted the target fragment into vector (ligation) that incubated in the refrigerator at room temperature (25°C) for 20 minutes. Then inserted products of ligation plasmid DNA into E. Coli DH5α (transformation) and spread on Luria-Bertani (LB) medium which contained antibiotics (50 µg/mL Ampicillin) and blue and white screening reagent (40 µg/mL X-gal and 24 µg/mL IPTG) to incubate at 37°C for 16 hours. Every LB medium contained 50 µl of blue and white screening reagent (X-gal: IPTG= 1: 4). Protocol for ligation using T&A™ cloning vector and LB medium preparation were shown in Table 3-12 and Table3-13, respectively. Due to the T&A™ cloning vector included Amp^r gene and therefore colony of incubation represented to contain vector. However, cut-off point of vector was signed on β- galactosidase gene and therefore if target fragment did not insert into T&A™ cloning vector that reacted with X-gal to produce the blue colony. On the contrary, if target fragment was successfully inserted into vector that did not react with X-gal and therefore it would produce the white colony. Due to the blue colony represented that did not insert target fragment into vector so only selected the white colony to streak onto the LB medium which included blue and white screening reagents to incubate at 37°C for 16 hours. This procedure would newly check whether the colony was white colony. It finally utilized primer M13 to execute PCR reaction to confirm target fragment and then did DNA Sequencing.

Table 3-12 Reagent and volume of protocol for ligation using T&ATM cloning vector.

Reagent	Standard control
Ligation buffer A	1 μ l
Ligation buffer B	1 μ l
T&A TM cloning vector	2 μ l
PCR product	3 μ l
yT ₄ DNA ligase	1 μ l
Deionized water	2 μ l

Table 3-13 LB medium for host cell growth and solution in cloning procedures.

Solution	Addition	Volume	Store Temperature	Brand
Luria-Bertani	12.5 g	To 500 ml	4°C	BD
Agar	7.5 g	(DI water)		
Ampicillin	0.05 g	To 1 ml (DI water)	4°C	Sigma
X-gal	0.04 g	To 1 ml (DMF)	-20°C (dark)	GeneMark
IPTG	0.024 g	To 1 ml (DI water)	-20°C	GeneMark

DMF: Dimethylformamide

3.6.7 Sequencing analysis

Samples of sequence trusted Mission Biotech Co., Ltd to do DNA sequencing. Due to the signals of two sides were feeble and therefore did the two-way sequencing. Then used DNA sequence reverse and complement online tool to reverse transcriptase the reverse of sequencing and combined with forward of sequencing that would get a complete gene sequencing fragment of 16S rRNA.

3.6.7.1 Basic Local Alignment Search Tool (Blast)

The complete combination of sequencing did comparison with GeneBank on the National Center for Biotechnology Information (NCBI). It would get much similar sequencing and then did consecutively the phylogenetic tree.

3.6.7.2 Phylogenetic Analysis

After comparison, employed the MEGA6 software to alignment all the sequencing and then utilized Neighbor-joining method to draw the phylogenetic tree under Bootstrap Replication for 500 times.

Chapter 4 Results and Discussion

4.1 The raw materials analysis

4.1.1 The basic characteristics of the raw materials

The WAS was sampled from the Futian water resource recycling center of Taichung City. The basic physical characteristic of domestic WAS and laterite results were shown in Table 4-1. The WAS had 2.07 % moisture content, 42.89 % flammable content and 55.04 % ash content while the laterite had 0.87 % moisture content, 6.74% flammable content and 92.39 % ash content. The laterite had the most component of ash content which increased the strength structure of pellets. Besides, the WAS possessed more component of flammable than the laterite. Therefore, these characteristics would provide the pellets possessed high porosity.

Table 4-1 Basic characteristics of the WAS of Futian water resource recycling center of Taichung city and laterite.

Basic characteristic	Dry WAS	Laterite
Moisture content, %	2.07±0.07 ¹	0.87±0.17
Flammable content, %	42.89±0.42	6.74±0.25
Ash content, %	55.04±0.56	92.39±0.19
pH	4.83±0.21	5.37±0.11

¹: mean ± standard deviation

n= 3

The WAS and laterite were ground into powder by mill machine (BM-072, Hong-Yu Instrument, Taiwan). The average diameters of WAS powder was mainly located at the 16 μm (Figure 4-1(a)) and laterite powder was at the 18 μm (Figure 4-1(b)). The powders of WAS and laterite were smaller than 75 μm which had a better effect in the form of pressed pellets (Gomes *et al.*, 2011; Santos *et al.*, 2012).

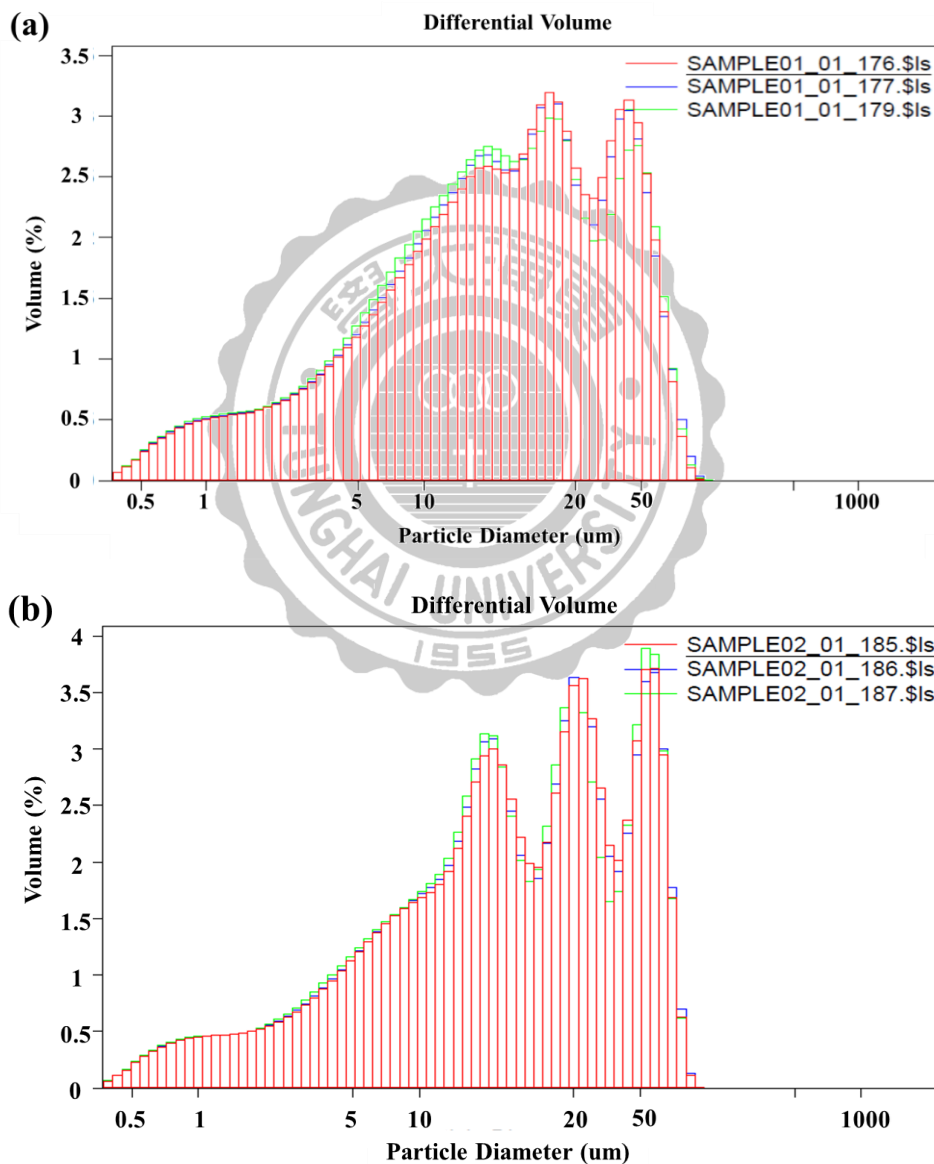


Figure 4-1 Particle size distribution analysis of (a) WAS powder and (b) laterite powder.

4.1.2 The TCLP of raw materials

The WAS and laterite were necessary to test the toxicity characteristic leaching procedure (TCLP) from NIEA before carrier pellets was used. The dehydrated sludge and laterite following wastewater treatment was used in this study, and the results of TCLP were shown in Table 4-2. Due to the concentration of WAS and laterite were lower than the standard in law (NIEA, 2004), hence the raw materials could be made as pellets.

Table 4-2 The TCLP tests for heavy metal concentration of Futian WAS and laterite.

Element	Concentration of WAS (mg/L)	Concentration of laterite (mg/L)	Regulatory concentration (mg/L)
Cu	0.086±0.004 ¹	0.011±0.002	15
Pb	0.006±0.001	0.013 ±0.001	5
Cr	N. D	0.006±0.002	5
Zn	3.021±0.008	0.051±0.007	25
Cd	N. D	N. D	1

¹: mean ± standard deviation

n= 3

N. D: not detected

4.2 The carrier pellet analysis

4.2.1 The characteristics of carrier pellet

The purpose of this study was to build carrier pellets for immobilized medium and enhanced nitrogen removal efficiency in the SBBR systems. Due to WAS was weakness reused directly to build carrier pellets. Therefore, the nutrients were added in the carrier pellets to increase compressive strength and durability in this study. Theoretically, the carrier pellets provided the high external surface area which was easily growth for biomass, high strong compression and high water absorption. The external surface area provided the supporter of biomass while the high water absorption could let the substrate penetrated into internal pellet easily. Ding *et al.* (2011) indicated that hydrophilic porosity carrier had stability in biofilm which was increased adsorbed rate of biofilm. Table 4-3 showed the basic characteristics of carrier pellets and other references. The optimal formula ratios of carrier pellets was 50% of WAS as raw material in this study. According to the regulation of general waste recycle and disposal, the strength must be exceeding the standard of recycling pellet compressive strength of 15 Kgf/cm². The compressive strength of this study: 46.1±1.2 Kgf/cm² was higher than previous study: 35.3±3.5 Kgf/cm² which was strong enough and with sufficient porosity. The plot of RSM by MINITAB[®] was showed in Figure 4-2 and 4-3. The result of RSM indicated that the 50% WAS mixed in carrier pellets which had the best compressive strength was 46.1 Kgf/cm² and the highest surface area was 2.9 m²/g, respectively. After numerous trials, this study obtained the optimal formula ratios of WAS: laterite: chemical additive was 5: 3: 2.

Table 4-3 Comparison of the basic characteristics of the porous WAS pellets in this study and previous study.

Water absorption ¹ (%)	Compressive Strength ^{1,2} (Kgf/cm ²)	Bulk Density ¹ (g/cm ³)	Specific external surface area ¹ (m ² /g)	Reference
52.7±4.4	46.1±1.2	2.2±0.5	2.9±0.2	This study
45.2±5.8	35.3±3.5	1.8±0.4	2.6±0.1	Wu (2012)
41.7±2.5	11.3±2.5	1.5±0.3	2.2±0.1	Huang (2010)
32.9	36.7	7.1	-	Su (2008)
60.49	2.44	0.67	-	Chen (2005)

¹: mean ± standard deviation; ²: Standard of recycling pellet compressive strength ≥ 15 Kgf/cm²

n= 3

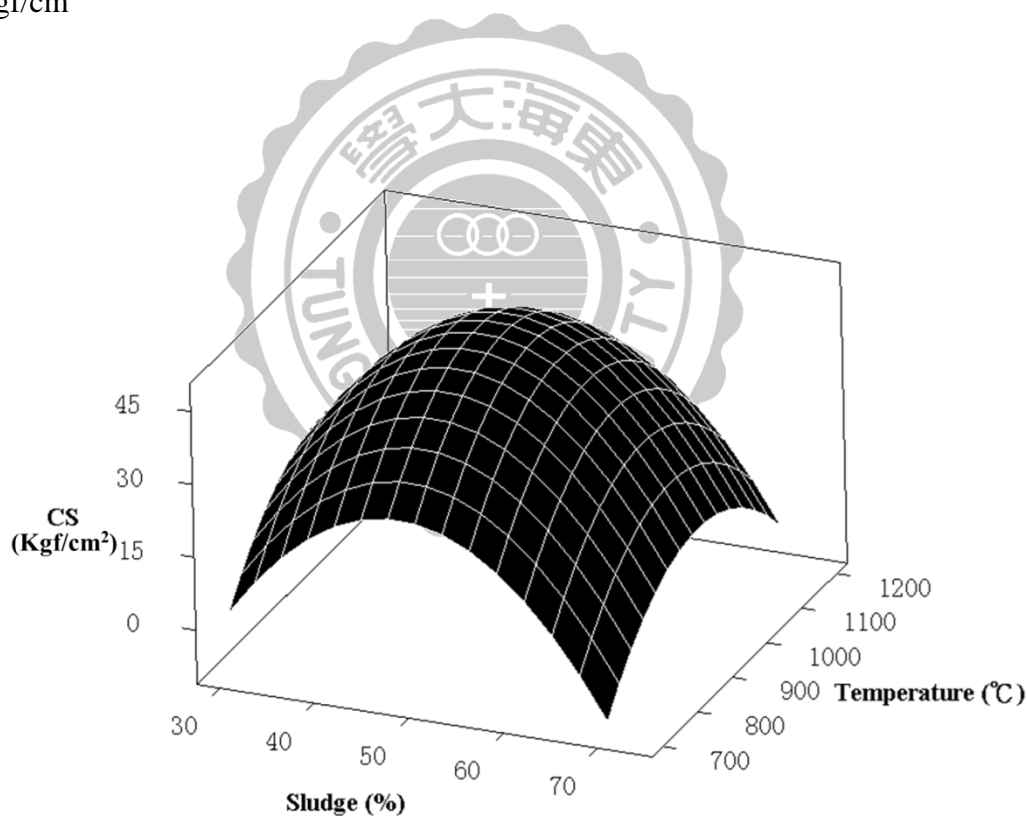


Figure 4-2 Surface plot of compressive strength (CS), dry sludge and temperature from RSM analysis.

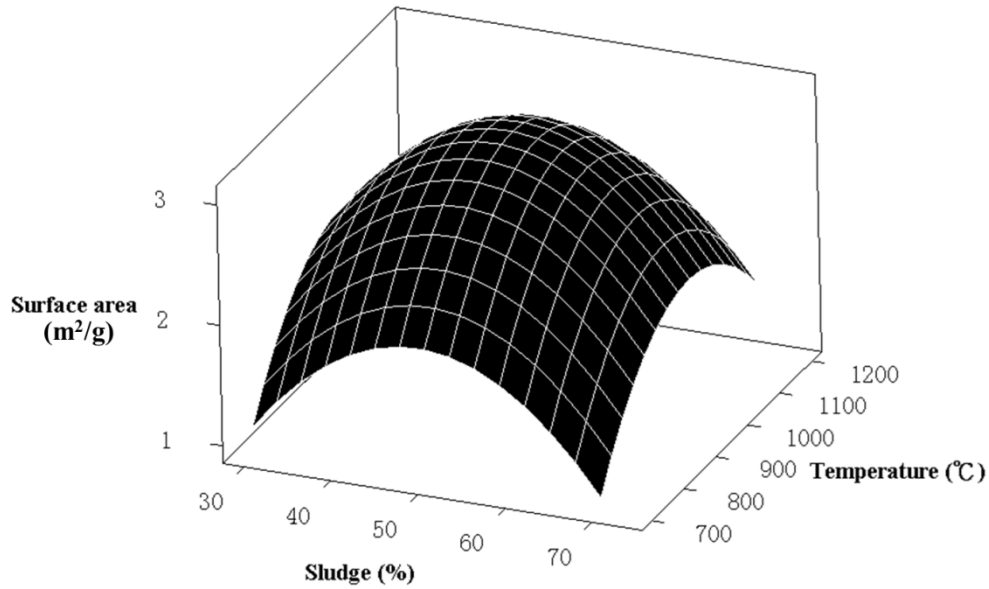


Figure 4-3 Surface plot of surface area, dry sludge and temperature from RSM analysis.

4.2.2 The TCLP of carrier pellets

The heavy metal concentrations of carrier pellets were analyzed by TCLP. The result of TCLP of carrier pellets was showed in Table 4-4. All concentrations of the pellets were lower than Taiwan's limitations (NIEA, 2004). Therefore, these pellets would not have the impact of pollution in the environment and could use as carrier in the SBBR system further.

Table 4-4 The TCLP test for heavy metal concentration of the porous WAS pallets.

Element	Concentration of pellet samples (mg/L) ¹	Regulatory concentration (mg/L)
Cu	0.176±0.002	15
Pb	0.157±0.005	5
Cr	0.007±0.003	5
Zn	0.085±0.002	25
Cd	N. D	1

¹: mean ± standard deviation; N. D: Not detected; n= 3

4.2.3 The composition and surface of the carrier pellets

Figure 4-4 showed the pellet of this study and the diameter (20 - 22 mm) was similar than that of previous studies. Due to increasing the external porosity and compressive strength this study used needle to prick and added the chemical additive, respectively. The bulk density was $2.2\pm 0.5 \text{ g/cm}^3$, the specific external surface area was $2.9\pm 0.2 \text{ m}^2/\text{g}$ and the compressive strength was $46.1\pm 1.2 \text{ Kg/cm}^2$ in this study. Due to the formula ratio of raw materials was different from Wu's study, the formula ratios of WAS: laterite: chemical additive were 5: 3: 2 (Figure 4-4 (a)) in this study and 5: 4: 1 (Figure 4-4 (b)) in Wu's study. All of the basic characteristics were better than previous study so that was good as carrier pellets in the SBBR system. Figure 4-5 showed the SEM image of carrier pellets from this study before used and compared with previous studies. As a result of the porous surface of carrier pellets in this study (Figure 4-5 (d)) was similar to that from Wu's study (Figure 4-5 (c)) which was better than previous others (Figure 4-5 (a) (b)). Therefore, the more porous surface was suitable for the bacteria to grow and attach on it.

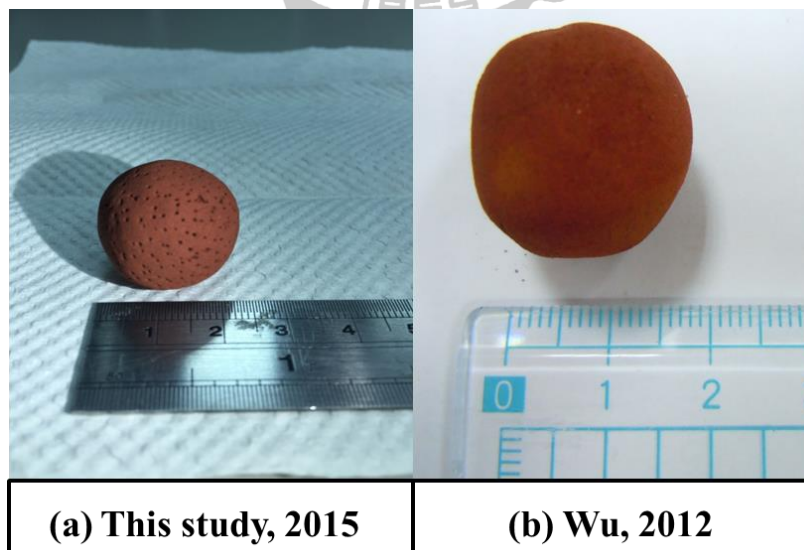
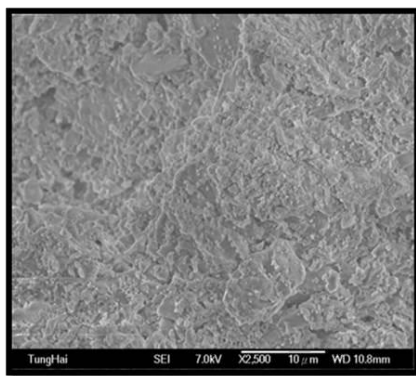
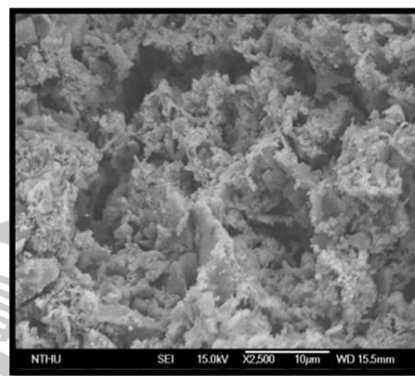


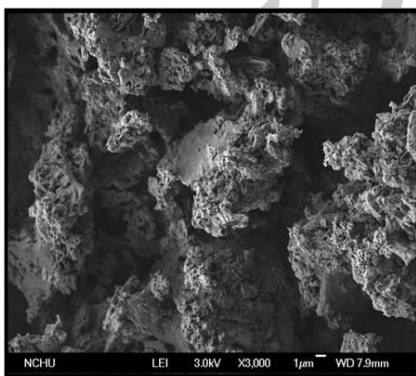
Figure 4-4 Surface of carrier pellet with the formula ratios of WAS: laterite: chemical additive are (a) 5: 3: 2 and (b) 5: 4: 1.



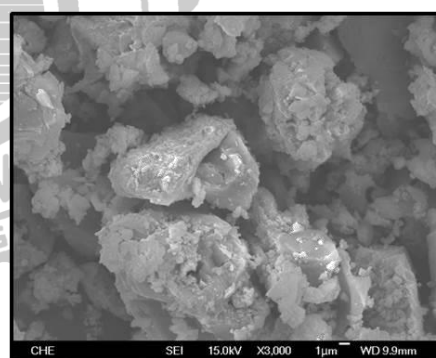
(a) Su, 2008



(b) Huang, 2010



(c) Wu, 2012



(d) This study, 2015

Figure 4-5 The SEM images of carrier pellets in this study and previous studies.

4.3 The carrier pellets were applied for SBBR systems

4.3.1 The daily monitor profiles in SBBRs

Two SBBR systems were designed with the pellet filling ratios of 40% and 60% (v/v) of carrier pellets to conduct the SND and also the BNR operation. Two SBBRs were operated for 156 days under three different phase. The phase I to phase III of food-to-microorganism ratio (F/M), volumetric loading and operation times were 0.476 kg COD/ kg MLSS-day, 0.058 kg NH₄⁺-N/ kg MLSS-day, 0.273 kg COD/ m³-day, 0.033 kg NH₄⁺-N/ m³-day for 70 days (phase I), 0.668kg COD/ kg MLSS-day, 0.078 kg NH₄⁺-N/ kg MLSS-day, 0.392 kg COD/ m³-day, 0.046 kg NH₄⁺-N/ m³-day for 47 days (phase II) and 0.845 kg COD/ kg MLSS-day, 0.102 kg NH₄⁺-N/ kg MLSS-day, 0.511 kg COD/ m³-day, 0.062 kg NH₄⁺-N/ m³-day for 39 days (phase III), respectively. This study maintained C/N at 8.2 - 8.6 in this range due to the C/N ratio of 5 -15 was suitable for bioreactor (Gieseke *et al.*, 2002; Xia *et al.*, 2008). Figure 4-6 showed the daily concentration change of COD in the influent and effluent. The three initial concentrations of COD were 455±17.1 mg/L, 653±15.7 mg/L and 852±12.4 mg/L for phase I, II and III. All effluent concentrations of COD were below 100 mg/L that conformed to regulations in law. Figure 4-7 showed the daily concentration change of ammonium in the influent and the effluent. The three initial concentrations of ammonium in the influent were 55±7.4 mg/L, 76±3.4 mg/L and 103±3.7 mg/L for phase I, II and III phases with COD/N ratios of 8.2, 8.6 and 8.2, respectively.

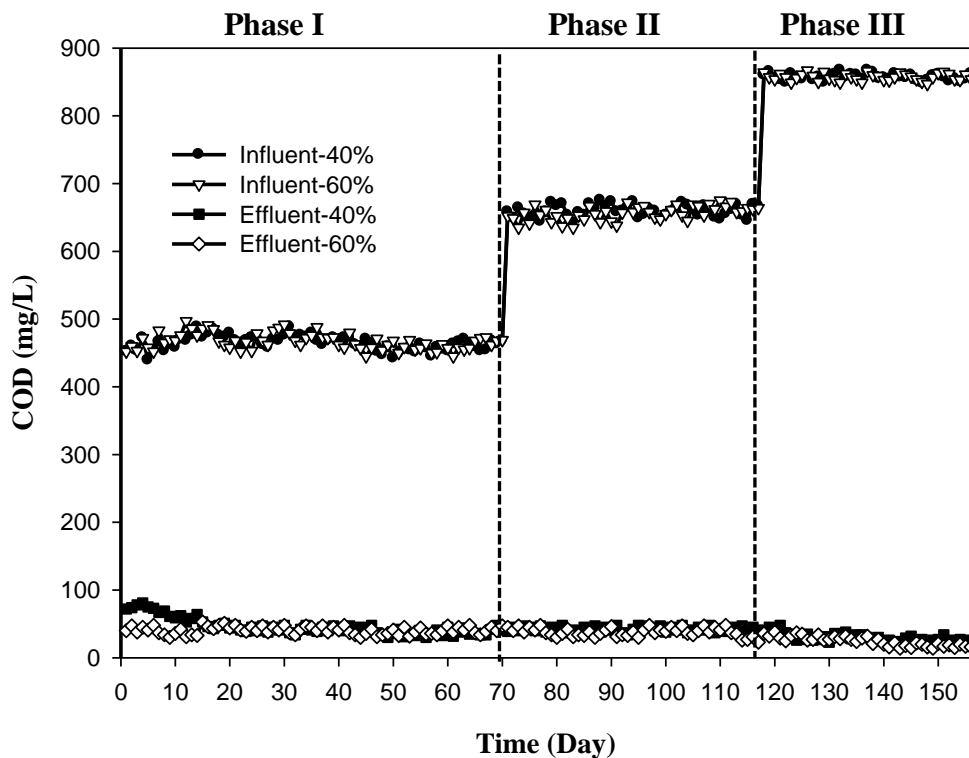


Figure 4-6 Concentration profiles of COD in the influent and effluent of SBBRs in this study. The daily profiles of COD in two types of system (SBBR with 40% and 60% filling ratio). The period of phase I (loading: 0.273 kg COD/ m³-day) under 70 days, phase II (loading: 0.392 kg COD/ m³-day) under 47 days and highest concentration was phase III (loading: 0.511 kg COD/ m³-day) under 39 days, respectively.

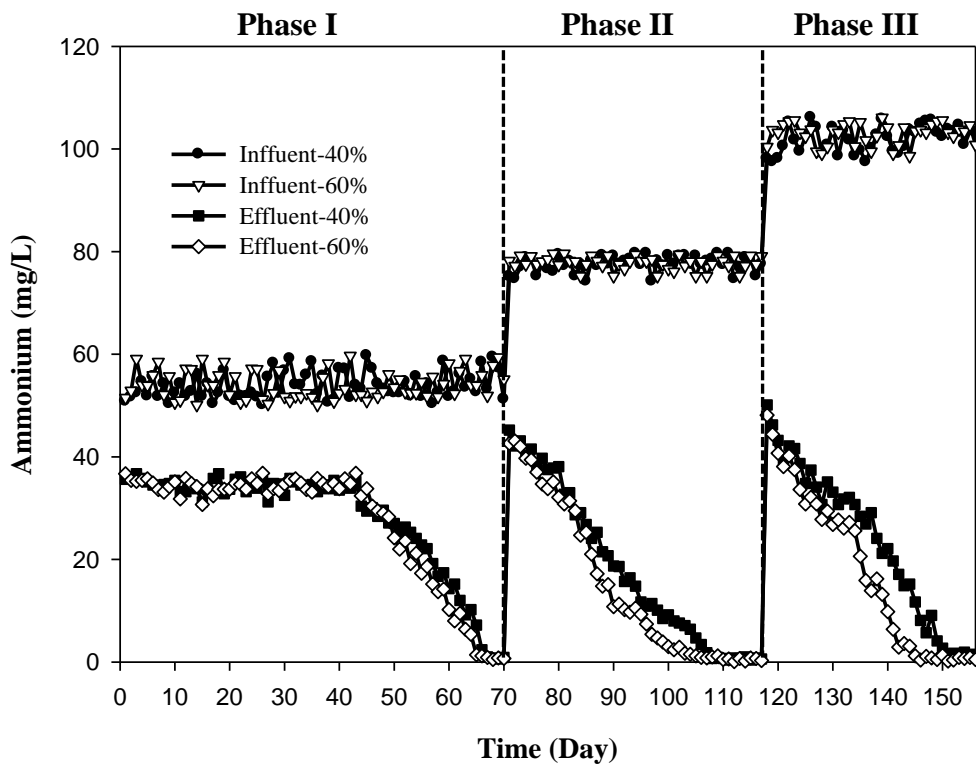


Figure 4-7 Concentration profiles of ammonium in the influent and effluent of SBBRs in this study. The daily profiles of ammonium in two types of system (SBBR with 40% and 60% filling ratio). The period of phase I (loading: $0.033 \text{ kg NH}_4^+ \text{-N/ m}^3 \text{-day}$) under 70 days, phase II (loading: $0.046 \text{ kg NH}_4^+ \text{-N/ m}^3 \text{-day}$) under 47 days and highest concentration was phase III (loading: $0.062 \text{ kg NH}_4^+ \text{-N/ m}^3 \text{-day}$) under 39 days, respectively.

4.3.2 Comparative profiles of two SBBRs

Two different filling ratios of carrier pellets in the SBBR systems were designing in this study. The filling ratios were 40% and 60%, respectively. Two SBBRs were run in parallel under the same operation conditions. Two SBBRs were operated at a hydraulic retention time (HRT) of 12 hours in an air conditioned room (with temperature under $25\pm 2^{\circ}\text{C}$) and the performances were observed regularly.

4.3.2.1 SBBR I (40% ratio)

Figure 4-8 showed the batch profiles of continuous monitoring under three loadings with filling ratios of 40% in the SBBR system. The DO concentration in the phase I was higher than others. Due to biomass and ammonium concentration of influent were not high enough that oxygen consumed less leads to higher DO concentration in the phase I. The pH was maintained among 6 to 8 and had a good stability. The nitrification reaction produced the acid which results the alkalinity were consumed by producing acid. Therefore supplying alkalinity was important in this SBBR system. The ORP under phase I was different from others. Because of DO concentration gradually increased 1 to 5 mg/L at 280 min to cause ORP with a large variation. Others had not much change that ORP controlled -125 to -45 mV at aeration and mix step.

The batch profiles of nitrogen removal were showed in Figure 4-9. The effluent concentration of COD in three loadings had a good treatment effect that all reduced below 100 mg/L of the law standard (Fig 4-9 (a)). It meant that carbon source was consumed effectively by heterotrophic bacteria. However, the concentration of COD in phase I decreased slowly at aeration and mix step. Due to the biofilm attached on the carrier pellets were not enough. The influents of ammonium under three loadings were

55, 78 and 99 mg/L, respectively. The effluents of ammonium under three loadings were below 1 mg/L at 620 min (Figure 4-9 (b)). The nitrate was produced few amounts in the SBBR-40% system (Figure 4-9(d)). However, most of the ammonium mainly converted to nitrite (Figure 4-9(c)) which like pathway of single reactor system for high-rate ammonium removal over nitrite (nitrification) process (Ahn, 2006). The maximum concentration of nitrite and nitrate was 5.4 and 2.2 mg/L at 360 min in the SBBR-40%, respectively. The phosphate was reduced during the aeration and mix step due to the aeration phosphate uptake (Figure 4-9(e)).

4.3.2.2 SBBR II (60% ratio)

The SBBR-60% and SBBR-40% had same conditions of operation that DO concentration in the phase I was higher than others (Figure 4-10(a)). The aeration decreased from 1 (phase I) to 0.5 (phase II) L/min. Figure 4-10 (a) showed DO decreased at the mix and aeration step in the phase II and phase III. The DO of SBBR-60% in the phase III had different with SBBR-40% in the phase III. The DO of SBBR-60% maintained at 0.8 - 1.5 mg/L that was lower than DO of SBBR-40% in the phase III. Because of different filling ratio of carrier pellets in the reactors caused the amount of biofilm differently, therefore, DO of SBBR-40% was consumed slowly. The pH was not much difference between two different filling ratios reactors that kept during 6 - 8 (Figure 4-10(b)). The ORP of SBBR-60% at mix and aeration step during three loadings were steady than SBBR-40% (Figure 4-10(c)). The COD of SBBR-60% also reduced below 20 mg/L (Figure 4-11 (a)) that was lower than standard in law (100 mg/L). Two SBBR systems had good removal effect for organic matters, and the ammonium removal in SBBR-60% system was finally reduced below 1 mg/L (Figure 4-11 (b)). While reactor

started the aeration and mix step, the ammonium converted to nitrite (nitrification) that SBBR-60% system showed nitrite produced more than SBBR-40%. It meant that SBBR-60% had a good convertibility which was better than SBBR-40%. Moreover, the pathway of few nitrites converted to nitrates (nitrification) (Figure 4-11 (d)) was similar to nitrification process. Besides, the maximum concentration of nitrite and nitrate was 5.7 and 0.5 mg/L at 420 min in the SBBR-60%, respectively. This result exhibited the nitrification occurred that most ammonium converted to nitrite and less nitrate production in this system. The SBBR-60% had a better nitrification than the SBBR-40% because the less nitrate production in the SBBR-60% during phase III. It might relate with DO concentration which was below 2 mg/L lower than the SBBR-40% during the phase III. Due to excessive DO would decrease activity of AOB that was good for growth of NOB. Finally, Figure 4-11 (e) showed that phosphate was reduced at mix and aeration step in SBBR-60% system. But SBBR-60% system had a better removal rate to remove phosphate at 320 min completely in the phase III which was faster than SBBR-40% at 560 min in the phase III.

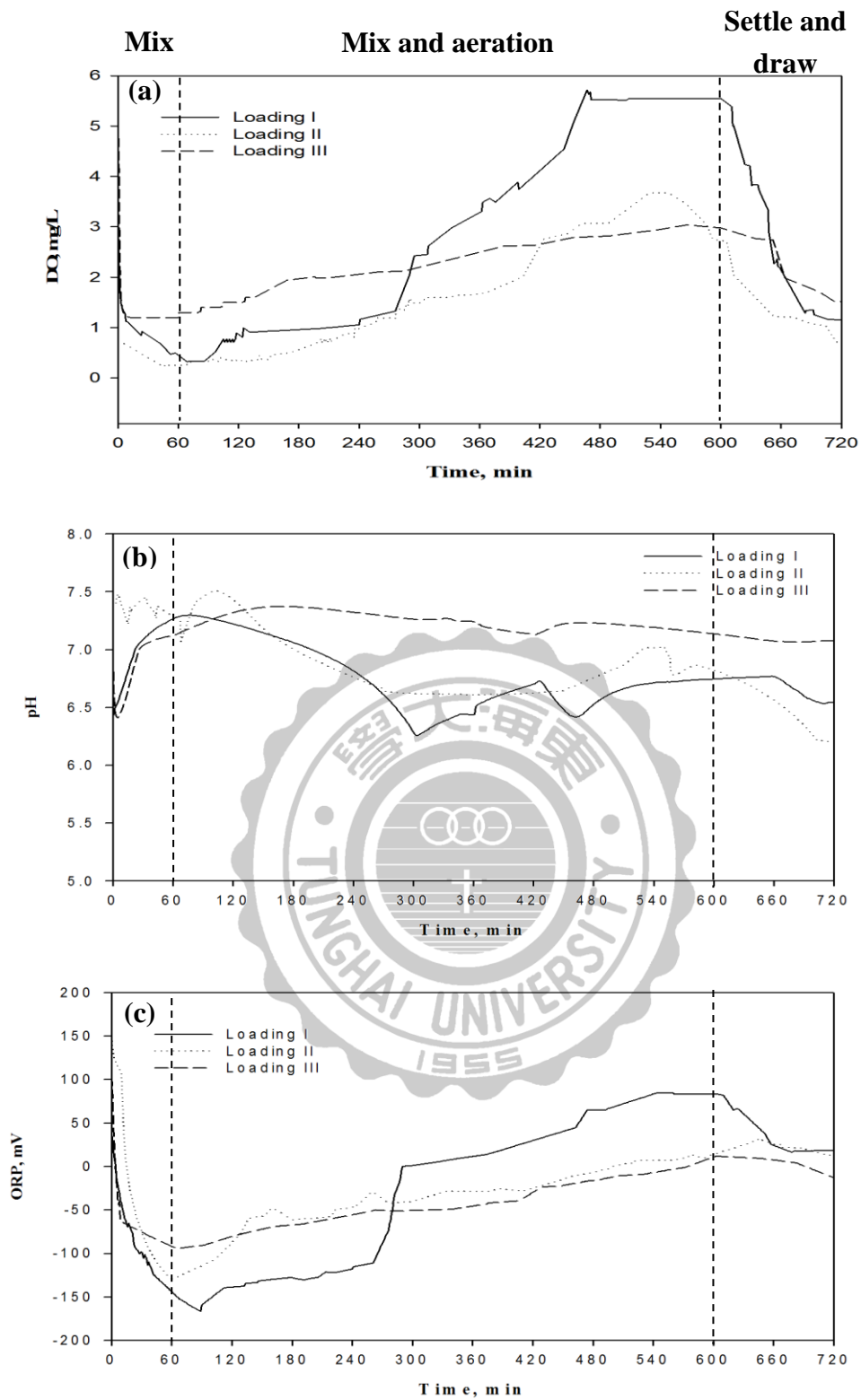


Figure 4-8 Batch profiles of on-line measured parameters under three loadings with filling ratio of 40% in the SBBR system (a) DO, (b) pH and (c) ORP.

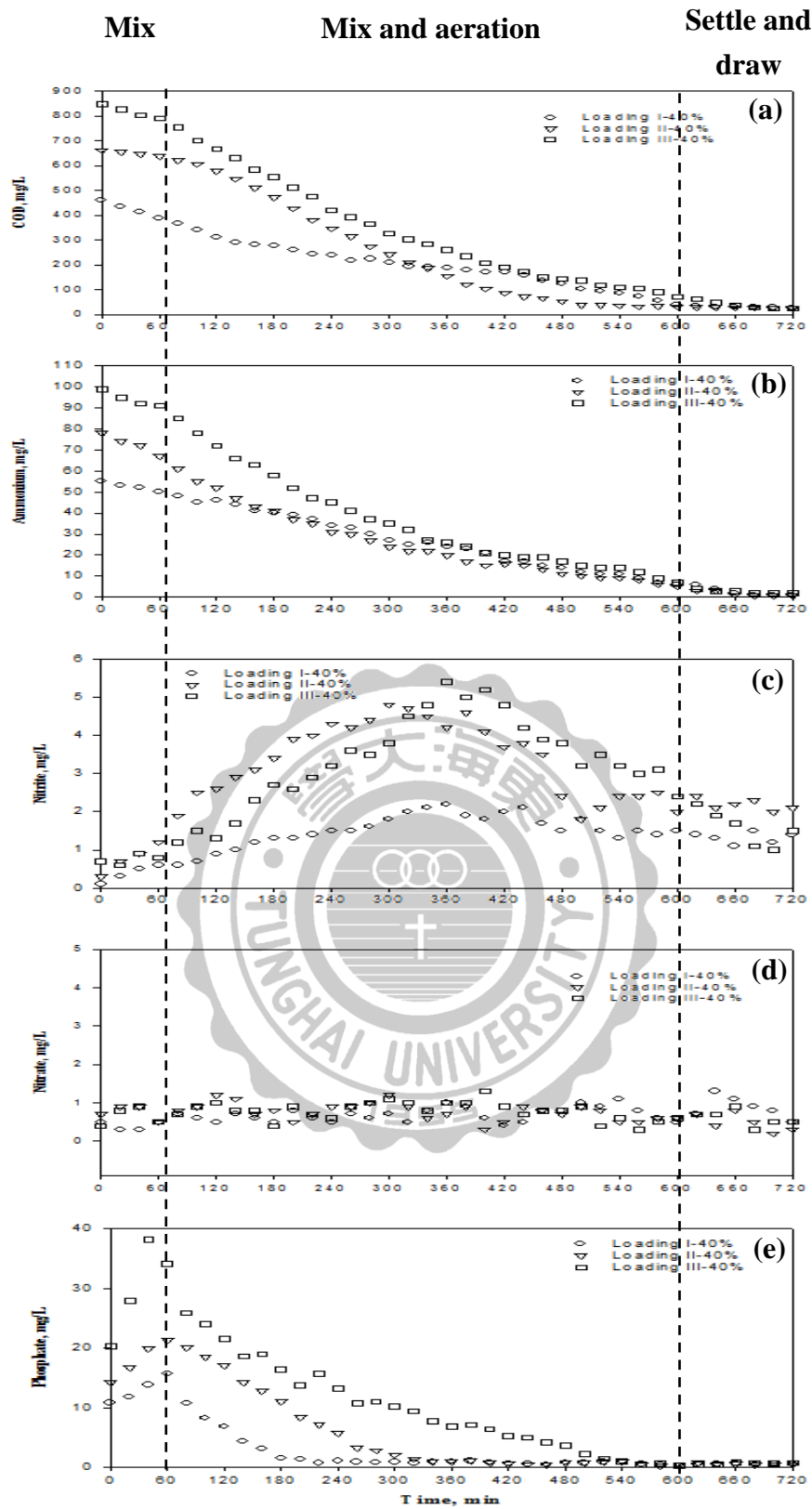


Figure 4-9 Batch profiles of continuous monitoring under three loadings with filling ratio of 40% in the SBBR system (a) COD, (b) Ammonium, (c) Nitrite, (d) Nitrate, (e) Phosphate.

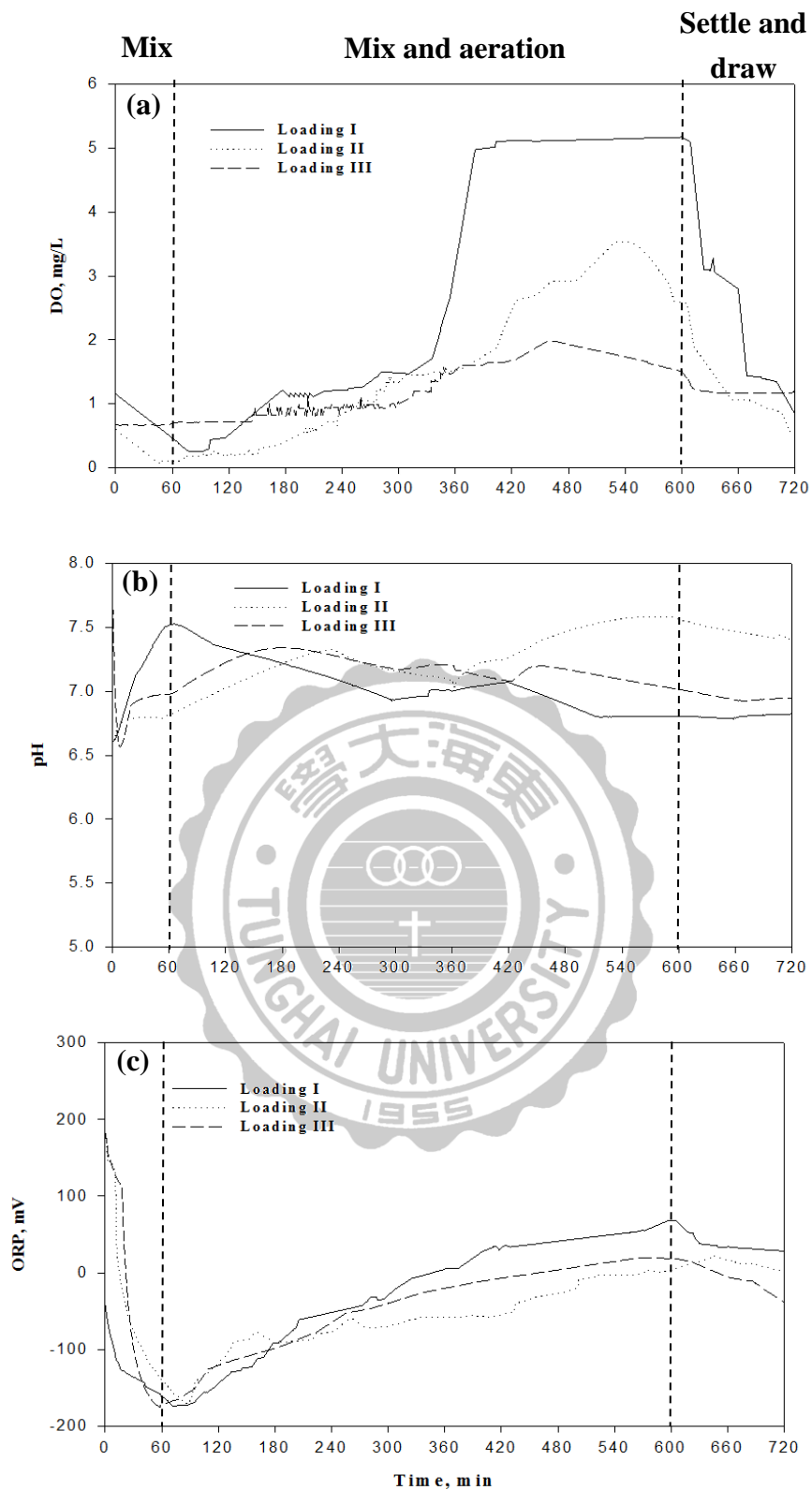


Figure 4-10 Batch profiles of on-line measured parameters under three loadings with filling ratio of 60% in the SBBR system (a) DO, (b) pH and (c) ORP.

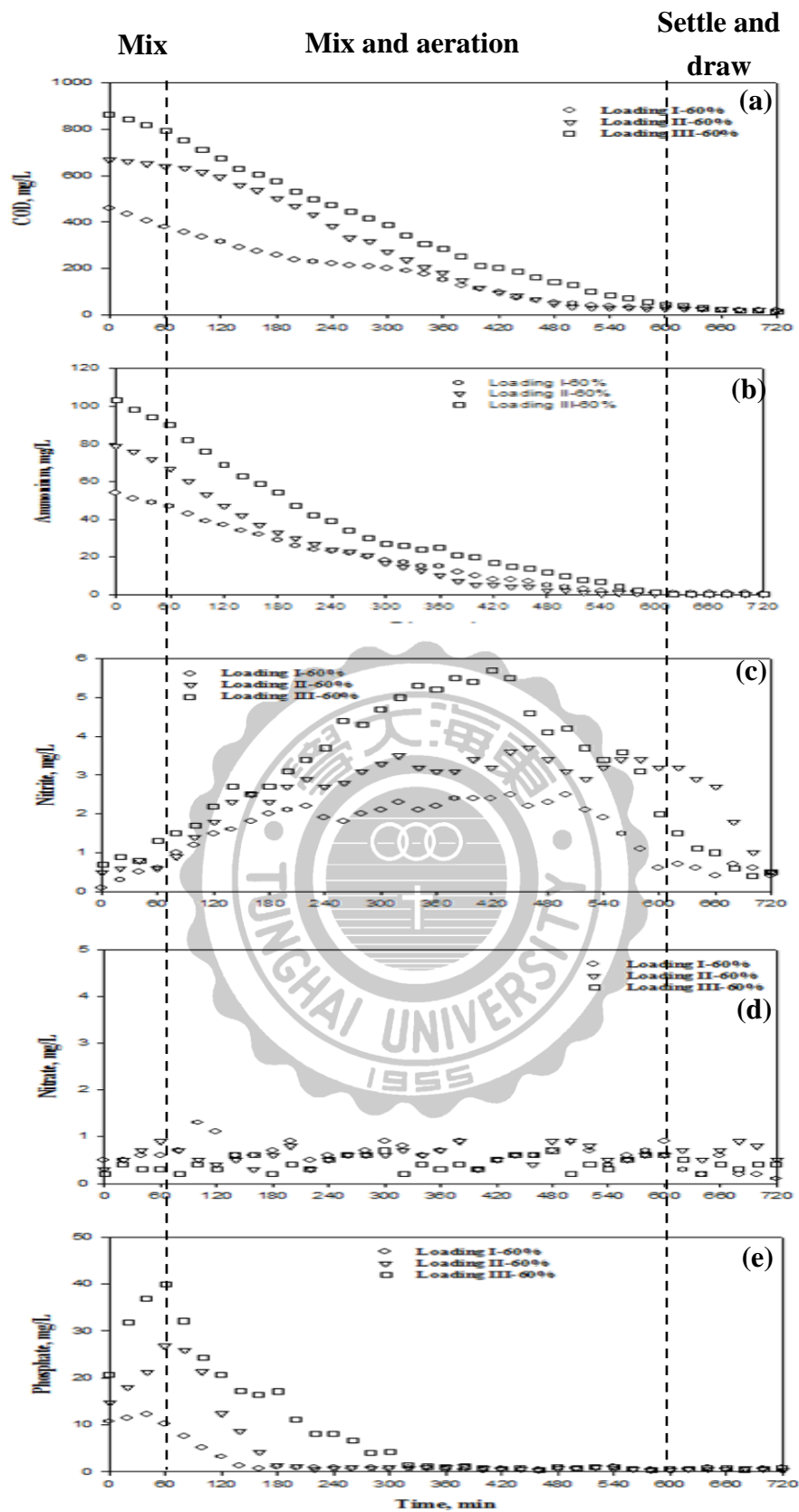


Figure 4-11 Batch profiles of continuous monitoring under three loadings with filling ratio of 60% in the SBBR system (a) COD, (b) Ammonium, (c) Nitrite, (d) Nitrate, (e) Phosphate.

4.3.3 Hydroxylamine produced in two SBBR systems

Hydroxylamine was an intermediate during the nitrification. The amount of hydroxylamine produced which could show the amount of ammonium converted to nitrite. Therefore, the higher influent ammonium concentration would produce more nitrite and hydroxylamine theoretically. Due to the ammonium concentration (about 1-10 mg/L) would affect growth of nitrite-oxidizing bacteria (NOB) but growing of ammonium-oxidizing bacteria (AOB) ineffectively (Hellingsa *et al.*, 1998). It could induce the ammonium converted to nitrite that produced few nitrate. The hydroxylamine would be generated when nitrification carried out the mix and aeration step. Figure 4-12 showed hydroxylamine was produced in SBBR-60% more than in SBBR-40% which two systems were the same phase.

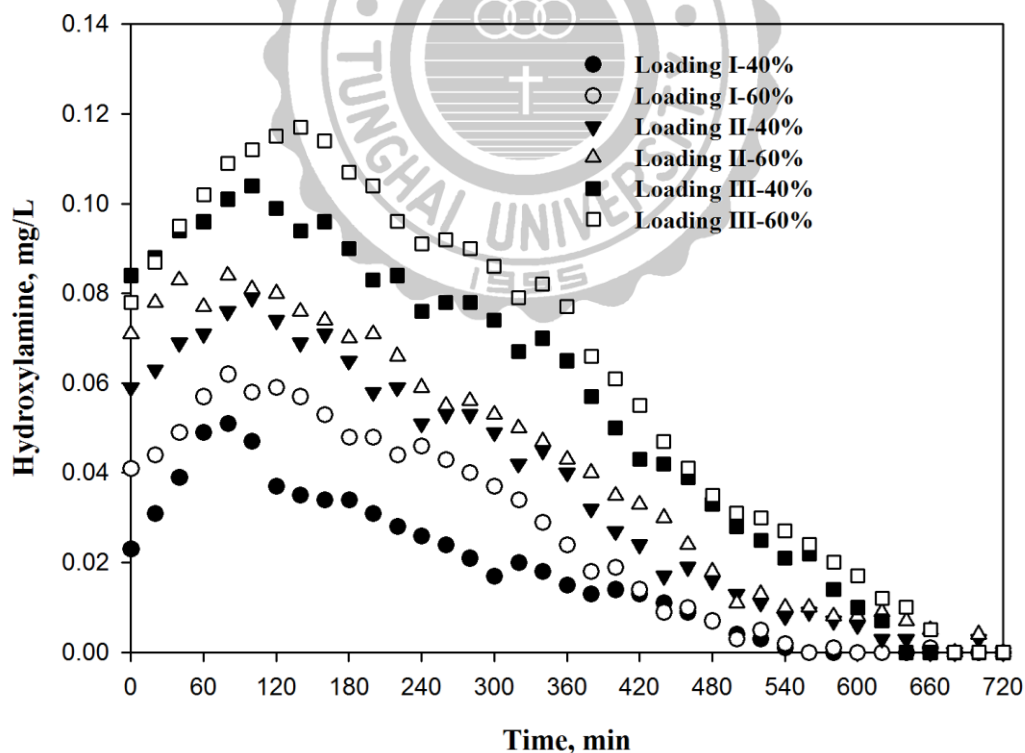


Figure 4-12 Concentration profiles of hydroxylamine under three loadings with filling ratio of 40% and 60% in the SBBR systems.

The influent ammonium concentration increased from phase I to phase III as well as the generation of hydroxylamine. When SBBR system started the mix and aeration step at 60 min, the hydroxylamine was on the rise and reduced gradually during ammonium removed completely.

4.3.4 Biomass growth of two SBBR systems

The carrier pellets were took out from two filling ratios of 40% and 60% to analyze biomass every 10 days. The carrier pellets would dry at 105°C and measured the weight until constant weight. After measuring, the carrier pellets would be marked and put back in two SBBR systems. The weight variations of biomass on carrier pellets in two SBBR systems were showed in Figure 4-13. The total growth of biomass in filling ratios of 40% and 60% were 9.2 g and 34.2g. The total growth biomass of SBBR-40% in this study was more than Wu's previous study with 11.2 g. Figure 4-14 showed the total growth profiles of biomass in this study and previous Wu's study. The total growth of biomass in this study had a significant increase compared with previous study. It meant that the ratios of carrier pellets enhanced in the SBBR systems beneficially to growth of biomass. Furthermore, the denitrifier bacteria would be good to perform the reduction of nitrite in the biofilm that balanced the nitrification and denitrification rate to increase the nitrogen removal efficiency of whole SBBR system.

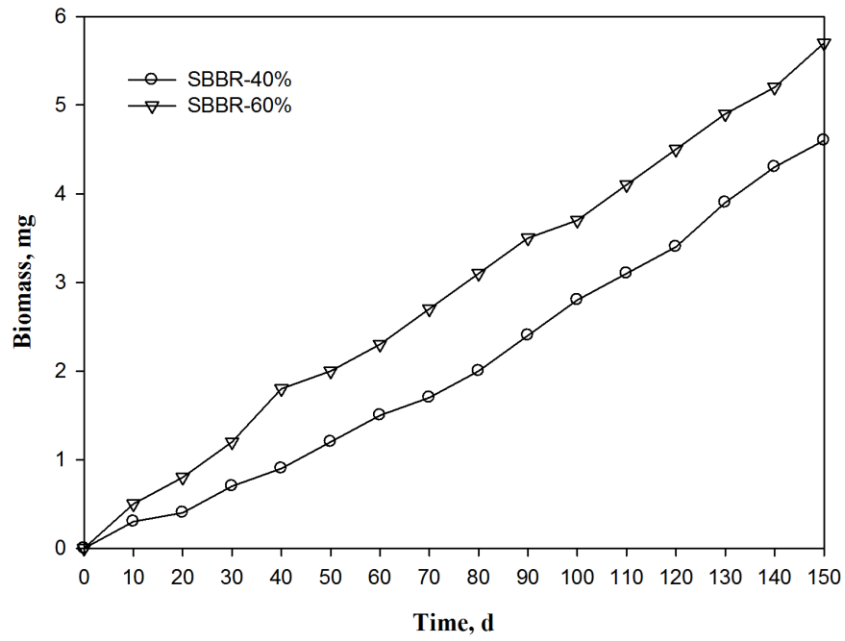


Figure 4-13 Growth profiles of biomass in two SBBR systems in each pellet.

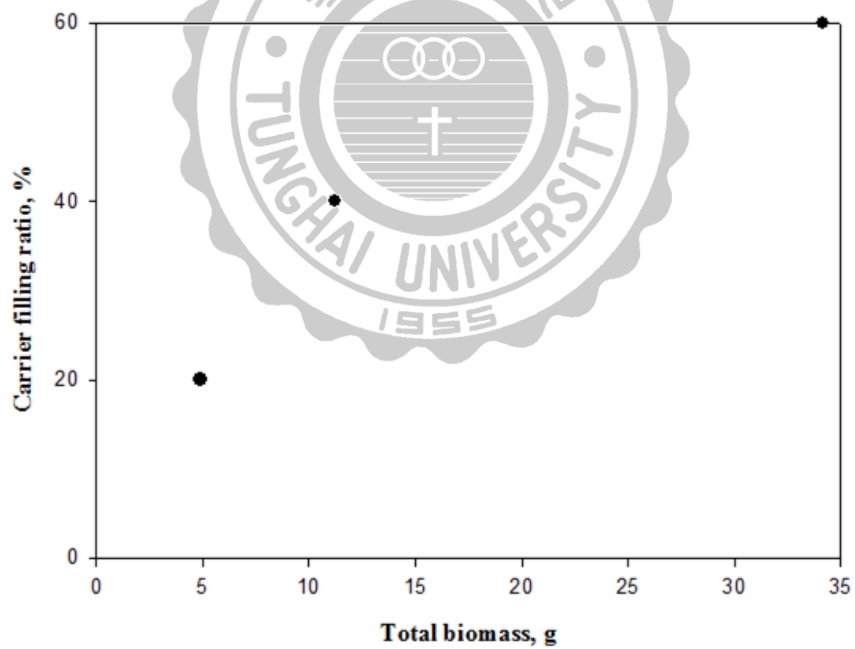


Figure 4-14 Total growth profiles of biomass in this study and previous study.

4.3.5 Compared removal rate with filling ratio of carrier pellets

Many references indicated the removal rate of ammonium depended upon the filling ratio of carriers as biofilm (Jin *et al.*, 2012b; Guo *et al.*, 2014; Yin *et al.*, 2015). Filling higher ratio of carrier would cause to produce thick biofilm. The carrier were filled in the reactor would reserve the majority biomass to avoid decreasing biomass loss. More carrier pellets were filled in SBBR system that could be conducive to denitrifier bacteria to grow and denitrification step (Park *et al.*, 2002; Jin *et al.*, 2012b). The different filling ratio and removal rate of ammonium and COD which the value compared with other references were showed in Table 4-5. The result indicated that filling ratio reached above 25% for a good removal rate of COD and ammonium in the SBBR system.

Table 4-5 Comparison of removal concentration of different filling ratios in this study and other references.

Wastewater	Carrier filling ratio (%)	Removal concentration (mg/L)		Reference
		NH ₄ ⁺	COD	
Synthesis	40	99 - 2	848 - 23	This study
	60	103 - 0	864 - 15	
Synthesis	20	90 - 5	750 - 27	Wu (2012)
	40	91 - 4	756 - 25	
Municipal	30	37 - 3	410 - 50	Yin <i>et al.</i> (2015)
Domestic	25	90 - 2	450 - 55	Ding <i>et al.</i> (2011)
Domestic	30	79 - 2	276 - 15	Guo <i>et al.</i> (2014)
Municipal	10	90 - 17	460 - 30	Jin <i>et al.</i> (2012b)

4.4 Comparison of the K_N , K_{DN} and SND efficiency of two SBBR systems

Due to this study showed few nitrite and nitrate produced at aeration stage so it indicated the efficient SND process occurred in the SBBR system. Some reports proposed the nitrification and denitrification rate were in a balance equilibrium that would produce low amount of NO_x in SBBR system (Munch *et al.*, 1996; Zeng *et al.*, 2003). The equation of SND efficiency (4-1) was used to calculate efficiency of the SND process (Third *et al.*, 2003).

$$Efficiency_{SND} (\%) = \left(1 - \frac{NO_x^- \text{ remained}}{NH_4^+ \text{ oxidized}} \right) \times 100\% \quad (4-1)$$

where NH_4^+ oxidized was the NH_4^+ oxidized after reaction, NO_x^- remained was the NO_x^- remained after reaction.

Table 4-6 summarized the calculated nitrification rate (K_N), denitrification rate (K_{DN}) and the SND efficiency. The results showed SND efficiencies in this study ranged between 97 – 99% which had a higher performance to compare with other references. The nitrification rate ($K_N = 9.7 \text{ mg } NH_4^+ \text{-N/ L-hr}$) and denitrification rate ($K_{DN} = 9.5 \text{ mg } NO_x^- \text{N/L-hr}$) of SBBR-60% system were obvious higher than SBBR-40% system with $K_N = 8.8 \text{ mg } NH_4^+ \text{-N/ L-hr}$ and $K_{DN} = 8.4 \text{ mg } NO_x^- \text{N/L-hr}$ under phase III. The results of SBBR-40% system in this study also had a similar performance with previous Wu's study. But SND efficiency during two studies had no significant variations. Both all studies had high SND efficiencies. The K_N and K_{DN} of SBBR-60% under phase III had better than others. It might be to grow more biomass to increase K_N so that K_{DN} also increased.

Table 4-6 Nitrification rate (K_N), denitrification rate (K_{DN}) and SND efficiency under different systems and comparison with other reported values.

Wastewater		System type	K_N^a	K_{DN}^b	SND efficiency (%)	Reference
Synthesis	Phase I	SBBR-40%	6.2	6.1	97	This study
	Phase II		7.8	7.5	97	
	Phase III		8.8	8.4	98	
Synthesis	Phase I	SBBR-60%	6.5	6.3	97	
	Phase II		8.3	8.0	98	
	Phase III		9.7	9.5	99	
Synthesis	-	SBR	3.3	-	78	Third <i>et al.</i> (2003)
Municipal	-	SHBR ^c	3.6	2.7	75	Wang <i>et al.</i> (2008)
Synthesis	Phase I	SBBR-20%	6.5	6.3	94	Wu (2012)
	Phase II		7.7	7.4	96	
	Phase III		8.3	7.8	96	
Synthesis	Phase I	SBBR-40%	6.8	6.5	97	
	Phase II		7.9	7.6	98	
	Phase III		8.6	7.9	98	
Synthesis	-	MBR	1.5	1.3	80	Paetkau and Cicek (2011)
Municipal	-	SBBR-10%	5.4	4.3	83	Jin <i>et al.</i> (2012b)

^a: Represent unit of nitrification rate (K_N) as $\text{mg NH}_4^+\text{-N/ L-hr}$. ^b: Represent unit of nitrification rate (K_{DN}) as $\text{mg NO}_x^-\text{-N/ L-hr}$.

^c: Sequence Hybrid Biological Reactor.

4.5 Molecular biotechnology analysis

4.5.1 Bacterial community analysis at different SBBR systems by PCR-DGGE and cloning

DGGE method was used to separate the length of base pair was near which between 200 to 900 bps. Figure 4-15 showed the DGGE profiles of 16S rDNA fragments of samples obtained from different SBBR systems during phase III. The results indicated that the length of fragments were too close to separate as a single band so it would cause the noise to affect the result of DNA sequencing subsequently. Therefore, this study was cut the obvious bands to cloning.

The method of molecular cloning would insert the DNA of target fragments (341F/926R) to cloning vector (ligation) and inserted the cloning vector into competent cell (*E. Coli* DH5 α) (transfection) to replicate. After transfection, the *E. Coli* was spread uniformly at LB media which contained the reagent of blue and white screening. The single white colony were selected at random and amplified by PCR (M13F/R) to confirm the colony contained target fragment. The colony contained the target fragments were sequenced by Mission Biotech and BLAST with GenBank.

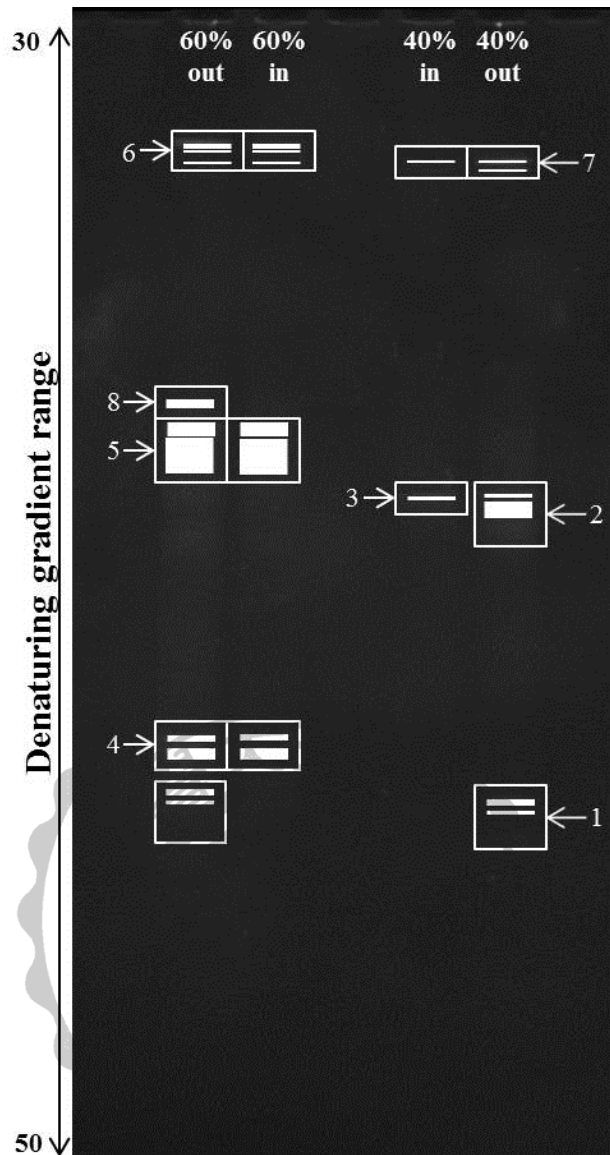
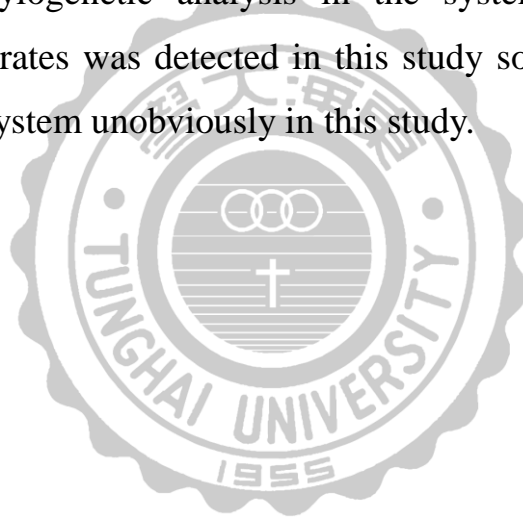


Figure 4-15 DGGE profile of bacterial communities under different SBBR systems. 6% (w/v) polyacrylamide (acrylamide-bisacrylamide (37.5:1)) gel with a denaturing gradient of 30% to 50% and carried out in 1X TAE buffer at 250V for 8h at 60°C.

4.5.2 Phylogenetic analysis

The sequences were rearranged after BLAST with GenBank and utilized the statistical method of Neighbor-joining method to draw the phylogenetic tree. The test of phylogeny used Bootstrap and with number of Bootstrap Replications was 500 times to analyze. Figure 4-16 showed the result of phylogenetic tree at different systems in this study. The results showed the bacteria of nitrifying and denitrifying were existed in the SBBR system. Nitrifying bacteria contained *Nitrospira*, *Nitrosococcus* and *Nitrosomonas*. Denitrifying bacteria included *Ralstonia*, *Azoarcus anaerobius*, *Enhydrobacter aerosaccus*, *Stenotrophomonas*, *Dokdonella immobilis*, *Acinetobacter sp.* and *Propionibacterium*. The function of *Methylophilus* was a bacterium of degradable organics. The AOB was detected in SBBR-60% system which was *Nitrosococcus* and *Nitrosomonas*. The NOB was detected in SBBR-40% and SBBR-60% systems which were *Nitrospira*. In addition, *Ralstonia* utilized hydrogen gas as an electron donor to enforce denitrification that might occur in the internal biofilm. The species of *Dokdonella* which belonged to the family *Xanthomonadaceae* and might be an aerobic denitrifier was indicated (Yoon *et al.*, 2006). Another aerobic denitrifier was *Acinetobacter sp.* which also indicated was a heterotrophic nitrifying–aerobic denitrifying bacterium. (Huang *et al.*, 2013; Yao *et al.*, 2013). Most denitrifying bacteria belonged to heterotrophic that could prove degradable of COD in the reactors. The bacterial community of SBBR-60% was more complex than SBBR-40% that the reason might be related to carrier pellet filling ratio. Therefore, K_N and K_{DN} of SBBR-60% were better than SBBR-40%. Due to low DO controlled in the SBBR system during the phase III so that decreased second step of nitrification occur to convert nitrite to nitrate (nitrataion).

The nitrifier bacteria belonged to autotrophic that carried out the first step nitrification without consuming organics. In addition, the denitrifier bacteria were part to heterotrophic performed the next step reduction with utilizing organic carbon which converted the nitrite and few nitrate to nitrogen gas. Due to *Nitrosomonas europaea* was a standard to verify nitrification process and pathway of nitrifier denitrification. However, the aerobic denitrifier (*Acinetobacter sp.*) was indicated to utilize nitrite as substrate to perform the reduction of nitrite later and few nitrates accumulation (Lu *et al.*, 2011). Therefore, the pathway of this study might perform most of nitrification, nitrifier denitrification which surmised the results of phylogenetic analysis in the system. As a result of production few nitrates was detected in this study so denitrification and carried out in the system unobviously in this study.



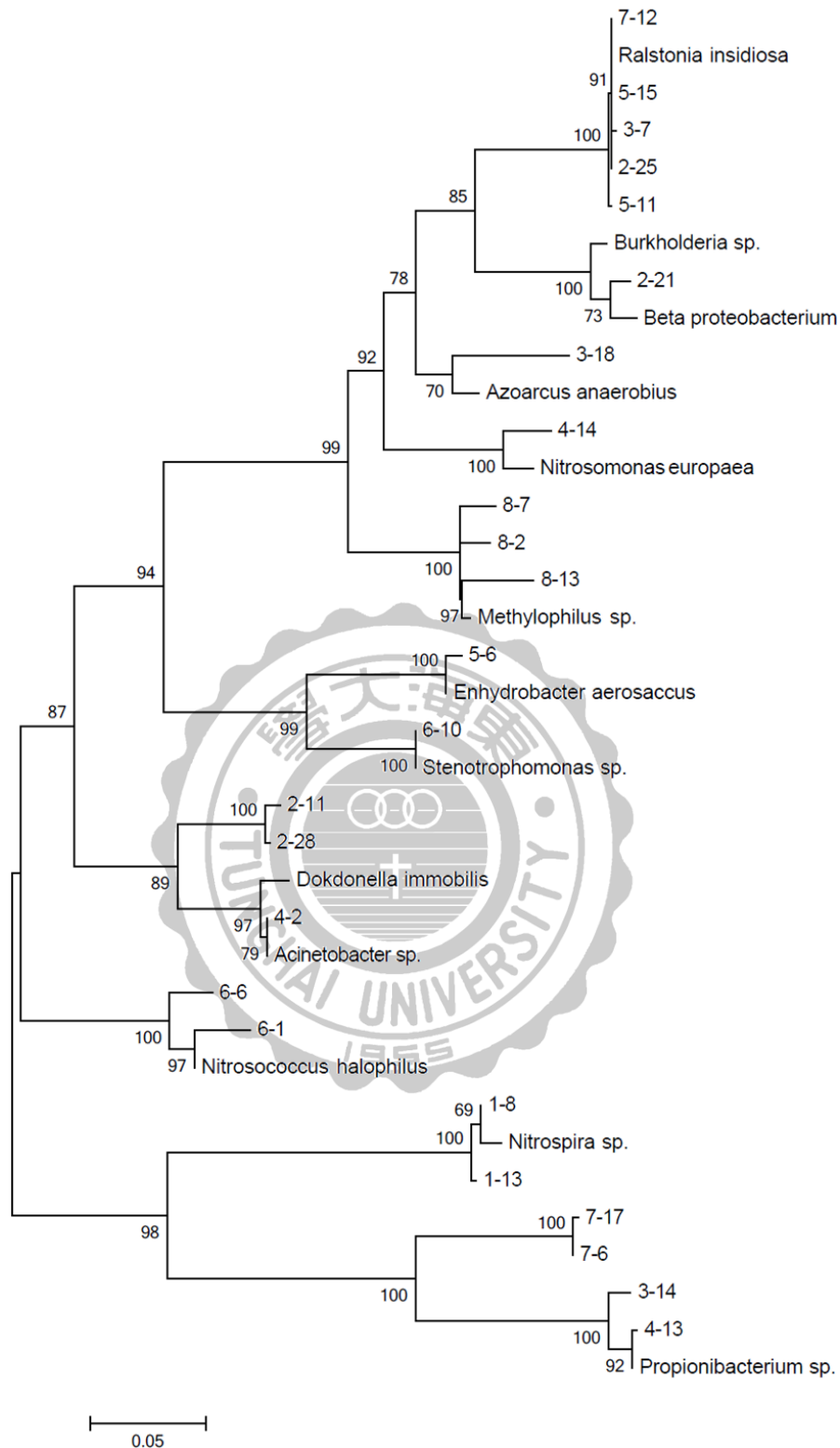


Figure 4-16 Phylogenetic tree of cloning from band of DGGE in two different SBBR systems. The phylogenetic tree of the interrelationship was constructed by using neighbor-joining method. Bootstrap replication values calculated from 500 times.

4.6 Nernst Equation Model Development in SND process

4.6.1 Nernst equation in the overall SND process

An efficient SND system occurred at the K_N and K_{DN} were in a balanced equilibrium producing low amount of NO_x in the SND system. The generalized Nernst equation to Eq. (4-2) and Eq. (4-3) could be obtained (Chang *et al.*, 2004). Besides, the excessive carbon substrate in the denitrification of SND process, the substrate concentration ($C_xH_yO_z$) could be assumed. Thence, the Eq. (4-4) could be obtained as following:

$$E = E^0 + \frac{RT}{nF} \ln \left(\frac{[NH_4^+](P_{O_2})^2}{[NO_3^-][H^+][H_2O]} \right) \quad (4-2)$$

$$E = i + j \ln([C_xH_yO_z]) + k \ln([NO_3^-]) + m \ln \left(\left[\frac{1}{OH^-} \right] \right) \quad (4-3)$$

$$E = a'' + b''pH + c'' \log(NO_3^-) + d'' \log(C_xH_yO_z) \quad (4-4)$$

4.6.2 Nernst equation established in the SND process (ammonium and nitrite removal)

Due to the SBBR system contained the anoxic and aerobic in SND process which could apply Nernst equation to simulate. Table 4-7 showed the Nernst equation modeling results of aerobic stages removed nitrogen and phosphate in the SBBR systems. The results of fitted models showed well coefficient of determination (R^2) value was 0.97 – 0.99 that indicated both *Eq. (4-4)* and *Eq. (4-5)* could predict the overall ORP profiles in SBBR systems. Simulation of the experimental data for SND process in the SBBR systems showed in Figure 4-17 that indicated a high correlation. Besides, the Nernst equations of “only mix” and “mix and aeration” were obtained as following *Eq. (4-6)* and *Eq. (4-7)*, respectively. It meant ORP model could be used as the further control strategy of nitrogen removal end point in SBBR systems.

$$E = a' + b'pH + c' \log \frac{[NH_4^+]}{[NO_2^-]} \quad (4-5)$$

$$E = -188.83 - 1.53 \text{ pH} + 31.63 \frac{[NH_4^+]}{[NO_2^-]} \quad (4-6)$$

$$E = -209.12 - 1.29 \text{ pH} - 2.40 \frac{[NH_4^+]}{[NO_2^-]} \quad (4-7)$$

Table 4-7 Results of regressive analysis on the Nernst equation for “only mix” and “mix and aeration” stages in two SBBR systems (ammonium and nitrite removal).

Stage	Nernst equation model constants			
	a'	b'	c'	R ²
Only mix	-188.83	-1.53	31.63	0.997
Mix and aeration	-209.12	-1.29	-2.40	0.971

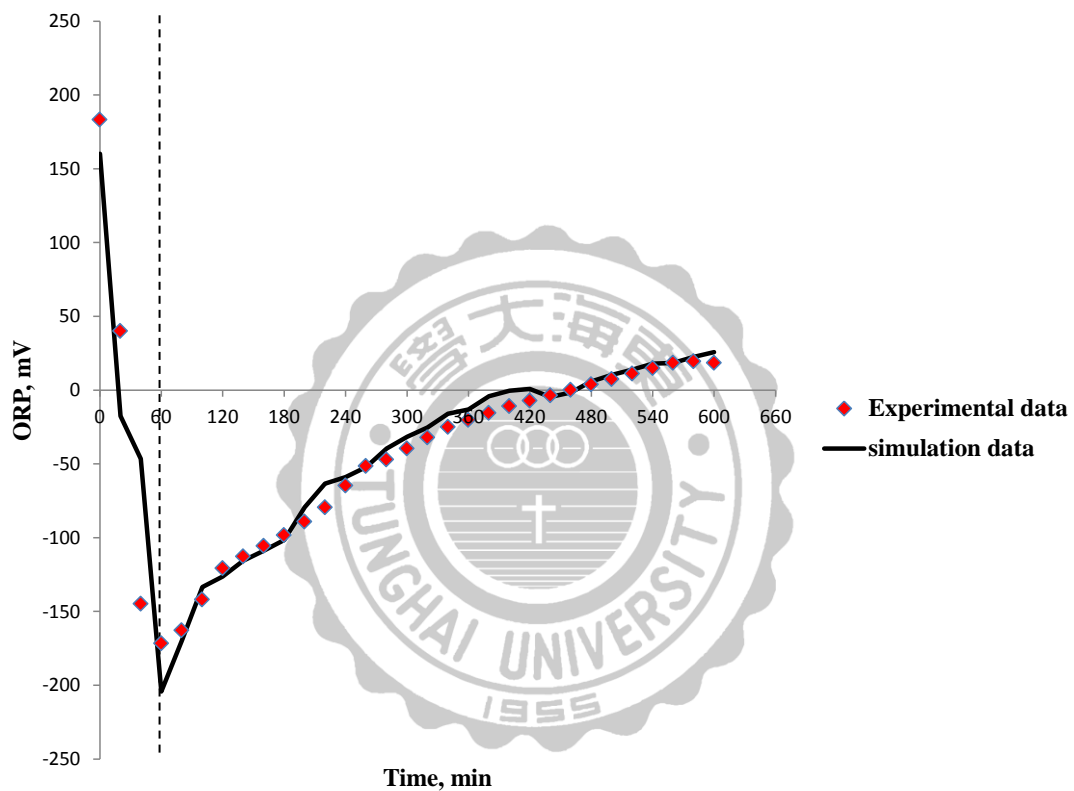


Figure 4-17 Comparison of simulation and experimental ORP profiles (ammonium and nitrite removal) for “only mix” and “mix and aeration” stages of SBBR system with filling ratio 60% carrier pellets.

4.6.3 Nernst equation established in the SND process (ammonium removal)

The Nernst equation which considered only ammonium for excessive carbon sources in SND process showed as (4-8) (Lee, 2004). When the phosphate were removed completely that (4-8) could predict the ammonium concentration in the SBBR system.

$$E = a' + b'pH + c' \ln([NH_4^+]) \quad (4-8)$$

Table 4-8 showed the Nernst equation model constant of mix and aeration stage which only considered ammonium removal in the SBBR systems. The simulation model displayed a good coefficient of determination (R^2) value was 0.993. Simulation of the experimental data for SND process in the SBBR systems in Figure 4-18 indicated a high correlation. The Nernst equation of “mix and aeration” was obtained as following (4-9).

$$E = 201.29 - 23.99 \text{ pH} - 2.28 \ln([NH_4^+]) \quad (4-9)$$

Table 4-8 Results of regressive analysis on the Nernst equation for “mix and aeration” stages in two SBBR systems (only ammonium removal).

Stage	Nernst equation model constants			
	a'	b'	c'	R ²
Mix and aeration	201.29	-23.99	-2.28	0.993

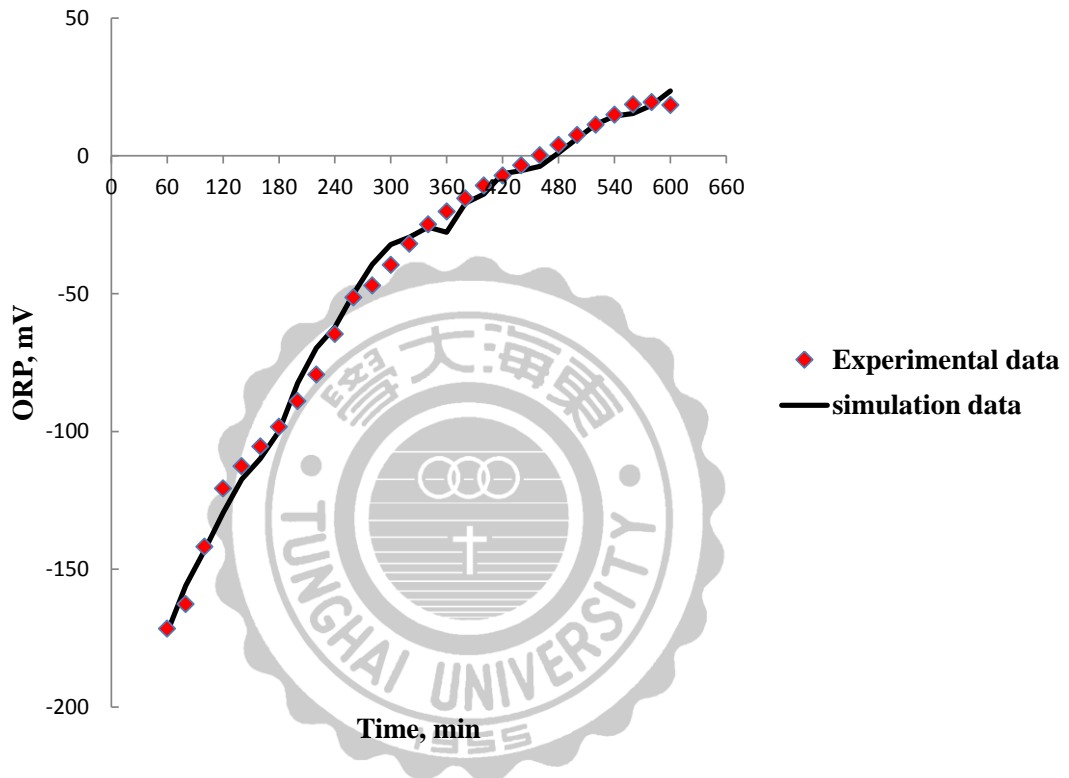


Figure 4-18 Comparison of simulation and experimental ORP profiles (only ammonium removal) for “mix and aeration” stage of SBBR system with filling ratio 60% carrier pellets.

Chapter 5 Conclusions and Suggestions

5.1 Conclusions

In this study, the waste activated sludge was sintered to form spherical pellets and two SBBR systems built with 40% and 60% pellet filling ratios were tested for biological nutrient removal. Both two systems were run with three different loadings to conduct SND reaction.

1. The basic characteristics of sintered raw pellets showed the bulk density was $2.2 \pm 0.5 \text{ g/cm}^3$, water absorption was $52.7 \pm 4.4 \%$, specific external surface area was $2.9 \pm 0.1 \text{ m}^2/\text{g}$ and the compressive strength was $46.1 \pm 1.2 \text{ Kgf/cm}^2$.
2. When the COD/N ratio was 8.2, the COD and ammonium removal efficiencies of SBBR-60% during phase III were 97% and 99%, respectively. The higher NH_2OH released, the more ammonium be converted to nitrite, and the SND efficiency also could increase due to the high K_N in the system.
3. The ammonium removal efficiency found in the SBBR-40% was 98% and 99% in the SBBR-60%. However, the K_N and K_{DN} of SBBR-60% were $9.7 \text{ mg NH}_4^+ \text{-N/L-hr}$ and $9.5 \text{ mg NO}_x^- \text{-N/L-hr}$ which were better than the K_N and K_{DN} of SBBR-40% were $8.3 \text{ mg NH}_4^+ \text{-N/L-hr}$ and $7.8 \text{ mg NO}_x^- \text{-N/L-hr}$.
4. Based on the results of phylogenetic analysis, the autotrophic bacteria such as *Nitrosococcus* and *Nitrosomonas* were detected in the SBBR-60% which converted ammonium to nitrite. Due to DO maintain at 0.8-1.6 mg/L during phase III in the SBBR-60% that conducted the SND process occurred. Therefore, the result of low DO was conducive to growth of heterotrophic denitrifier. Moreover, the

species of *Dokdonella* which belonged to the family *Xanthomonadaceae* and might be an aerobic denitrifier was indicated. Another aerobic denitrifier (*Acinetobacter sp.*) was indicated to utilize nitrite as substrate to perform later the reduction of nitrite and few nitrates accumulation. The bacterial community of SBBR-60% was detected more denitrifier and AOB than SBBR-40% that caused the K_N and K_{DN} had a significant difference during the phase III. The pathway of this study might perform most of nitrification, nitrifier denitrification which surmised that the results of phylogenetic analysis in the system.

5. According to the amount of biomass that the total growth of biomass in SBBR-60% was more than SBBR-40%. It meant the SBBR-60% provided a suitable surrounding of growing biomass and conducted SND process.

5.2 Suggestion

1. Each loading is necessary to analyze DNA identification that would understand the variation of bacterial community in different loading and be in favor of adjusting operating conditions of SBBR.
2. Decreasing the carbon/nitrogen ratio and increased the influent ammonium loading to investigate overall nitrogen removal rate.
3. Control the DO concentration ranges 0.5-1 mg/L to inhibit the occurrence of second step nitrification (nitrification) that accomplishes complete nitrification to reduce oxygen consumption and organic carbon demand.

Reference

Ahn, Y.H. (2006). Sustainable nitrogen elimination biotechnologies: A review. *Process Biochem*, 41(8), pp. 1709-1721.

APHA, (2005). *Standard Methods for the Examination of Water and Wastewater*, 21st ed. American Public Health Association, Washington, DC.

Bagheri, M., Mirbagheri, S.A., Ehteshami, M., Bagheri, Z. (2015). Modeling of a sequencing batch reactor treating municipal wastewater using multi-layer perceptron and radial basis function artificial neural networks. *Process Saf Environ*, 93, pp. 111-123.

Bhatty, J.I., Redit, K.J. (1989). Moderate strength concrete from lightweight sludge ash aggregates. 11(3), pp. 179-187.

Boopathy, R., Bonvillain, C., Fontenot, Q., Kilgen, M. (2007). Biological treatment of low-salinity shrimp aquaculture wastewater using sequencing batch reactor. *Int Biodeter Biodegr*, 59(1), pp. 16-19.

Chang, C.N., Cheng, H.B., Chao, A.C. (2004). Applying the nernst equation to simulate redox potential variations for biological nitrification and denitrification processes. *Environ Sci Technol*, 38(6), pp. 1807-1812.

Cheeseman, C.R., Sollars, C., McEntee, S. (2003). Properties, microstructure and leaching of sintered sewage sludge ash. *Resour Conserv Recy*, 40(1), pp. 13-25.

Chen, C.H. (2005). *Recovery of Industrial Waste Activated Sludge by Baking Technology*. Master Thesis, Department of Environmental Science and Engineering, Tunghai University, Taichung, ROC.

Chen, H.H. (2008). *Research on Performance of Wastewater Purification Unit and Recycling of Wastewater and sludge Dewatering of In-Site in Feng Shan Wate Treatment Plant*. Master Thesis, Institute of Environmental Engineering, National Sun Yat-sen University, Kaohsiung, ROC.

Chiang, Y.P., Liang, Y.Y., Chang, C.N., Chao, A.C. (2006). Differentiating ozone direct and indirect reactions on decomposition of humic substances. *Chemosphere*, 65(11), pp. 2395-2400.

Chinelatto, A.S.A., Chinelatto, A.L., Ojaimi, C.L., Ferreira, J.A., Pallone, E.M.D.A. (2014). Effect of sintering curves on the microstructure of alumina-zirconia nanocomposites. *Ceram Int*, 40(9), pp. 14669-14676.

Chiu, Y.C., Lee, L.L., Chang, C.N., Chao, A.C. (2007). Control of carbon and ammonium ratio for simultaneous nitrification and denitrification in a sequencing batch bioreactor. *Int Biodeter Biodegr*, 59(1), pp. 1-7.

Chong, L. (2001). *Molecular cloning - A laboratory manual*, 3rd edition. Science, 292(5516), pp. 446-446.

Cocolin, L., Aggio, D., Manzano, M., Cantoni, C., Comi, G. (2002). An application of PCR-DGGE analysis to profile the yeast populations in raw milk. *Int Dairy J*, 12(5), pp. 407-411.

Cusido, J.A., Soriano, C. (2011). Valorization of pellets from municipal WWTP sludge in lightweight clay ceramics. *Waste Manage*, 31(6), pp. 1372-1380.

Czerwionka, K., Makinia, J., Pagilla, K.R., Stensel, H.D. (2012). Characteristics and fate of organic nitrogen in municipal biological nutrient removal wastewater treatment plants. *Water Res*, 46(7), pp. 2057-2066.

da Silva, J.C.G.E., Dias, J.R.M., Magalhaes, J.M.C.S. (2001). Factorial analysis of a chemiluminescence system for bromate detection in water. *Anal Chim Acta*, 450(1-2), pp. 175-184.

Daniel, L.M.C., Pozzi, E., Foresti, E., Chinalia, F.A. (2009). Removal of ammonium via simultaneous nitrification-denitrification nitrite-shortcut in a single packed-bed batch reactor. *Bioresource Technol*, 100(3), pp. 1100-1107.

Das, D., Badri, P.K., Kumar, N., Bhattacharya, P. (2002). Simulation and modeling of continuous H₂ production process by *Enterobacter cloacae* IIT-BT 08 using different bioreactor configuration. *Enzyme Microb Tech*, 31(6), pp. 867-875.

de Silva, D.G.V., Urbain, V., Abeyasinghe, D.H., Rittmann, B.E. (1998). Advanced analysis of membrane-bioreactor performance with aerobic-anoxic cycling. *Water Sci Technol*, 38(4-5), pp. 505-512.

Dewil, R., Baeyens, J., Neyens, E. (2005). Fenton peroxidation improves the drying performance of waste activated sludge. *J Hazard Mater*, 117(2-3), pp. 161-170.

Ding, D.H., Feng, C.P., Jin, Y.X., Hao, C.B., Zhao, Y.X., Suemura, T. (2011). Domestic sewage treatment in a sequencing batch biofilm reactor (SBBR) with an intelligent controlling system. *Desalination*, 276(1-3), pp. 260-265.

Donatello, S., Cheeseman, C.R. (2013). Recycling and recovery routes for incinerated sewage sludge ash (ISSA): A review. *Waste Manage*, 33(11), pp. 2328-2340.

Duan, L., Jiang, W., Song, Y.H., Xia, S.Q., Hermanowicz, S.W. (2013). The characteristics of extracellular polymeric substances and soluble microbial products in moving bed biofilm reactor-membrane bioreactor. *Bioresource Technol*, 148, pp. 436-442.

Edwards, U., Rogall, T., Blocker, H., Emde, M., Bottger, E.C. (1989). Isolation and Direct Complete Nucleotide Determination of Entire Genes - Characterization of a Gene Coding for 16s-Ribosomal Rna. *Nucleic Acids Res*, 17(19), pp. 7843-7853.

Fan, A.M., Steinberg, V.E. (1996). Health implications of nitrate and nitrite in drinking water: An update on methemoglobinemia occurrence and reproductive and developmental toxicity. *Regul Toxicol Pharm*, 23(1), pp. 35-43.

Fang, P., Tang, Z.J., Huang, J.H., Cen, C.P., Tang, Z.X., Chen, X.B.

(2015). Using sewage sludge as a denitration agent and secondary fuel in a cement plant: A case study. 137, pp. 1-7.

Fasoli, S., Marzotto, M., Rizzotti, L., Rossi, F., Dellaglio, F., Torriani, S. (2003). Bacterial composition of commercial probiotic products as evaluated by PCR-DGGE analysis. *Int J Food Microbiol*, 82(1), pp. 59-70.

Feng, L.J., Yang, G.F., Zhu, L., Xu, X.Y., Gao, F., Xu, Y.M. (2015). Enhancement removal of endocrine-disrupting pesticides and nitrogen removal in a biofilm reactor coupling of biodegradable *Phragmites communis* and elastic filler for polluted source water treatment. 187, pp. 331-337.

Ga, C.H., Ra, C.S. (2009). Real-time control of oxic phase using pH (mV)-time profile in swine wastewater treatment. *J Hazard Mater*, 172(1), pp. 61-67.

German, R.M., (1996). *Sintering theory practice*. An Imprint of Wiley.

Ghehi, T.J., Mortezaeifar, S., Gholami, M., Kalantary, R.R., Mahvi, A.H. (2014). Performance evaluation of enhanced SBR in simultaneous removal of nitrogen and phosphorous. *J Environ Health Sci*, 12(134), pp.

Gieseke, A., Arnz, P., Amann, R., Schramm, A. (2002). Simultaneous P and N removal in a sequencing batch biofilm reactor: insights from reactor- and microscale investigations. *Water Res*, 36(2), pp. 501-509.

Gomes, M.D., Santos, D., Nunes, L.C., de Carvalho, G.G.A., Leme, F.D., Krug, F.J. (2011). Evaluation of grinding methods for pellets preparation aiming at the analysis of plant materials by laser induced breakdown spectrometry. *Talanta*, 85(4), pp. 1744-1750.

Gunawan, E.R., Basri, M., Rahman, M.B.A., Salleh, A.B., Rahman, R.N.Z.A. (2005). Study on response surface methodology (RSM) of lipase-catalyzed synthesis of palm-based wax ester. *Enzyme Microb Tech*, 37(7), pp. 739-744.

Guo, J., Peng, Y.Z., Wang, S.Y., Zheng, Y.A., Huang, H.J., Wang, Z.W. (2009). Long-term effect of dissolved oxygen on partial nitrification performance and microbial community structure. *Bioresource Technol*, 100(11), pp. 2796-2802.

Guo, Y.M., Liu, Y.G., Zeng, G.M., Hu, X.J., Xu, W.H., Liu, Y.Q., Liu, S.M., Sun, H.S., Ye, J., Huang, H.J. (2014). An integrated treatment of domestic wastewater using sequencing batch biofilm reactor combined with vertical flow constructed wetland and its artificial neural network simulation study. *Ecol Eng*, 64, pp. 18-26.

Hai, R.T., He, Y.Q., Wang, X.H., Li, Y. (2015). Simultaneous removal of nitrogen and phosphorus from swine wastewater in a sequencing batch biofilm reactor. *Chinese J Chem Eng*, 23(1), pp. 303-308.

Hamer, K., Karius, V. (2002). Brick production with dredged harbour sediments. An industrial-scale experiment. *Waste Manage*, 22(5), pp. 521-530.

Hellinga, C., Schellen, A.A.J.C., Mulder, J.W., van Loosdrecht, M.C.M., Heijnen, J.J. (1998). The SHARON process: An innovative method for nitrogen removal from ammonium-rich waste water. *Water Sci Technol*, 37(9), pp. 135-142.

Henze, M., Van Loosdrecht, M.C.M., Ekama, G.A., Brdjanovic, D., (2008). *Biological Wastewater Treatment: Principles, Modelling and Design*. IWA Publishing, London, UK.

Hesham, A., Qi, R., Yang, M. (2011). Comparison of bacterial community structures in two systems of a sewage treatment plant using PCR-DGGE analysis. *J Environ Sci-China*, 23(12), pp. 2049-2054.

Holakoo, L., Nakhla, G., Bassi, A.S., Yanful, E.K. (2007). Long term performance of MBR for biological nitrogen removal from synthetic municipal wastewater. *Chemosphere*, 66(5), pp. 849-857.

Huang, C.H., Wang, S.Y. (2013). Application of water treatment sludge in the manufacturing of lightweight aggregate. *Constr Build Mater*, 43, pp.

174-183.

Huang, H.H. (2010). Recycled the wasted sludge to rebuild the nutrient biofilm carrier in simultaneous nitrification and denitrification (SND) system by design of experiment (DOE). Master Thesis, Department of Environmental Science and Engineering, Tunghai University, Taichung, ROC.

Huang, X.F., Li, W.G., Zhang, D.Y., Qin, W. (2013). Ammonium removal by a novel oligotrophic *Acinetobacter* sp Y16 capable of heterotrophic nitrification-aerobic denitrification at low temperature. *Bioresource Technol*, 146, pp. 44-50.

Jefferson, K.K. (2004). What drives bacteria to produce a biofilm? *Fems Microbiol Lett*, 236(2), pp. 163-173.

Jenicek, P., Svehla, P., Zabranska, J., Dohanyos, M. (2004). Factors affecting nitrogen removal by nitrification/denitrification. *Water Sci Technol*, 49(5-6), pp. 73-79.

Jin, R.C., Yang, G.F., Yu, J.J., Zheng, P. (2012a). The inhibition of the Anammox process: A review. *Chem Eng J*, 197, pp. 67-79.

Jin, Y.X., Ding, D.H., Feng, C.P., Tong, S., Suemura, T., Zhang, F. (2012b). Performance of sequencing batch biofilm reactors with different control systems in treating synthetic municipal wastewater. *Bioresource Technol*, 104, pp. 12-18.

Joss, A., Salzgeber, D., Eugster, J., Konig, R., Rottermann, K., Burger, S., Fabijan, P., Leumann, S., Mohn, J., Siegrist, H. (2009). Full-Scale Nitrogen Removal from Digester Liquid with Partial Nitrification and Anammox in One SBR. *Environ Sci Technol*, 43(14), pp. 5301-5306.

Jun, L., Peng, Y.Z., Gu, G.W., Wei, S. (2007). Factors affecting simultaneous nitrification and denitrification in an SBBR treating domestic wastewater. 1(2), pp. 246-250.

Kampschreur, M.J., Poldermans, R., Kleerebezem, R., van der Star,

- W.R.L., Haarhuis, R., Abma, W.R., Jetten, M.S.M., van Loosdrecht, M.C.M. (2009). Emission of nitrous oxide and nitric oxide from a full-scale single-stage nitrification-anammox reactor. *Water Sci Technol*, 60(12), pp. 3211-3217.
- Kim, C.G., Lee, H.S., Yoon, T. (2003). Resource recovery of sludge as a micro-media in an activated sludge process. *Adv Environ Res*, 7(3), pp. 629-633.
- Kim, E.H., Cho, J.K., Yim, S. (2005). Digested sewage sludge solidification by converter slag for landfill cover. *Chemosphere*, 59(3), pp. 387-395.
- Kose, S., Bayer, G. (1982). Schaumbildung im System Altglas-SiC und die Eigenschaften derartiger Schaumgläser. 55(7), pp. 151-160.
- Kulkarni, P. (2013). Nitrophenol removal by simultaneous nitrification denitrification (SND) using *T. pantotropha* in sequencing batch reactors (SBR). *Bioresource Technol*, 128, pp. 273-280.
- Lafhaj, Z., Samara, M., Agostini, F., Boucard, L., Skoczylas, F., Depelsenaire, G. (2008). Polluted river sediments from the North region of France: Treatment with Novosol (R) process and valorization in clay bricks. *Constr Build Mater*, 22(5), pp. 755-762.
- Lee, L.L. (2004). The feasibility study of establishing automatic control strategy in simultaneous nitrification and denitrification (SND). Master, Department of Environmental Science and Engineering, Tunghai University, Taichung, ROC.
- Li, L., Fan, M., Brown, R.C., Koziel, J.A., van Leeuwenach, J. (2009). Production of a new wastewater treatment coagulant from fly ash with concomitant flue gas scrubbing. *J Hazard Mater*, 162(2-3), pp. 1430-1437.
- Lin, D.F., Weng, C.H. (2001). Use of sewage sludge ash as brick material. *J Environ Eng-Asce*, 127(10), pp. 922-927.

- Liu, Y., Lin, Y.M., Yang, S.F., Tay, J.H. (2003). A balanced model for biofilms developed at different growth and detachment forces. *Process Biochem*, 38(12), pp. 1761-1765.
- Lu, C., Zhang, F.J., Lu, Y., Liu, Y., Zhong, S., (2011). Screening and identification of aerobic denitrifier with nitrite as substrate. *IEEE, Hohhot*, pp. 3418 - 3421.
- Ma, Y., Sundar, S., Park, H., Chandran, K. (2015). The effect of inorganic carbon on microbial interactions in a biofilm nitrification-anammox process. *Water Res*, 70, pp. 246-254.
- Mudliar, S., Banerjee, S., Vaidya, A., Devotta, S. (2008). Steady state model for evaluation of external and internal mass transfer effects in an immobilized biofilm. *Bioresour Technol*, 99(9), pp. 3468-3474.
- Munch, E.V., Lant, P., Keller, J. (1996). Simultaneous nitrification and denitrification in bench-scale sequencing batch reactors. *Water Res*, 30(2), pp. 277-284.
- Muyzer, G., Dewaal, E.C., Uitterlinden, A.G. (1993). Profiling of Complex Microbial-Populations by Denaturing Gradient Gel-Electrophoresis Analysis of Polymerase Chain Reaction-Amplified Genes-Coding for 16s Ribosomal-Rna. *Appl Environ Microb*, 59(3), pp. 695-700.
- Muyzer, G., Smalla, K. (1998). Application of denaturing gradient gel electrophoresis (DGGE) and temperature gradient gel electrophoresis (TGGE) in microbial ecology. *Anton Leeuw Int J G*, 73(1), pp. 127-141.
- Nagaoka, H. (1999). Nitrogen removal by submerged membrane separation activated sludge process. *Water Sci Technol*, 39(8), pp. 107-114.
- Ni, S.Q., Meng, J. (2011). Performance and inhibition recovery of anammox reactors seeded with different types of sludge. *Water Sci Technol*, 63(4), pp. 710-718.

Nowok, J.W., Benson, S.A., Jones, M.L., Kalmanovitch, D.P. (1990). Sintering Behavior and Strength Development in Various Coal Ashes. *Fuel*, 69(8), pp. 1020-1028.

Paetkau, M., Cicek, N. (2011). Comparison of nitrogen removal and sludge characteristics between a conventional and a simultaneous nitrification-denitrification membrane bioreactor. *Desalination*, 283, pp. 165-168.

Park, S.J., Lee, H.S., Yoon, T.I. (2002). The evaluation of enhanced nitrification by immobilized biofilm on a clinoptilolite carrier. *Bioresource Technol*, 82(2), pp. 183-189.

Peng, M.C. (2002). Ammonia-oxidizing Bacteria in Aquaculture Pond. Master Thesis, Department of Marine Biotechnology and Resources, National Sun Yat-sen University, Kaohsiung, ROC.

Pritchard, L., Corne, D., Kell, D., Rowland, J., Winson, M. (2005). A general model of error-prone PCR. *J Theor Biol*, 234(4), pp. 497-509.

Queiroz, L.M., Aun, M.V., Morita, D.M., Sobrinho, P.A. (2011). Biological Nitrogen Removal over Nitritation/Denitritation Using Phenol as Carbon Source. *Braz J Chem Eng*, 28(2), pp. 197-207.

Rafiei, B., Naeimpoor, F., Mohammadi, T. (2014). Bio-film and bio-entrapped hybrid membrane bioreactors in wastewater treatment: Comparison of membrane fouling and removal efficiency. *Desalination*, 337, pp. 16-22.

Regmi, P., Miller, M.W., Holgate, B., Bunce, R., Park, H., Chandran, K., Wett, B., Murthy, S., Bott, C.B. (2014). Control of aeration, aerobic SRT and COD input for mainstream nitritation/denitritation. *Water Res*, 57, pp. 162-171.

Ruscalleda Beylier, M., Balaguer, M.D., Colprim, J., Pellicer-Nàcher, C., Ni, B.J., Smets, B.F., Sun, S.P., Wang, R.C. (2011). Biological Nitrogen Removal from Domestic Wastewater. 6, pp. 329-340.

- Saby, S., Djafer, M., Chen, G.H. (2002). Feasibility of using a chlorination step to reduce excess sludge in activated sludge process. *Water Res*, 36(3), pp. 656-666.
- Sanchez-Monedero, M.A., Mondini, C., de Nobili, M., Leita, L., Roig, A. (2004). Land application of biosolids. Soil response to different stabilization degree of the treated organic matter. *Waste Manage*, 24(4), pp. 325-332.
- Santos, D., Nunes, L.C., de Carvalho, G.G.A., Gomes, M.D., de Souza, P.F., Leme, F.D., dos Santos, L.G.C., Krug, F.J. (2012). Laser-induced breakdown spectroscopy for analysis of plant materials: A review. *Spectrochim Acta B*, 71-72, pp. 3-13.
- Semmens, M.J., Dahm, K., Shanahan, J., Christianson, A. (2003). COD and nitrogen removal by biofilms growing on gas permeable membranes. *Water Res*, 37(18), pp. 4343-4350.
- Shahabadi, S.M.S., Reyhani, A. (2014). Optimization of operating conditions in ultrafiltration process for produced water treatment via the full factorial design methodology. *Sep Purif Technol*, 132, pp. 50-61.
- Siegrist, H., Salzgeber, D., Eugster, J., Joss, A. (2008). Anammox brings WWTP closer to energy autarky due to increased biogas production and reduced aeration energy for N-removal. *Water Sci Technol*, 57(3), pp. 383-388.
- Siripong, S., Rittmann, B.E. (2007). Diversity study of nitrifying bacteria in full-scale municipal wastewater treatment plants. *Water Res*, 41(5), pp. 1110-1120.
- Skrifvars, B.J., Hupa, M., Backman, R., Hiltunen, M. (1994). Sintering Mechanisms of Fbc Ashes. *Fuel*, 73(2), pp. 171-176.
- Stuven, R., Bock, E. (2001). Nitrification and denitrification as a source for NO and NO₂ production in high-strength wastewater. *Water Res*, 35(8), pp. 1905-1914.

- Su, W.F. (2008). Application of recycle porous diffusers in a SND-sequencing batch biofilm reactor (SBBR). Master Thesis, Department of Environmental Science and Engineering, Tunghai University, Taichung, ROC.
- Sun, S.P., Nacher, C.P.I., Merkey, B., Zhou, Q., Xia, S.Q., Yang, D.H., Sun, J.H., Smets, B.F. (2010). Effective Biological Nitrogen Removal Treatment Processes for Domestic Wastewaters with Low C/N Ratios: A Review. *Environ Eng Sci*, 27(2), pp. 111-126.
- Tay, J.H., Yip, W.K. (1989). Sludge Ash as Lightweight Concrete Material. *J Environ Eng-Asce*, 115(1), pp. 56-64.
- Third, K.A., Burnett, N., Cord-Ruwisch, R. (2003). Simultaneous nitrification and denitrification using stored substrate (PHB) as the electron donor in an SBR. *Biotechnol Bioeng*, 83(6), pp. 706-720.
- Tsuneda, S., Ohno, T., Soejima, K., Hirata, A. (2006). Simultaneous nitrogen and phosphorus removal using denitrifying phosphate-accumulating organisms in a sequencing batch reactor. *Biochem Eng J*, 27(3), pp. 191-196.
- Tuan, B.L.A., Hwang, C.L., Lin, K.L., Chen, Y.Y., Young, M.P. (2013). Development of lightweight aggregate from sewage sludge and waste glass powder for concrete. *Constr Build Mater*, 47, pp. 334-339.
- Upadhyaya, G.S. (2001). Some issues in sintering science and technology. *Mater Chem Phys*, 67(1-3), pp. 1-5.
- Volland, S., Brötz, J. (2015). Lightweight aggregates produced from sand sludge and zeolitic rocks. 85, pp. 22-29.
- Volland, S., Kazmina, O., Vereshchagin, V., Dushkina, M. (2014). Recycling of sand sludge as a resource for lightweight aggregates. *Constr Build Mater*, 52, pp. 361-365.
- Wang, J.L., Peng, Y.Z., Wang, S.Y., Gao, Y.Q. (2008). Nitrogen Removal by Simultaneous Nitrification and Denitrification via Nitrite in a

Sequence Hybrid Biological Reactor. *Chinese J Chem Eng*, 16(5), pp. 778-784.

Warburg, O., Christian, W. (1942). Isolierung und kristallisation des garungsferments enolase. 310, pp. 384 - 421.

Weemaes, M., Grootaerd, H., Simoens, F., Verstraete, W. (2000). Anaerobic digestion of ozonized biosolids. *Water Res*, 34(8), pp. 2330-2336.

Weissenbacher, N., Loderer, C., Lenz, K., Mahnik, S.N., Wett, B., Fuerhacker, M. (2007). NO_x monitoring of a simultaneous nitrifying-denitrifying (SND) activated sludge plant at different oxidation reduction potentials. *Water Res*, 41(2), pp. 397-405.

Weng, C.H., Lin, D.F., Chiang, P.C. (2003). Utilization of sludge as brick materials. *Adv Environ Res*, 7(3), pp. 679-685.

Wijffels, R.H., Tramper, J. (1995). Nitrification by Immobilized Cells. *Enzyme Microb Tech*, 17(6), pp. 482-492.

Wolff, E., Schwabe, W.K., Conceição, S.V. (2015). Utilization of water treatment plant sludge in structural ceramics. 96, pp. 282-289.

Won, S.G., Ra, C.S. (2011). Biological nitrogen removal with a real-time control strategy using moving slope changes of pH(mV)- and ORP-time profiles. *Water Res*, 45(1), pp. 171-178.

Wrage, N., Velthof, G.L., van Beusichem, M.L., Oenema, O. (2001). Role of nitrifier denitrification in the production of nitrous oxide. *Soil Biol Biochem*, 33(12-13), pp. 1723-1732.

Wu, Y.T. (2012). Application Hydroxylamine to Identify and Model Simultaneous Nitrification and Denitrification (SND) Process. Master Thesis, Department of Environmental Science and Engineering, Tunghai University, Taichung, ROC.

Xia, S., Li, J., Wang, R. (2008). Nitrogen removal performance and

microbial community structure dynamics response to carbon nitrogen ratio in a compact suspended carrier biofilm reactor. *Ecol Eng*, 32(3), pp. 256-262.

Xu, W., Xu, J.C., Liu, J., Li, H.X., Cao, B., Huang, X.F., Li, G.M. (2014). The utilization of lime-dried sludge as resource for producing cement. *J Clean Prod*, 83, pp. 286-293.

Yao, S., Ni, J.R., Ma, T., Li, C. (2013). Heterotrophic nitrification and aerobic denitrification at low temperature by a newly isolated bacterium, *Acinetobacter* sp HA2. *Bioresource Technol*, 139, pp. 80-86.

Yi, X.S., Shi, W.X., Yu, S.L., Li, X.H., Sun, N., He, C. (2011). Factorial design applied to flux decline of anionic polyacrylamide removal from water by modified polyvinylidene fluoride ultrafiltration membranes. *Desalination*, 274(1-3), pp. 7-12.

Yin, J., Zhang, P.Y., Li, F., Li, G.P., Hai, B.H. (2015). Simultaneous biological nitrogen and phosphorus removal with a sequencing batch reactor biofilm system. pp. 1-6.

Yoon, J.H., Kang, S.J., Oh, T.K. (2006). *Dokdonella koreensis* gen. nov., sp nov., isolated from soil. *Int J Syst Evol Micr*, 56(145-150).

Zeng, R.J., Lemaire, R., Yuan, Z., Keller, J. (2003). Simultaneous nitrification, denitrification, and phosphorus removal in a lab-scale sequencing batch reactor. *Biotechnol Bioeng*, 84(2), pp. 170-178.

Zeng, W., Li, L., Yang, Y.Y., Wang, S.Y., Peng, Y.Z. (2010). Nitritation and denitritation of domestic wastewater using a continuous anaerobic-anoxic-aerobic (A(2)O) process at ambient temperatures. *Bioresource Technol*, 101(21), pp. 8074-8082.

Zhu, G.B., Peng, Y.Z., Wang, S.Y., Wu, S.Y., Ma, B. (2007). Effect of influent flow rate distribution on the performance of step-feed biological nitrogen removal process. *Chem Eng J*, 131(1-3), pp. 319-328.

Zhu, G.B., Peng, Y.Z., Wu, S.Y., Wang, S.Y. (2005). Automatic control

strategy for step feed anoxic/aerobic biological nitrogen removal process.
J Environ Sci-China, 17(3), pp. 457-459.

NIEA, (2004) “一般廢棄物回收清除處理辦法”。

NIEA R205.01C, (2004) “廢棄物中灰份、可燃份測定方法”。

NIEA R201.14C (2004) “事業廢棄物毒性特性溶出程序”。

NIEA W415.52B, (2005) “水中陰離子檢測方法-離子層析法”。

中國國家標準 CNS-487 “細粒料比重及吸水率試驗法”。

中國國家標準 CNS1010 R3032 “水硬性水泥壩料抗壓強度檢驗法”。

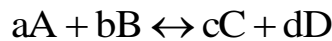


Appendix

Appendix 1

Nernst Equation for a General Oxidation-Reduction Reaction

A general oxidation-reduction reaction can be represented as (a1-1).



A and B: Reactants

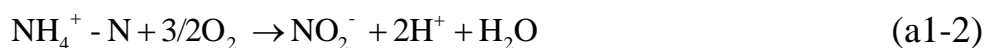
C and D: Products

a, b, c and d: Stoichiometric Coefficients for A, B, C, and D, respectively. All species involved in the chemical reaction are assumed to be dissolved solutes. If the reagent is a pure substrate rather than the component of a solution, the partial molar free energy equal to the free energy of 1 mole of the substrate. The Nernst equation for a general oxidation-reduction reaction can be obtained:

$$E = E^0 - \frac{RT}{nF} \ln \frac{(a_C)^c (a_D)^d}{(a_A)^a (a_B)^b} \quad \text{or} \quad E = E^0 + \frac{RT}{nF} \ln \frac{(a_A)^a (a_B)^b}{(a_C)^c (a_D)^d} \quad (\text{a1-1})$$

Nitrification of immobilized SND process

The process converts ammonium nitrogen to nitrite is a heterotrophic SND process. For the conversion of ammonium nitrogen to nitrite, the following chemical reaction is assumed:



Applying the generalized Nernst Equation to the (a1-2), then (a1-3) is obtained.

$$E = E^0 + \frac{RT}{nF} \ln \left(\frac{[\text{NH}_4^+](P_{\text{O}_2})^2}{[\text{NO}_2^-][\text{H}^+]} \right) \quad (\text{a1-3})$$

The above equation could be further modified as:

$$E = E^0 + \frac{RT}{nF} \ln ([\text{NH}_4^+]) + \frac{2RT}{nF} \ln (P_{\text{O}_2}) + \frac{RT}{nF} \ln \left(\frac{1}{[\text{NO}_2^-]} \right) + \frac{2RT}{nF} \ln \left(\frac{1}{[\text{H}^+]} \right) \quad (\text{a1-4})$$

Both the P_{O_2} and temperature in (a1-4) are assumed unchanged during the nitrification of the SND process, and regarded as constants. Replacing

$\ln \left(\frac{1}{[\text{H}^+]} \right)$ for $2.3026 \times (\text{pH})$, (a1-5) is obtained.

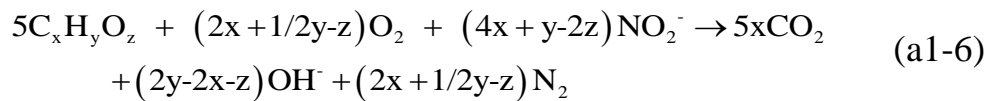
$$E = a' + b' \text{pH} + c' \log \left[\frac{[\text{NH}_4^+]}{[\text{NO}_2^-]} \right] \quad (\text{a1-5})$$

The three constants, a' , b' , and c' are defined as:

$$\begin{aligned} a' &= E^0 + \frac{2RT}{nF} \ln P_{\text{O}_2} \\ b' &= \frac{2.302 \times 2RT}{nF} \\ c' &= \frac{2.306 \times RT}{nF} \end{aligned}$$

Denitrification of immobilized SND process

The main biological denitrification converts nitrite to nitrogen gas under oxic condition is heterotrophic and can be expressed with the following generic stoichiometric (a1-6)



Applying the generalized Nernst equation for the denitification of SND process is:

$$E = E^0 + \frac{RT}{nF} \ln \left(\frac{[C_x H_y O_z]^b [NO_2^-] (4x + y - 2z) (P_{O_2})^{2x+1/2y-z}}{(P_{CO_2})^{5x} (P_{N_2})^{2x+1/2y-z} (2y - 2x + z) [OH^-]^{4x+y-2z}} \right) \quad (a1-7)$$

(a1-7) is simplified with different constants of i, j, h and k, which defined as follows:

$$i = E^0 + \frac{(2x + 1/2y - z)RT}{nF} \ln\left(\frac{1}{P_{O_2}}\right) + \frac{(5x)RT}{nF} \ln\left(\frac{1}{P_{CO_2}}\right) + \frac{(2y - 2x + z)}{nF} \ln\left(\frac{1}{P_{N_2}}\right)$$

$$j = \frac{5RT}{nF}$$

$$h = \frac{(4x + y - 2z)RT}{nF}$$

$$k = \frac{(4x + y - 2z)RT}{nF}$$

Then the (a1-9) can be simplified further as (a1-8).

$$E = i + j \ln([C_x H_y O_z]) + h \ln([NO_2^-]) + k \ln\left(\frac{1}{[OH^-]}\right) \quad (a1-8)$$

Replacing $2.3026 \times (14 - \text{pH})$ for $\ln\left(\frac{1}{[OH^-]}\right)$ then obtains (a1-9).

$$E = a'' + b'' \text{pH} + c'' \log(NO_2^-) + d'' \log(C_x H_y O_z) \quad (a1-9)$$

where a'' , b'' , c'' and d'' are defined as:

$$a'' = i + 2.3026 \times 14 \times k$$

$$b'' = -2.3026 \times k$$

$$c'' = 2.3026 \times j$$

$$d'' = 2.3026 \times j$$

Appendix 2



國立成功大學永續環境實驗所 藥物毒物分析實驗室
Chemicals and Toxics Substances Analysis Laboratory
Sustainable Environment Research Laboratories, National Cheng Kung University

測試報告

報告編號：ERC103-015

報告日期：2014/04/11

以下資料由委託檢驗廠商提供及確認

委託單位：東海大學
委託地址：台中市西屯區臺灣大道四段 1727 號
理學院 S206

收樣日期：2014/03/24

測試日期：2014/04/02

測試結果：

項次	原樣名稱	檢項	單位	測試結果	偵測範圍
1	Sample 1	粒徑分析	um	16.47	0.04~2000
2	Sample 2	粒徑分析	um	18.79	0.04~2000
備註	1. 本報告不得分離使用，分離使用無效。 2. 本報告僅對該樣品負責，且未經本中心書面同意不得隨意摘錄複製使用。 3. 檢驗報告僅就委託者之委託事項提供檢驗結果，至若本產品之合法性，仍應由主管機關依法判斷。				



本報告是依照本所訂定之通用服務規則製作發散，將本中心之義務、免責、管轄權皆有明確之規範，除非另有說明，此報告結果僅對檢驗之樣品負責。本報告未經本中心書面許可，不可部份複製；對報告內容或者外觀任何未經授權之變更、竄改、偽造皆屬非法，違反者將會被依法起訴。This Test Report is issued by Sustainable Environment Research Laboratories, National Cheng Kung University. Attention is drawn to the limitations of indemnification, liability and jurisdictional issues defined therein. The results shown in this test report refer only to the sample(s) tested. This test report can not be reproduced, except in full, without prior written permission of the Center. Any unauthorized alteration, forgery or falsification of the content or appearance of this report is unlawful and offenders may be prosecuted to the fullest extent of the law.

國立成功大學永續環境實驗所藥物毒物分析實驗室地址：台南市安南區安明路三段 500 號電話：(06)384-0136ext 520 傳真：(06)384-0960
Sustainable Environment Research Laboratories, National Cheng Kung University, No.500, Sec. 3, Anming Rd., Annan District, Tainan City, Taiwan (R.O.C.) 1 of 1